uOttawa

L'Université canadienne
Canada's university

FACULTÉ DES ÉTUDES SUPÉRIEURES ET POSTOCTORALES

u Ottawa

L'Université canadienne
Canada's university

FACULTY OF GRADUATE AND POSDOCTORAL STUDIES

Christopher Ryan McLaughlin
AUTEUR DE LA THÈSE / AUTHOR OF THESIS

Ph.D. (Cellular and Molecular Medicine)
GRADE / DEGREE

Department of Cellular and Molecular Medicine
FACULTÉ, ÉCOLE, DÉPARTEMENT / FACULTY, SCHOOL, DEPARTMENT

Tissue Engineered Biomimetic Corneas for Promoting Corneal Regeneration

TITRE DE LA THÈSE / TITLE OF THESIS

May Griffith
DIRECTEUR (DIRECTRICE) DE LA THÈSE / THESIS SUPERVISOR

CO-DIRECTEUR (CO-DIRECTRICE) DE LA THÈSE / THESIS CO-SUPERVISOR

Rosalind Labow

James Zieske (Harvard Medical School)

Alan Mears

Catherine Tsilfidis

Gary W. Slater
Le Doyen de la Faculté des études supérieures et postdoctorales / Dean of the Faculty of Graduate and Postdoctoral Studies

Tissue Engineered Biomimetic Corneas for Promoting Corneal Regeneration

Christopher Ryan McLaughlin

Thesis submitted to the
Faculty of Graduate and Postdoctoral Studies
In partial fulfillment of the requirements
For the PhD degree in Cellular and Molecular Medicine

Cellular and Molecular Medicine
Faculty of Medicine
University of Ottawa

Your file Votre référence
ISBN: 978-0-494-65560-3
Our file Notre référence
ISBN: 978-0-494-65560-3

Dedication

I would like to dedicate this work to my wife Tammy, for believing in me and being my inspiration all along the way.

Authorization

Sections 1.1.1, 1.2, 1.2.1-1.2.2, 1.3.1, 1.4, 1.5.2-1.5.5 were adapted from **Bioengineered corneas for transplantation and in vitro toxicology**. McLaughlin CR, Tsai RJ, Latorre MA, Griffith M. Front Biosci. 2009 Jan 1;14:3326-37. with permission as found on the Frontiers in Biosciences website (http://www.bioscience.org/permit.htm)

Educational use :

Frontiers in Bioscience grants permission to all authors, readers and third parties of educational nature to reproduce and use published material and online resources as part of another publication or entity. This permission is granted free of charge provided that

1. there is no charge, submission fee, royalty, honorarium, or any other monetary rewards for the use of the figure by the author, user, WebSite, Publisher, Organizer or any other entity using the material.

2. the material is properly credited by including the reference within the text or legend and including the full citation of the article in the reference section of educational material. When available the DOI link should also be provided. If reproduced in CD format, the reference should be included in the same page that the material is included. If reproduced on a Web Site, the reference should be linked to the article published in the Frontiers in Bioscience. Users who do not know the URL of the link can request it by providing the citation in an Email to fbs@bioscience.org .

The educational use includes, for example, the use of a figure, table or text in a presentation, another article, a book chapter, newsletter, theses, dissertations, classroom material, academic course, academic conference material, training material or posting of an abstract on a Web site. If your use complies with the above guideline, you do not need to obtain permission from Frontiers in Bioscience for the use of material. However, if in doubt or if the use does not comply with the above guideline, please write to fbs@bioscience.org .

Manuscript 1: Journal of Toxicological Sciences, Oxford publishing.

From the publishers' website:
http://www.oxfordjournals.org/access_purchase/publication_rights.html
Rights retained by ALL Oxford Journal Authors

- The right, after publication by Oxford Journals, to use all or part of the Article and abstract, for their own personal use, including their own classroom teaching purposes;
- The right, after publication by Oxford Journals, to use all or part of the Article and abstract, in the preparation of derivative works, extension of the article into book-length or in other works, provided that a full acknowledgement is made to the original publication in the journal;
- The right to include the article in full or in part in a **thesis or dissertation**, provided that this not published commercially;

For the uses specified here, please note that there is no need for you to apply for written permission from Oxford University Press in advance. Please go ahead with the use ensuring that a full acknowledgment is made to the original source of the material including the journal name, volume, issue, page numbers, year of publication, title of article and to Oxford University Press and/or the learned society.

The only exception to this is for the re-use of material for commercial purposes, as defined in the information available via the above url. Permission for this kind of re-use is required and can be obtained by using Rightslink:

Manuscript 2: Cornea, Published by Lippincott Williams & Wilkins, Inc.
Permission requested via Rightslink© Copyright Clearance Center
Accessible through:
https://s100.copyright.com/CustomerAdmin/PLF.jsp?lID=2009071_1248130295952
Licence Number 2233300935952

Manuscript 3: Biomaterials, Published by Elsevier
Permission requested via Rightslink© Copyright Clearance Center
Accessible through:
https://s100.copyright.com/CustomerAdmin/PLF.jsp?lID=2009071_1248129628870
Licence Number 2233300268870

Manuscript 5: IOVS, Published by Association for Research in Vision and Ophthalmology

From: Debbie Chin
Sent: Tuesday, July 21, 2009 9:17:15 AM
To: McLaughlin, Christopher
Subject: RE: Copyright permission to use article in doctoral thesis
Auto forwarded by a Rule
Dear Dr. McLaughlin,
Thank you for your e-mail. Yes, as an author of the IOVS article, you may reprint it in your doctoral thesis without obtaining formal permission, as long as you include a full article citation and acknowledge ARVO as the copyright holder.
Best regards,
Debbie Chin
IOVS Editorial Office

ARVO 2010
For Sight: The Future of Eye and Vision Research
May 2-6 * Fort Lauderdale, FL

Abstract

Corneal transplantation with allograft tissue is currently the gold standard treatment for treating corneal damage following trauma or disease. However the supply of good quality donor tissue cannot meet the demand, especially in developing countries. Currently, the only alternative treatment option has been the use of corneal prostheses (keratoprostheses) but these do not permit integration with the host tissue. We utilized a regenerative medicine approach to enhance the natural ability of the cornea to regenerate by providing an acellular but highly bioactive scaffold to serve as a corneal extracellular matrix (ECM) substitute. The corneal substitutes tested were based on the predominant ECM protein found in the cornea, which is type I collagen. Cross-linked collagen corneal scaffolds were formed into the appropriated dimensions and cross linked using a simple methodology, and tested *in vitro* to assure that they would support cellular growth of epithelial cells and nerves. The most promising candidate implants were then implanted into a range of animal models as either lamellar grafts, or full thickness grafts by lamellar and penetrating keratoplasties, respectively. Following implantation, it was observed that the scaffolds promoted regeneration of the corneal epithelial and stromal cells. The implants themselves were remodelled, observed through biotin conjugation, to give a seamless host-graft interface. The grafts remained stably integrated. At 12 months post implantation, the implanted corneas had comparable mechanical properties compared to contralateral controls. Nerves had reinnervated the cornea at densities comparable to controls and were shown to be functionally active, capable of responding to external stimuli through electrophysiological testing. We were also able to improve the mechanical properties of our gels by incorporating the biomimetic molecule 2-methacryloyloxyethyl phosphorylcholine (MPC), which allowed

for full thickness transplantation into guinea pigs. Finally, with the advent of recombinant human collagen, we were able to create a novel class of human based materials for corneal implantation, which were successfully transplanted into pigs. Type III recombinant human collagen, a minor component of the human cornea, showed superior optical transmission compared to type I collagen gels, and both showed stable integration, with corneal regeneration of cells, tear film, and nerves. Substantially more work is needed to determine the limits of this approach in treating corneal blindness, i.e. what clinical causes of blindness can be treated in this manner. Nevertheless, we have demonstrated that a simple, ECM mimetic could promote the regeneration of corneal cell types, and the reinnervation of functional nerves, in a stable and seamless fashion.

Table of Contents

Dedication ii
Authorization iii
Abstract vi
Table of Contents viii
List of Tables xi
List of Figures xii
List of Abbreviations xiv
Acknowledgments xix
Chapter 1 1
1.1 The Cornea 1
1.1.1 Overview 1
1.1.2 Corneal Nerves 2
1.2 In Vitro Corneal Models 4
1.2.1 Tissue Engineered Full Thickness Models 5
1.2.2 Innervated Corneal Model 6
1.3 Corneal Damage and Vision Loss 6
1.3.1 Neurotrophic Effects on the Cornea 6
1.3.2 Corneal Nerve Injury 7
1.4 Current Allograft Transplantation Techniques and Tissue Availability Issues 8
1.5 Corneal Substitutes for Transplantation 10
1.5.1. Scaffold Materials 10
1.5.2 Completely Synthetic Corneal Replacements: Keratoprostheses 12
1.5.3 Keratoprostheses with Cell Coverage 15
1.5.4 Self-assembled Corneal Substitutes 16
1.5.5. Biomimetic Corneal Implants 18
1.6 Research Summary 20
1.6.1 Rationale 20
1.6.2 Hypothesis 20
1.6.3 Thesis Objectives 21
1.6.4 Research Approach 21
1.7 Summary 25
Chapter 2 26
2.1 Manuscript 1 26
Functional Innervation in Tissue Engineered Models for in vitro Study and Testing Purposes. 27
Abstract 30
Introduction 31
Materials and Methods 32
Results 38
Discussion 44
Chapter 3 52
3.1 Manuscript 2 52
Regeneration of Corneal Cells and Nerves in an Implanted Collagen Corneal Substitute 53
Co-author Contributions to Manuscript 55

Abstract 57
Introduction 58
Materials and Methods 60
Results 66
Discussion 76
Chapter 4 82
4.1 Manuscript 3 82
Collagen-phosphorylcholine Interpenetrating Network Hydrogels as Corneal Substitutes. 83
Co-author Contributions to Manucript 84
Abstract 87
Introduction 88
Materials and Methods 90
Results 97
Discussion 107
Chapter 5 113
5.1 Manuscript 4 113
Regeneration of Functional Nerves within Full Thickness Collagen-Phosphorylcholine Corneal Substitute Implants in Guinea Pigs. 114
Co-author Contributions to Manucript 115
Abstract 117
Introduction 118
Materials and Methods 120
Results and Discussion 129
Chapter 6 145
6.1 Manuscript 5 145
Tissue Engineered Recombinant Human Collagen-based Corneal Substitutes for Implantation: Performance of Type I versus Type III Collagen 146
Co-author Contributions to Manuscript 148
Abstract 151
Introduction 152
Materials and Methods 153
Results 160
Discussion 169
Chapter 7 172
General Discussion 172
7.1 Significant Scientific Contributions 173
7.2 Novel Technologies, Methods, or Results 174
7.3 Current Progress 176
References 180
Chapter 1 180
Chapter 2 190
Chapter 3 195
Chapter 4 199
Chapter 5 204
Chapter 6 209

Chapter 7 213

List of Tables

Chapter 3

Table 1. Nerve Density 73
Table 2. Averaged tensile properties of pig corneas harvested from control and implanted eyes and of the cross-linked collagen hydrogel alone. 75

Chapter 4

Table 1. Comparison of key properties of optimized porcine and recombinant human collagen-MPC hydrogels with their respective collagen only benchmarks 99

Chapter 5

Table 1. Functional properties of corneal sensory units recorded from contralateral and implanted eyes at 3 months post-surgery. 137
Table 2. Response to chemical stimulation (a 30s-pulse of 98.5% CO_2) of corneal polymodal nociceptors recorded from implanted and contralateral eyes. 140

Chapter 6

Table 1. Primary antibody specifications. 159
Table 2. Comparison of key properties of optimized EDC/NHS cross-linked recombinant human collagen type I (RHC-I) and type III (RHC-III) corneal substitutes to excised human eye bank corneas. 161

List of Figures

Chapter 1

Fig. 1. Diagram of the layers of the cornea. 1

Chapter 2

Fig. 1. TE cornea construction and neurite growth promotion. 33
Fig. 2. Effects of innervation on properties of the epithelium. 39
Fig. 3. Epithelial cell viability. 41
Fig. 4. Visualization with 2-photon microscopy. 42
Fig. 5. Na^+ channels and internal Na^+ concentration in nerve fibres of the TE cornea. 43

Chapter 3

Fig. 1. Sections through biotinylated cornea substitutes implanted by penetrating keratoplasty into corneas of mice. 68
Fig. 2. Corneal implantation by lamellar keratoplasty in pigs at 12 months. 70
Fig. 3. IVCM and TEM images at 12 months from pigs. 71
Fig. 4. Nerve fibre bundle length density calculated by analysis of serial in vivo confocal micrographs. 74

Chapter 4

Fig. 1. The solid state ^{13}CNMR spectra of freeze-dried (A) pure porcine collagen hydrogel and (B) APS-initiated porcine collagen-MPC hydrogel (collagen:MPC=1:1,w/w) 98
Fig. 2. The solid state ^{31}PNMR spectra of freeze-dried (A) pure porcine collagen hydrogel and (B) APS-initiated porcine collagen-MPC hydrogel (collagen:MPC=1:1,w/w). 98
Fig. 3. In vitro biodegradation collagen and collagen-MPC hydrogels in collagenase. .. 101
Fig. 4. Absorption spectrum before (thick) and after (thin) solar exposure for 20 hours. 102
Fig. 5. Typical in vivo confocal images of the cornea of mini-pigs at 12 months post-operative 104
Fig. 6. Sections through representative pig corneas at 12 months post-implantation. 105
Fig. 7. TEM of the epithelial-stromal interface region of mini-pig implant. 106
Fig. 8. TEM image showing regenerated collagen fibrils in the stroma of the mini-pig cornea received implant 107

Chapter 5

Fig. 1. Schematic diagram of the recording set-ups used in the experiments 125
Fig. 2. Corneal implantation by penetrating keratoplasty 129
Fig. 3. Histology of control (left panels) and collagen MPC corneal substitute (right panels) at 6 months post implantation. 131
Fig. 4. Penetration of corneal nerves into collagen MPC corneal substitutes. 134
Fig. 5. Response of regenerating corneal polymodal nociceptive units to noxious stimuli. 141
Fig. 6. Sample recording of the response to temperature reduction of a cold corneal nerve terminal located inside a corneal implant at eight months after surgery. 143

Chapter 6

Fig. 1. H&E stained sections through RHC-I and RHC-III hydrogels implanted sub-cutaneously into rats. 162
Fig. 2. Fundus and IVCM images at 12 months from pigs. 164
Fig. 3. Postsurgical corneal regeneration at 12 months. 166

Fig. 4. TEM of epithelial-stromal compartment interface. 167
Fig. 5. Nerve density per central cornea 12 months after surgery in unoperated control corneas and in various corneal graft types. 168

List of Abbreviations

AM: acetoxymethyl

ANOVA: analysis of variance

APS: ammonium persulphate

ATPase: adenosine triphosphatase

BDNF: brain derived neurotrophic factor

BSA: bovine serum albumin

CGRP: calcitonin gene related peptide

^{13}CNMR: ^{13}Carbon nuclear magnetic resonance

CS: chondroitin - 6 - sulphate

CT: cold thermoreceptors

CTT: corneal touch threshold

DAB: 3,3-diaminobenzidine

DAPI: 4',6-diamidino-2-phenylindole

DLKP: deep lamellar keratoplasty

DMEM: Dulbecco`s modified eagle medium

DMSO: dimethyl sulfoxide

DRG: dorsal root ganglia

ECM: extracellular matrix

EDC: 1-ethyl-3-(3-dimethylaminopropyl) carbodiimide hydrochloride

FBS: fetal bovine serum

FCS: fetal calf serum

FITC: fluorescein isothiocyanate

HCEC: human corneal epithelial cells

HCE-T: human corneal epithelial cell line

HIV: human immunodeficiency virus

HRP: horseradish peroxidase

HSV-1: herpes simplex virus 1

IGF-1: insulin-like growth factor 1

IL-1: interleukin 1

IPN: interpenetrating network

ISO: International Organization for Standardization

IVCM: *in vivo* confocal microscopy

K^+: potassium

KPro: keratoprosthesis

KSFM: keratinocyte serum free media

LASIK: laser-assisted *in situ* keratomileusis

MES: morpholinoethanesulfonic acid

MMP: matrix metallo proteases

MMPC: 2-(methacryloyloxy)ethyl-[N-(2 methacryloyloxy)ethyl]phosphorylcholine

MN: mechano nociceptor

MPC: 2-methacryloyloxyethyl phosphorylcholine

MTT: (3-(4,5-Dimethylthiazol-2-yl)-2,5-diphenyltetrazolium bromide

Na^+: sodium

NAMSA: North American Science Associates

NFB: nerve fibre bundle

NGF: nerve growth factor

NHS: N-hydroxysuccinimide

NMR: nuclear magnetic resonance

OOKP: osteo-odonto keratoprosthesis

PAA: poly(acrylic acid)

PBS: phosphate buffered saline

PDMS: poly(dimethyl siloxane)

PDSGR: Pro-Asp-Ser-Gly-Arg

PEG: poly(ethylene glycol)

PEGDA: poly(ethylene glycol) diacrylate

PFA: paraformaldehyde

PHEMA: poly(2-hydroxyethyl methacrylate)

PMMA: poly(methyl methacrylate)

PN: polymodal nociceptor

^{31}PNMR: ^{31}Phosphorous nuclear magnetic resonance

PRK: photorefractive keratectomy

PTFE: poly(tetrafluoroethylene)

PVA: poly(vinyl alcohol)

RA: retinoic acid

RF: receptive field

RGD: Arg-Gly-Asp

RGDS: Arg-Gly-Asp-Ser

RHC-I: recombinant human collagen type I

RHC-III: recombinant human collagen type III

RT: room temperature

SBFI: sodium – binding benzofuran-isophthalate

SBP: subbasal nerve plexus

SD: Sprague Dawley

SDS: sodium dodecyl sulphate

SEM: standard error of mean

SP: Substance P

SMA: smooth muscle actin

TBS: tris buffered saline

TCT: TBS containing 0.6% carrageenan and 0.3% Triton-X 100

TE: tissue engineered

TEM: transmission electron microscopy

TEMED: N,N,N',N'- tetramethyl ethylene diamine

TEP: transepithelial permeability

TMEDA: N,N,N',N'- tetramethyl ethylene diamine

TTX: tetrodotoxin

UEA: *Ulex europaeus* agglutinin

UV: ultraviolet

UVA: ultraviolet A

UVB: ultraviolet B

WHO: World Health Organization

XPS: X-ray photoelectron spectroscopy

YIGSR: Tyr-Ile-Gly-Ser-Arg

Acknowledgments

I would like to thank Dr. May Griffith, for being the greatest supervisor and mentor from the very beginning, to the very end. Over the years, she has afforded me the opportunities and given me the guidance to become the researcher I am today.

To my committee members, Dr. Peter Stys, Dr. Margaret Sonnenfeld, Dr. Heather Sheardown, Dr. Catherine Tsilfidis and Dr. Stefanie Bennett, I truly appreciate all the time and guidance you have given me over the years.

For financial support, I am very grateful for a fellowship from the National Science and Engineering Research Council, an Ontario Graduate Student Scholarship and Excellence scholarships from the University of Ottawa.

To all of my lab mates, and staff involved from the University of Ottawa, Ottawa Health Research Institute and the Eye Institute, I thank you for your help and humour over the years.

Most importantly, I thank my mother Corinne, and my father James as well the rest of my family for their unwavering encouragement and belief in me.

Chapter 1

INTRODUCTION

1.1 The Cornea

1.1.1 Overview

The average human cornea is about 500 μm thick centrally and about 750 μm peripherally (Jonas and Holbach 2005). It can be viewed as a largely collagenous matrix containing cells (a stroma) sandwiched between an outer epithelium and an inner endothelium (Fig. 1). It is avascular but very highly innervated by sensory and autonomic nerves, making the cornea an estimated 300 times more sensitive than skin (Rozsa and Beuerman 1982). A unique property of the cornea is its optical clarity, which accounts for over 70% of the light that is transmitted to the retina for vision. Corneal clarity is now believed to result from a combination of refractive index matching, and the presence of structural components well below the wavelength of visible light (Freegard 1997; Meller et al. 1997). Another unique property of the cornea is that it is avascular, as well as immune privileged (Niederkorn 1990).

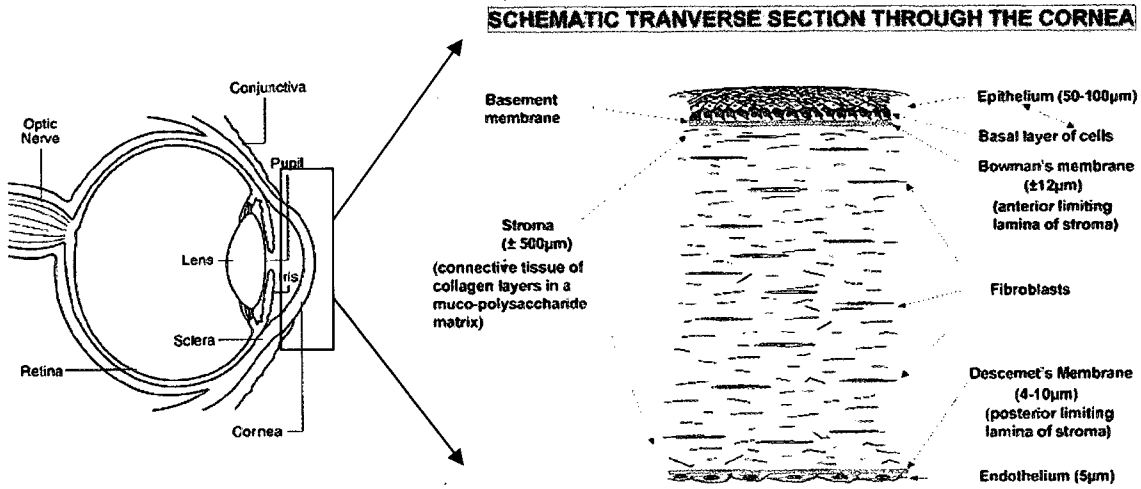

Fig. 1. Diagram of the layers of the cornea.

The corneal epithelium consists of stratified, non-keratinizing epithelial cells, and is approximately 50 μm thick. The basal layer of the epithelium consists of progenitor cells that proliferate and differentiate to replace the superficial cells lost at the anterior surface (Ren and Wilson 1996). These progenitors are in turn replenished by a population of corneal stem cells that reside within the corneal/scleral limbus (Dua and Azuara-Blanco 2000). The epithelium is overlain by a tear film that comprises several defined layers. The mucous layer apposing the epithelium is secreted by the epithelial cells along with several anti-inflammatory and anti-microbial factors (Gipson and Argueso 2003; Sack et al. 2001)

The stroma can be thought of as a largely hydrated extracellular matrix (ECM) containing fibroblast-like cells referred to as keratocytes. Biochemically, the stroma is comprised of type I collagen (13.6%), 0.9% glycosaminoglycans, and 80% water, making the stroma in essence a hydrated gel or hydrogel. The keratocytes are localized in lamellar networks within this hydrogel.

Lastly, the endothelium, which is a single cell layer, functions to regulate the hydration level of the corneal stroma, which helps to maintain central corneal thickness. Sodium/potassium ATPase pumps within the endothelium circulate aqueous humor between the anterior chamber and stroma. A detailed review of the corneal layers is given in Nishida (Nishida 1997).

1.1.2 Corneal Nerves

The mammalian cornea and conjunctiva receive sensory innervation from a modest amount (50- 450 depending on the species) of primary sensory neurons that are derived from the ophthalmic branch of the trigeminal ganglion (LaVail et al. 1993; Marfurt et al. 1989; Morgan et al. 1978). Nerves enter the periphery of the cornea in a radial manner, losing their

myelin sheath and subdividing into smaller fragments, bifurcate forming a subepithelial plexus, which then enters the basal epithelium running parallel to the surface forming leashes that eventually terminate in the superficial epithelium (Muller et al. 2003). Due to the extensive branching of the corneal neurons, and the size of the tissue, the cornea is one of the most densely innervated tissues of the body (de Castro et al. 1998; De Felipe and Belmonte 1999; Muller et al. 2003). Corneal neurons can be classified morphologically as either thin myelinated A-delta (30%), or unmyelinated C axons (70%). Immunohistochemical analysis reveals that approximately 60% of corneal sensory neurons are immunoreactive to calcitonin gene related peptide (CGRP), and 20% contain the neuropeptide substance P (Muller et al. 2003).

Perhaps the most meaningful way to functionally classify sensory neurons is through electrophysiological studies. Approximately 15% of corneal fibres are the A-delta type, which rapidly conduct mechanical forces, with the threshold stimulus being lower than that for skin. These fire impulses in response to brief contact of the corneal surface. The majority of corneal fibres (70%) are polymodal receptors which are activated by near noxious mechanical insult, as well as thermoresponsiveness to temperatures above 39 °C and noxious cold below 29 °C. Also, they respond to exogenous chemical irritants, as well as endogenous chemical mediators produced from damaged corneal tissue, by inflammatory cells, or derived from plasma leaking from limbal vessels (potassium ions, protons, ATP, prostaglandins, kynins, growth factors, arachidonic acid metabolites) (Belmonte et al. 2004; Chen et al. 1997). These polymodal receptors can elicit irregular, continuous discharge that produces sustained sensation of pain. Some of the polymodal nociceptors are of the thin myelinated type, but the majority are of the C type. Finally, approximately 10-15% of the corneal nerve

fibres are cold-sensitive receptors, which discharge spontaneously at rest and increase their firing when the temperature at the surface of the cornea decreases due to evaporation, blowing of cold air, or application of cold solutions (Belmonte et al. 2004), and are transiently silenced upon warming (Gallar et al. 1993). It has also been suggested that there is a separate class of "sleepy" nociceptors which are only activated when local inflammation occurs (Schaible and Schmidt 1983), but this has not been proven experimentally (Tanelian and Beuerman 1984).

Unlike most tissues, the avascular cornea is unique in its dependence upon its nerve source and the nerve-corneal cell interaction to maintain tissue integrity and for wound healing (Lambiase et al. 1999). Irreversible nerve damage due to trauma or infection can lead to loss of transparency and vision loss or blindness.

1.2 *In Vitro* Corneal Models

Alternatives for animal research in the field of ocular toxicity testing, has prompted several groups to design tissue engineered *in vitro* corneal alternatives. The Gillette *In vitro* Testing and Research Laboratory have previously created a human corneal epithelial cell line (HCE-T) for *in vitro* test protocols. Fluorescein transepithelial permeability (TEP) is measured via a dose dependent effect of test substances on the HCE-T TEP cell line. The cells are grown on a simplified collagen membrane, induced to stratify at an air liquid interface, which allows for the formation of tight junctions and a true epithelial barrier (Wertz 2006). The MatTek Corporation has developed a simple three dimensional model based on human foreskin keratinocytes, allowed to stratify in a specialized medium at an air liquid interface in 24-well plates for cellular viability testing using an MTT assay (Klausner et al. 2003). Although these models are becoming popular, they are not able to predict

responses to chemicals that may affect the other cell layers of the cornea, or that are dependent upon the interactions of the epithelial cells with other cell types within the cornea.

1.2.1 Tissue Engineered Full Thickness Models

In an effort to reproduce the true three dimensional structure of the cornea, Zieske *et al.* (Zieske et al. 1994) utilized a stroma comprised of neutralized type I collagen blended with rabbit stromal fibroblasts, and seeded with rabbit corneal epithelial cells. Immortalized mouse endothelial cells were seeded on the reverse side, making a true three dimensional corneal construct (Zieske et al. 1994). Our group sought to fabricate a full thickness cornea using immortalized human corneal epithelium, endothelium, and keratocyte cell lines, which reproduced the biochemical and morphological functions of normal human corneas. The tissue engineered artificial corneas were developed around a type I collagen/ chondroitin sulphate stroma, and crosslinked with glutaraldehyde to provide a more physiologically relevant and robust structure. To select appropriate cells for the constructs, immortalized cell lines were screened electrophysiologically through patch clamping, and tested for proper expression of biochemical markers indicative of the specific corneal cell types. The epithelium was allowed to stratify at an air liquid interface. Constructs were tested for opacity changes in response to irritating chemicals, as well as for changes in the expression of wound healing genes such as c-fos, and IL-1 alpha (Griffith et al. 1999). The main limitation of this model was that it lacked innervation, and could not address the important role of corneal nerves.

1.2.2 Innervated Corneal Model

In Suuronen et al. (Suuronen et al. 2004), we showed that our previous *in vitro* corneal model could be functionally innervated using a sensory nerve source. Laminin and nerve growth factor (NGF) were crosslinked into the type I rat-tail collagen and chondroitin sulphate hydrogel scaffolds, through glutaraldehyde crosslinking. Both laminin and NGF had previously been shown to promote the differentiation and guidance of nerves (Chan and Haschke 1982; Riggott and Moody 1987). Chicken dorsal root ganglia explants (DRG) were selected as the sensory neuron source, and were implanted within the hydrogel scaffold prior to gelling. In order to promote neurite extension, the medium was supplemented with retinoic acid, which has been shown to induce neurite outgrowth from embryonic mouse dorsal root ganglia explants (Corcoran et al. 2000). Using innervated constructs the structural morphology found in the human cornea was able to be reproduced. DRGs extended neurites that contained both smooth fibres traversing the corneal stroma, along with smaller beaded fibres that entered the epithelium, which is similar to the structural morphology found in the human cornea (Muller et al. 1996; Muller et al. 1997). As well, transmission electron microscopy showed individual neurite terminals within epithelial cells (Suuronen et al. 2004).

1.3 Corneal Damage and Vision Loss

1.3.1 Neurotrophic Effects on the Cornea

A peripheral nerve supply is necessary for the proper function of various types of innervated tissue (Holzer 1988). Corneal nerve fibres have been known to have important

trophic effects on the corneal epithelium. Releasing Substance P (SP) from neurons has been shown to have a synergistic effect with IGF-1 on corneal epithelial migration, adhesion, and wound closure (Chikama et al. 1999). Damage to the corneal nerve supply leads to a condition known as neurotrophic keratitis. This can be caused by trigeminal nerve damage associated with head surgery, or keratorefractive procedures such as photorefractive keratectomy and LASIK (laser-assisted *in situ* keratomileusis), leading to transiently mild or severe epithelial alterations (Davis and Dohlman 2001; Tervo and Moilanen 2003). Surgical damage of the rabbit trigeminal ganglion leads to significant inhibition of corneal epithelial wound healing, and predisposes the newly healed corneas to recurrent, spontaneous epithelial aberrations (Araki et al. 1994).

Just as normal corneal function requires innervation, it has been shown that corneal nerves benefit from the presence of corneal cells. Neurotrophic factors secreted by corneal epithelial cells, including nerve growth factor (NGF), and brain derived neurotrophic factor (BDNF), have been shown to aid in guidance and survival of corneal nerves (Emoto and Beuerman 1987; You et al. 2000). Overexpression of NGF leads to hypertrophy and nerve sprouting, whereas neutralizing antibodies against NGF reduce collateral axon branching (Albers et al. 1994). Together, it can be seen that the epithelium and neurons in the cornea are mutually beneficial towards each other.

1.3.2 Corneal Nerve Injury

Corneal nerve damage can be caused by a wide range of mediators, including: corneal transplantation surgery, photorefractive surgery (LASIK and PRK), contact lens wear, wounds, keratitis and inflammation as a secondary result of infections such as herpes simplex

virus -1 (HSV-1). Local tissue damage leads to sensitization, which is a decrease in the firing frequency and decrease in the threshold of nociceptors, and an increase in ongoing activity (Belmonte et al. 2004). Inflammatory mediators released from inflammatory cells, or extravasated plasma interact with receptor proteins on nociceptor membranes which leads to activation of intracellular pathways that ultimately activate ion channels leading to depolarization and increased excitability (Handwerker and Reeh 1991). Also, when polymodal nerves are depolarized, they release neuropeptides which travel antidromically to activate neighbouring nerve terminals. These neuropeptides act as proinflammatory substances, causing neurogenic inflammation (Brock et al. 1998).

Injury to corneal nerves often leads to hypoaesthesia to natural stimuli, but paradoxically abnormal activity occurs leading to the sensation of pain, burning or itching. Nerves that are cut begin to form neuromas at axonal stumps, and eventually regenerate. It is accompanied by molecular changes in the neurons encoding for membrane receptor proteins and ion channels, which change the functional behaviour of the nerves, and their excitability, which leads to spontaneous activity and abnormal responses (Waxman et al. 1999). These changes in expression of membrane proteins and ion channels in response to growth factors, cytokines and inflammatory mediators released from injured tissue leads to long lasting and permanent changes in excitability (Ehlers et al. 1995).

1.4 Current Allograft Transplantation Techniques and Tissue Availability Issues

The function of the cornea is dependent upon its optical clarity. When loss of clarity due to disease or damage is irreversible, corneal blindness results. The World Health Organization's (WHO) definition of blindness includes individuals who have a visual acuity

of 3/60 or less. That being said, it is estimated that there are 50 million people worldwide who possess bilateral blindness, as well as at least 150 million people who have impaired vision in both eyes (Foster 2003; Whitcher et al. 2001). While cataracts are responsible for almost half the cases of blindness, corneal damage and disease due to various etiologies is the next largest culprit, with corneal trachoma, a bacterial infection caused by *Chlamydia trachomatis*, affecting roughly 5 million people worldwide (Foster 2003). Furthermore, it is estimated that corneal ulceration and ocular trauma is responsible for 1.5 to 2 million new cases of corneal blindness annually (Whitcher et al. 2001). At present, transplantation of human donor tissue is the only widely acceptable treatment.

Depending upon the nature of the damage, replacement of one or more corneal layers is performed, using corneal allografts or progenitor cell grafts, (e.g., limbal stem cell grafts). In other conditions such as keratoconus, where stromal matrix is damaged or weakened, attempts to strengthen the matrix by *in situ* crosslinking have been attempted.

One of the main issues with the above mentioned surgical techniques, is that they all rely on donor corneas, which have traditionally been in adequate supply in the US, but are in shortage in other countries (Ehlers et al. 1995). This is due to the lack of proper organ banking procedures in developing countries, and an increasing lack of suitability of donor tissue (due to transmissible diseases such as HIV, Creutzfeldt–Jakob disease or hepatitis C) or to the increase in refractive surgical techniques, such as LASIK treatment, which renders corneas unsuitable for grafting. This has caused an increase in the shortage of corneas worldwide (Rama et al. 2001).

1.5 Corneal Substitutes for Transplantation

1.5.1. Scaffold Materials

The majority of tissue engineering approaches to building *in vitro* models of organs require a scaffold material to allow three dimensional support, upon which cells can attach to proliferate and differentiate into physiologically functional tissues that are structurally similar to the native tissue. The cells used in tissue engineered tissues can either be pre-seeded cells, which can be derived from stem cells, primary cells, and cells with extended lifespans, or cells influenced to grow into the matrix from surrounding tissue. Often, co-factors such as extracellular matrix proteins or growth factors, can be added to the gels to promote and maintain proper cellular differentiation.

Most tissue engineered scaffolds are polymeric arrangements of either synthetic materials or naturally occurring materials, which can be further processed through cross-linking methods to increase physical properties. Typically, synthetic materials have the benefit of having greater mechanical strength, easier batch processing with high reproducibility, and a firmer control over pore size. However, fully synthetic materials often initiate a higher immune response in the host, causing an increase of inflammatory infiltrate and the deposition of fibrin around host tissue. An exception to this is synthetic biodegradable polymers, such as poly (L)-(lactic acid) and poly(glycolic acid), which are being used increasingly in *in vitro* models and drug delivery vehicles (Jain 2000; Ryu et al. 2007).

Many tissue engineering strategies rely on the use of extracellular matrix (ECM) proteins in order to provide a suitable scaffold. The ECM is a secreted product of cells into the surrounding organ that helps to direct and maintain the phenotype of the cells (Boudreau

et al. 1995). Typically, ECM is comprised of both structural and functional proteins, glycosaminoglycans, glycoproteins, and other small molecules that are arranged into a specific three dimensional structure (Baldwin 1996).

The most abundant protein found in the ECM is collagen, a family of glycosylated proteins with over 25 members, including both fibrillar and non fibrillar forms (Gelse et al. 2003). All collagens are comprised of triple helixes of polypeptide chains. The fibril forming collagens, type I, II, III, V, and XI, often impart high strength and structural stability, whereas non fibrillar collagens such as type IV collagen are often found in basement membranes of epithelial tissues with vascular components. Type I collagen is the most common form of collagen found in the body, the most extensively studied and, therefore, the most common form of collagen used in tissue engineering. It forms 300nm triple helices of up to 1000 aa's, based on the tri-peptide repeat of Gly-X-Y. Type I collagen can be extracted from ligaments and tendons, acid solubilized and then reconstituted into a three dimensional matrix. It is further stabilized through crosslinking, which *in vivo* occurs via disulfide bridges, glycation, as well as enzymatic modifications (Nimni 1988). *In vitro*, this crosslinking can be reproduced through the use of chemical cross linkers such as glutaraldehyde (Nimni et al. 1987), carbodiimides (Girardot and Girardot 1996; Liu et al. 2006), polyepoxy compounds (Imamura et al. 1989), and synthesized co-polymers (Li et al. 2005). Typically, crosslinking has an effect on reducing bio-degradation and immunogenicity (Badylak 2002).

1.5.2 Completely Synthetic Corneal Replacements: Keratoprostheses

The osteo-odonto keratoprosthesis (OOKP), developed by Strampelli (Strampelli 1963), consists of autologous tissue derived from tooth and bone which surrounds a central poly(methyl methacrylate) PMMA optic. Before implantation, the osteodental skirt is pre-implanted into the buccal mucosa to allow colonization of fibroblasts to support integration when implanted ocularly. This KPro has been one of the most successful as it has a low extrusion rate, due to the excellent integration of the skirt material (mostly hydroxypatite) with the host tissue (Mehta et al. 2005). Complications associated with this KPro include retroprosthetic membrane formation, glaucoma and decentration of the central optic, due to absorption of the osteodental skirt (Falcinelli et al. 2005).

Another KPro that has been developed utilizing PMMA is the Boston KPro, or the Dohlman-Doane Kpro, in which there are two types, with the most common one being the single collar button. This design consists of a front plate that is 5.5-7 mm in diameter, connected by a 3.5 mm stem piece to a 7 mm back plate. This KPro is used in patients who have had multiple graft rejections, including those with chemical burns, congenital glaucoma and herpetic keratitis (Khan et al. 2007).

The Seoul-type KPro consists of an optic surrounded by a skirt, with additional haptics for increased mechanical biostability post implantation. The haptics are secured to the eye through suturing of the skirt to the cornea as well as fixation to the sclera. The optics are comprised of a (PMMA) surface modified with poly(ethylene glycol) (PEG), while the skirt was made initially of poly(tetrafluoroethylene) (PTFE) but more recently of either poly(propylene) or poly(urethane). The haptics are designed using polypropylene

monofilaments. A recent study was published that followed nine patients at 62 months post operative, who had severe intractable ocular surface disease. Average visual acuity preservation time was 31.6 months. However, complications associated with this device included retroprosthetic membrane formation, extrusion and retinal detachment. Regardless of the skirt materials used in the study, tissue melt occurred with full skirt exposure at a mean interval of 12.9 months, necessitating mucosal, amniotic membrane or scleral grafting to compensate. In all the cases where KPro exchange was required due to polyurethane skirt degeneration, retinal detachment occurred, suggesting retinal management techniques are required for long term survival, as well as exchange (Kim et al. 2007).

The current generation of the original Chirila KPro has undergone multicentre clinical trials. The first generation consisted of a poly(2-hydroxyethyl methacrylate) PHEMA hydrogel core-skirt model that was sutured in place through a traditional penetrating keratoplasty technique, which has given rise to the current two-stage lamellar procedure. The newer device that has gained market approval is known as the AlphaCor™ KPro. This device consists of an interpenetrating network of transparent PHEMA, with an opaque sponge skirt also made of PHEMA. The skirt differs in water content, resulting in a KPro that does not have any glued joints, or mechanical junctions (Chirila et al. 1994). The surgical procedure consists of implanting the KPro in an intrastromal pocket via removal of the central posterior corneal lamellae, and closing over with a conjunctival flap. After three months, the flap and anterior corneal lamellae are removed, exposing the central optic. While this device has been shown to have low complication rates in normal healthy eyes, it was also meant for eyes that were already pathologic, in patients that had experienced multiple graft failures, or were not eligible for conventional donor tissue transplants. Complications with

these KPro's include corneal melting, formation of retroprosthetic membranes and optic depositions, as well as rare cases of device extrusion. Contraindications for this device include abnormal tear film, as well as uncontrollable high intraocular pressure. Topical administration of medroxyprogesterone has been shown to limit corneal melting of the device. In the most recent report on the clinical outcomes of AlphaCor™ implantation, it has been stated that HSV-1 (herpes simplex virus 1) infection is no longer considered a contraindication for implantation (Hicks et al. 2006).

Another group (Hollick et al. 2006) has tested a KPro that is comprised of a central optic made of silicone, surrounded by an opaque skirt of PTFE. The BioKPro III is inserted in a similar fashion to the AlphaCor™ through a two-stage process, of initial implantation covered with either a conjunctival or buccal mucous membrane back, and three months later the central optic is exposed. Follow up occurred between 18-48 months, with failure in six of seven patients due to extrusion, although it is noted that all the patients had extensive corneal pathologies, including thermal injury, chemical injury, congenital rubella, measles keratitis and Steven's Johnson syndrome. Also, with the one implant that was not extruded, the patient recorded mucous accumulation on the optic which required clearing. The authors' observed that more work needed to be performed on this implant in order for it to be a viable option (Hollick et al. 2006).

Recent developments include a KPro developed by Storsberg and co-workers at the Fraunhofer Institute for Applied Polymer Research, Germany. The "new artificial cornea adheres to eye cells without needing to be held in place by sutures - a major advantage over other artificial corneas, which can cause inflammation and infection". According to the German team, the skirt portion is coated with a "special protein" that has been described to

"connect to the natural cells of the eye". The optic, however, is cell free (http://www.rsc.org/chemistryworld/News/2007/October/18100701.asp).

1.5.3 Keratoprostheses with Cell Coverage

Researchers believe that it is important for the epithelium to cover the KPro in order to maintain the tear film, and prevent infection and extrusion of the implant (Trinkaus-Randall 2000). Materials such as PMMA, poly(vinyl alcohol) (PVA), and PHEMA are utilized for traditional KPro's. As these materials are non-cell adhesive, improvements have been made to modify the ability of corneal cells to adhere, and migrate over the surface. Naturally occurring extra cellular matrix proteins, and other cell adhesive peptides have been grafted onto the KPros to alleviate this problem.

Sheardown *et al.* (Aucoin et al. 2002) covalently attached cell adhesion peptides from laminin and fibronectin, including laminin derived YIGSR, and its synergistic peptide PDSGR, as well as fibronectin based RGDS and PDSGR. These were attached to poly(dimethyl siloxane) (PDMS) surfaces. It was found that surface modification with multiple peptides had a synergistic effect of corneal epithelial cell attachment compared to single peptides on their own (Aucoin et al. 2002).

Jacob *et al.* (Jacob et al. 2005) investigated the coupling of cell adhesion peptides and various cytokines to polymethacrylic acid-co-2-hydroxyethyl methacrylate (PHEMA/MAA). The bioactive factors included fibronectin, laminin, substance P, IGF-1 (insulin-like growth factor 1) and RGD. They tested whether corneal epithelial cell growth rate and adhesion were increased when the bioactive factors were directly coated on the surfaces, or if they were tethered through PEG spacers. It was found that the spacer molecules provided the

correct microenvironment for the epithelial cells by exposure of the bioactive motifs, in order to allow the cells to reach confluence, compared to little to no epithelial growth on the surfaces that were only coated with the bioactive factors (Jacob et al. 2005). It is also of importance to note that the peptides and factors are exposed to biodegradation, and effort must be taken to ensure long term attachment of the epithelial cells on the surface is maintained.

The Stanford keratoprosthesis has been developed based on a mechanically enhanced core and skirt method, consisting of a double network of PEG and poly(acrylic acid) (PAA) as its central optic, allowing for the overgrowth of corneal epithelial cells. The use of a double network of polymers increases the mechanical strength, optical transparency and biocompatibility of the polymer. The Stanford KPro has also been designed using polymer technology that allows for microperforation of the outer skirt, to further enhance integration with the host tissue. As well, they have been able to utilize a photochemical surface modification strategy to tether bioactive factors to specific sites of the polymer to promote cell adhesion (Myung et al. 2008; Myung et al. 2005). The KPro has been shown to be tolerated well in animal models up to six weeks, and further studies are ongoing (Bakri et al. 2006).

1.5.4 Self-assembled Corneal Substitutes

Germain and co-workers (Gaudreault et al. 2003) at the Laboratoire d'Organogenèse Expérimentale (LOEX) used a self-assembly approach for a corneal substitute. Ascorbic acid is used to stimulate the secretion of collagen and other ECM molecules by dermal fibroblast cells. Resulting sheets of matrix macromolecules are stacked together to form a

stroma, allowed to further integrate in culture, and then an epithelium is seeded on top of the stack. These constructs show excellent corneal morphology and cells express appropriate tissue-specific markers. The primary drawback is the time needed to produce enough transplantable material rapidly for transplantation. More recently, Carrier *et al.* (Carrier et al. 2008) followed up with a new self-assembled model comprising a stroma consisting of human corneal and dermal fibroblasts. The authors contend that the combination of the corneal and dermal fibroblasts was more conducive to the formation of a well-differentiated epithelium that showed higher re-epithelialization rates than just corneal fibroblasts alone. They showed that this model reproduced the microanatomy of the native human cornea. In addition, this model was able to reproduce a mechanistically accurate wound healing process. This suggests that this model could be used as a tool for studying wound healing, screening bioactive factors that could modulate wound healing or as a pre-screen prior to animal testing (Carrier et al. 2008).

Guo *et al.* (Guo et al. 2007) characterized the ECM macromolecules deposited by primary human corneal fibroblasts in such self-assembled corneal substitutes. The average culture took four weeks to produce a multi-layered construct about 36 μm thick. These constructs were highly cellular and are morphologically similar to the stroma of mammalian corneas, with multiple, parallel layers of cells and small fibrillar ECM arrays. The fibrils and collagen, were approximately 27 to 51 nm, with a mean of 38.1 ± 7.4 nm, compared to the 31 ± 0.8 nm reported in adult human corneas (Meek and Leonard 1993).

1.5.5. Biomimetic Corneal Implants

Since type I collagen is the dominant biopolymer found in the human cornea (70% dry weight), and is amenable to modification, it has been investigated for its use as a scaffold for artificial cornea construction. Type I collagen scaffolds have been used previously to culture human corneal stromal fibroblasts. It was observed that the cell scaffold interactions caused a change in the mechanical properties of the gels, as well as the permeability of the gels when cultured *in vitro* (Borene et al. 2004; Crabb et al. 2006). This indicated the remodeling of the matrix by the stromal cells changed the properties to be more like the natural stroma. Resultant tissue had a lamellar like microstructure following 21 days of incubation, as compared to its initial spongy structure.

Our laboratory have developed various collagen-based corneal substitutes that have been successfully implanted as either deep lamellar grafts, or full thickness implants into mice, rabbits, guinea pigs, dogs and pigs. These gels can be fabricated to the appropriate dimensions and curvatures, which allow for transmission of 90% or higher of white light. Collagen sources have included both porcine and bovine extracted collagens, as well as the more current use of recombinant human collagen. To make the gels mechanically strong enough to permit suturing, and resist biodegradation, crosslinking, co-polymerization and development of interpenetrating networks have been used. We recently demonstrated that a simple type I collagen-based cornea stroma mimic (fabricated by crosslinking porcine collagen with 1-ethyl-3-(3-dimethylaminopropyl) carbodiimide hydrochloride (EDC) and N-hydroxysuccinimide (NHS)) could be successfully implanted into mini-pigs with stable host-graft integration (Liu et al. 2006). Without the use of post operative steroids, the implants

resisted any adverse inflammatory response, and were not rejected. At 12 months post implantation, the implants were integrated and optically clear. Histology showed that a regenerated, stratified, epithelium covered the surface of the implant, with proper barrier function and tear film restoration. Stromal cells were observed to enter into the implant. Of importance, it was observed that corneal nerves had re-innervated the implant, through *in vivo* confocal microscopy (IVCM), as well as through transmission electron microscopy (TEM). Nerve density found in the implanted corneas was at levels similar to the contralateral control. Mechanically, corneas harvested from implanted eyes mimic normal pig corneas in key mechanical properties. Generally, mechanical properties of implants were found to be either similar or superior to the ones for control pig corneas.

We have also shown that synthetic materials can be combined with our collagen based corneal alternatives, in order to enhance interaction with the host cornea. By incorporating an artificial polymer, poly(N-isopropylacrylamide-coacrylic acid-coacryloxysuccinimide) into our collagen corneal alternatives, we were able to modify the gels to include the laminin derived pentapeptide, YIGSR into the matrix (Li et al. 2005). Upon deep lamellar keratoplasty implantation into mini pigs, it was observed that the incorporation of YIGSR into the corneal alternatives had a significant effect on nerve regeneration, which was shown through restoration of corneal touch sensitivity within a six week period, compared to allografts.

1.6 Research Summary

1.6.1 Rationale

Due to the increase in the need for human donor corneas to replace damaged corneas, the need for artificial corneas has also risen. It is known that a sensory nerve supply is important for optimal tissue function in both normal and wounded corneas. However, current keratoprostheses are not designed to permit reinnervation and often lead to complications with graft acceptance. By creating a tissue engineered artificial cornea comprised of collagen, which is the main ECM molecule found in the cornea, this will lead to better graft integration. Our laboratory has shown previously that this can be utilized for a partial thickness replacement of the cornea, but further work needed to be performed to increase the properties to make it suitable for full thickness implantation, and ultimately for human transplantation.

1.6.2 Hypothesis

My hypothesis is that an ECM scaffold consisting of collagen will likely contribute to wound healing and regeneration, and allow gradual remodelling through integration with host cells and permit reinnervation. Synthetic materials will be used to reinforce the mechanical strength.

1.6.3 Thesis Objectives

1. To investigate *in vitro* the suitability of gel formulations to be amenable to transplantation
2. To develop a tissue engineered artificial cornea for partial thickness and full thickness keratoplasty that permits regrowth of corneal cell types and nerves *in vivo*.
3. To test the reinnervated cornea for normal nerve activity following implantation.
4. To create an artificial cornea that can be clinically accepted for human transplantation.

1.6.4 Research Approach

This summary of the research approach is given to direct the progression through the following chapters (collection of manuscripts).

Manuscript 1: Functional innervation in tissue engineered models for *in vitro* study and testing purposes.

The innervated *in vitro* corneal model that was described in Suuronen *et al.* (Suuronen et al. 2004) was further characterized for toxicological testing purposes. The artificial cornea was fabricated with type I rat tail collagen crosslinked with glutaraldehyde. It contained human derived immortalized corneal cell types (epithelial cells, stromal cells and endothelial cells) and was innervated by a chicken dorsal root ganglion. The inclusion of nerves in the model resulted in a thicker stratified epithelium, and the formation of a mucin layer. Innervation also provided greater protection to the epithelium from chemical irritants,

measured through epithelial cell death. A differential response in the nerve fibres was assessed by 2 photon microscopy measurement of internal sodium concentration to various chemical stimuli. Combined, the epithelial cell death, and the differential changes in internal sodium concentration of the nerves, allows for an *in vitro* model to assess the toxicology of potential ocular irritants. Ultimately, it was shown that the artificial cornea permitted innervation, and that this allowed for a functional model for toxicology testing, and led to the rationale for creating an artificial cornea comprised of type I collagen.

Manuscript 2: Regeneration of corneal cells and nerves in an implanted collagen corneal substitute.

Our lab's previous work on *in vitro* corneal models, led to the creation of artificial corneas based on crosslinked type I porcine derived collagen (Li et al. 2003; Liu et al. 2006) as well as methodology and rationale for *in vitro* testing to determine suitable gel formulations for implantation. In this manuscript, we utilized high concentration collagen (10% w/v) crosslinked with a watersoluble carbodiimide crosslinker for implantation and progressive recruitment of autologous cells, to promote functional integration with the host tissue. We also developed a novel non toxic method for labelling the implants that wouldn't interfere with light transmission, but would allow for visualization of the implant within the host tissue. Following twelve months implantation into pigs, it was shown through histology, *in vivo* confocal microscopy, and TEM, the successful regeneration of host corneal epithelium, stroma and nerves. Nerve density and corneal mechanical properties were observed to be comparable to the unoperated control after twelve months. The labelling method was shown to be effective and monitoring the integration of the tissue engineered

cornea within the host tissue. Therefore, this implantable ECM mimetic allowed seamless and stable integration of host tissue, as well as gradual remodelling.

Manuscript 3: Collagen-phosphorylcholine interpenetrating network hydrogels as corneal substitutes.

While partial thickness (lamellar) keratoplasties are performed, the majority of transplantations are still performed through penetrating keratoplasty. Our previous studies have involved successful lamellar transplantation of our artificial corneas, but these have not been amenable to full thickness implantation, due to their lower mechanical strength, compared to the native cornea. In this article, we explored the use of incorporating a biomimetic monomer, 2-Methacryloyloxyethyl phosphorylcholine (MPC), as an interpenetrating network with type I porcine collagen. The resultant artificial corneas showed an increase in mechanical properties compared to non-MPC containing corneas, and retained the biointeractive properties, despite the known anti-adhesive properties of MPC. The gels showed increased resistance to collagenase and ultraviolet light degradation. Upon implantation into pigs, stable integration with the host tissue was observed after 12 months, showing the regeneration of corneal cell types and nerves into the implants.

Manuscript 4: Regeneration of Functional Nerves Within Full Thickness Collagen-phosphorylcholine Corneal Substitute Implants in Guinea Pigs.

The type I collagen MPC gels that were previously used for lamellar keratoplasties showed an improvement in their mechanical properties, and were deemed suitable for full thickness implantation into guinea pigs. Following implantation, the grafts remained stable,

but were translucent for a month, and cleared after 5 weeks implantation. The implants showed complete regeneration of corneal epithelium, stroma, and nerves after six months. While the operated corneas showed a return to normal sensitivity, as monitored through aesthesiometry, the nerves were tested through electrophysiology. General nociceptive units reinnervating corneal implants showed only slightly different properties from unoperated corneas, presenting a slightly increased spontaneous impulse firing and a slightly delayed response to natural stimulation (mainly to chemical stimuli). These results are similar to corneas that have undergone microkeratome lesions, similar to those that occur during a LASIK operation.

Manuscript 5: Tissue Engineered Recombinant Human Collagen-based Corneal Substitutes for Implantation: Performance of Type I versus Type III Collagen.

Our previously designed artificial corneas have all been based upon animal derived collagen for implantation. While they have been shown to promote corneal regeneration of corneal cells and nerves when implanted into pigs, there was a low level of immunogenic reaction when implanted xenogeneically into mice (Liu et al. 2007). Since the ultimate goal is clinical implantation into humans, there is also the risk of safety concerns with the use of animal derived collagen, including the potential for disease transmission. In this study, we utilized type I and type III recombinant human collagen produced in yeast cells. While type I collagen is the predominant form found in the cornea, type III is present, and has the advantageous feature of forming more tightly packed gels, as a result of smaller fibril diameter. These gels were found to have better optical and mechanical properties compared to the type I porcine collagen MPC gels that were used in the previous manuscript, as well as

having better optical properties. Upon implantation into pigs, both gel types supported corneal epithelial cell proliferation and stratification, as well as innervation. The use of recombinant human collagen has allowed us to develop a wholly synthetic, biomimetic artificial cornea, that is free of safety concerns regarding the use of animal source proteins. It also allowed us to proceed to human clinical testing.

1.7 Summary

As the medical need for artificial corneas has risen, the importance of creating an implant that allows for integration with the host's cells, and permits reinnervation has become apparent. By fabricating artificial corneas from collagen, the predominant polymer found in the native cornea, we have observed stable implantation and regrowth of functional, corneal cell types. Furthermore, by utilizing recombinant human collagen, we have addressed the concerns regarding animal based proteins, and have created a synthetic biomimetic implant that is suitable for human implantation.

Chapter 2
2.1 Manuscript 1

Functional Innervation in Tissue Engineered Models for *in vitro* Study and Testing Purposes.

Toxicol Sci. 2004 Dec;82(2):525-33. Epub 2004 Sep 1

Functional Innervation in Tissue Engineered Models for *in vitro* Study and Testing Purposes.

Erik J. Suuronen[1], Christopher R. McLaughlin[1], Peter K. Stys[2], Masatsugu Nakamura[3], Rejean Munger[1], and May Griffith[1,4]

[1]University of Ottawa Eye Institute, Ottawa Health Research Institute – Vision Centre, and Department of Cellular and Molecular Medicine, University of Ottawa, 501 Smyth Rd., Ottawa, Ontario, K1H 8L6, Canada, [2]Ottawa Health Research Institute – Division of Neuroscience, University of Ottawa, Ottawa, Ontario, K1Y 4E9, Canada, [3]Santen Pharmaceutical Company Ltd., Ikoma-shi, Nara, 630-0101, Japan

Emails: EJS: esuuronen@ohri.ca; CRM: chmclaughlin@ohri.ca; PS: pstys@ohri.ca; MN: nakamuram@santen.co.jp; RM: rmunger@ohri.ca

[4]Corresponding author

email: mgriffith@ohri.ca; phone: (613) 737-8899, ext. 74011; fax: (613) 739-6070

Running title: Innervation of *In vitro* Models

Suggested section: *In vitro* toxicology and alternative testing

Co-author Contributions to Manuscript

Suuronen, Eric

Dr. Suuronen , now an Assistant Professor at the University of Ottawa Dept. of Surgery, was a PhD student at the time of the publication. He was responsible for designing, coordinating and conducting the experiments.

Stys, Peter.

Dr. Stys was a neuroscience professor at the University of Ottawa, and performed the electrophysiology experiments on the tissue engineered corneal nerves, as well as the developer of the ImageTrak Software that was used for data analysis.

Nakamura, Masatsugu

Dr. Nakamura, General Manager of Cornea R&D, Santen Pharmaceuticals Inc., performed the immunoassays for Substance P. He contributed to the development of efficacy tests for the *in vitro* model.

Munger, Rejean

Dr. Munger, an optical physicist at the University of Ottawa Eye Institute, performed optical characterization of the tissue engineered cornea, as well as confocal microscopy for visualization of structures in the tissue engineered cornea.

Griffith, May

Dr. Griffith supervised both Erik and myself. She helped us with the overall experimental design, troubleshooting and edited our manuscript.

My contributions to this manuscript were to assist in finishing up the publication. I tissue engineered corneal constructs, treated them with various drugs, and performed live/dead

assays, analyzing the data, and creating the figures for that section. My photomicrograph was selected for the cover publication for the journal.

Abstract

The biotech industry is rapidly expanding and the emerging field of tissue engineering is projected to have a high impact in the near future. Recently the field of cellular, drug, and prosthetic delivery has melded with the field of tissue engineering to make simulated tissues. In addition to their roles as tissue substitutes for transplantation, these simulated tissues may provide more accurate models and environments for toxicology testing and the study of peripheral nerves. The current study demonstrates the importance of innervation, in general, for the function of engineered tissues. We observe that the presence of nerves in a tissue engineered (TE) human cornea model enhances the growth of the epithelium and the formation of its protective mucin layer. Innervation also confers protection to the epithelium from chemical insult, as determined by the level of post-treatment epithelial cell death. We demonstrate differential responses of the nerves to chemical stimuli by changes in intracellular sodium as measured by 2-photon microscopy. Two-photon imaging techniques also allow for the visualization and study of the fine sensory axon fibers within the 3-dimensional tissue. This work demonstrates a role for innervation in the protective quality and function of the engineered tissue, and the potential to use the nerves themselves as indicators of the severity of an insult. These results are important to consider for the development of any optimized TE models for *in vitro* study and testing purposes.

KEYWORDS

innervation / tissue engineering / toxicology / 2-photon microscopy / cornea

Introduction

Tissue engineering can be described as the fabrication of biological or semi-synthetic living tissue in the laboratory for use as replacement tissues for damaged or diseased body parts. It is a rapidly growing area and the development of tissue engineered (TE) substitutes for several organs including liver, heart, skin, kidney and cornea is being pursued by a variety of approaches (Atala and Lanza, 2002). Although optimal function, homeostasis and wound healing of many tissues is dependent in part on proper peripheral sensory innervation (Anand et al., 1996; Gover et al., 2003; Holzer, 1988), the restoration of innervation to engrafted engineered tissue replacements is often overlooked.

In addition to their proposed use for transplantation, TE substitutes also have the potential to provide new toxicology models. While tissues need to confer function as a replacement to a tissue or organ in transplantation, for use as an *in vitro* model for testing, TE tissues need to mimic key morphological, physiological and biochemical properties of the natural tissue as closely as possible. Like TE constructs for transplantation, *in vitro* models may also require a sensory nerve supply to be mechanistically accurate. With the ban on animal testing for development of consumer products expected to expand from Europe (European Union Directive 76/768/EEC) into North America, the demand for *in vitro* methods for safety and efficacy testing (e.g. toxicology and drug testing) is expected to grow. Currently, the response of many TE constructs to external stimuli is overly sensitive, possibly due to a lack of innervation (Griffith et al., 1999).

We recently described the fabrication of a fully innervated *in vitro* human corneal model that demonstrated basic anatomical and physiological similarities to the natural tissue *in situ* (Suuronen et al., 2004). In this paper we demonstrated the importance of nerve-target

cell interactions in the overall functioning of the engineered tissue. In the present study, we examined in greater detail the contributions of sensory innervation to the function of an engineered tissue. In particular, 2-photon confocal microscopy was used to examine in detail the reaction of fine, terminal sensory nerves to external stimuli.

The innervated TE cornea demonstrates the potential of TE substitutes to serve as replacements to animals for *in vitro* ocular toxicology testing or as models for the study of fine sensory nerves. The cornea's transparency, structural simplicity and the importance of innervation for optimal corneal function make it an ideal tissue model for studying sensory nerve function. We observe that innervation affects the characteristics of the TE cornea and confers protection to its epithelium from chemical insult. Two-photon imaging techniques allow for the visualization and study of the fine sensory axon fibers within the 3-dimensional tissue. We demonstrate differential responses of the nerves to chemical stimuli by changes in intracellular sodium as measured by 2-photon microscopy. This work demonstrates a role for innervation in the protective quality and function of the engineered tissue, and the potential to use the nerves themselves as indicators of the severity of an insult. These results are important to consider for the development of any optimized, TE substitutes for *in vitro* use, either as toxicology models or for the study of peripheral sensory innervation.

Materials and Methods

Corneal Construction

Corneal cell lines with extended life spans (Araki-Sasaki et al., 2000; Griffith et al., 1999) were used. Innervated corneas were constructed as described previously (Suuronen et al., 2004), with modifications. Briefly, collagen matrix was prepared using blended neutralized,

type I rat tail collagen (0.3% (w/v), Becton-Dickinson, Oakville, Canada) and chondroitin-6-sulfate (CS) (1:5 w/w of these biopolymers; Sigma, Oakville, Canada) and cross-linked with glutaraldehyde (0.02% (v/v)). Residual aldehyde groups were inactivated by reaction with 0.8% aqueous glycine (w/v) solution. This collagen-CS mixture is liquid at 4°C, but forms a hydrated gel at 37°C. Corneal stromal matrix was constructed with a laminin (Becton-Dickinson) gradient of increasing concentrations from bottom to top of 0, 10 and 20 μg/ml. Cornea stromal cells (3 X 10^4 cells/ml) were added to all three layers of the collagen mix, nerve growth factor (NGF; 100 ng/ml; Sigma) was added to the top layer of collagen mix, and the stromal matrix was layered within 0.4 μm pore culture inserts (Costar, Fisher Scientific, Ottawa, Canada). Dorsal root ganglia (DRG), isolated from chick embryos (E8.0) were used for the neural source. These were embedded within the collagen matrix (Fig. 1) after an overnight pre-incubation in M199 at 37°C to remove contaminating fibroblasts. The construct was then thermo-gelled by incubation at 37°C for 2 hours. Corneal epithelial cells at a density of 70 cells/mm^2 were then seeded onto the construct, which was supplemented with a modified SHEM medium (Jumblatt and Neufeld, 1983) containing 2% B27 and 1% N2 nerve growth supplements (Life Technologies, Burlington, Canada) with 1 nM of retinal acetate (RA; Sigma). At epithelial confluence, the constructs were maintained at an air liquid interface for up to 10 days until used.

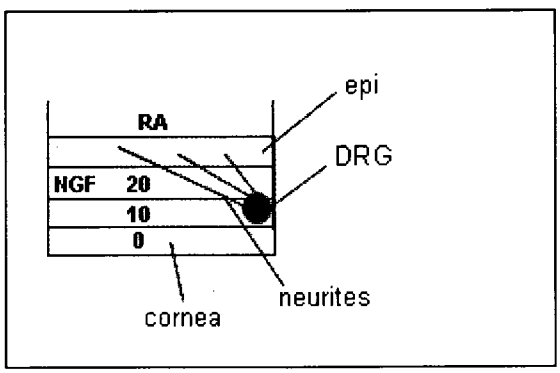

Fig. 1. TE cornea construction and neurite growth promotion. The schematic shows the TE cornea with DRG (black circle) placed in the stromal matrix and neurites extending into the corneal epithelium (epi). Note the concentration gradient of laminin (0, 10, 20), NGF in the uppermost stromal layer and RA in the medium.

Immunohistochemistry

For Na^+ channel labeling, whole tissue constructs were fixed in 4% paraformaldehyde (PFA) for 30 minutes, then rinsed in 0.05 M Tris buffer, pH 7.4 and permeabilized in Tris buffer containing 0.3% Triton X-100. After blocking with 10% normal goat serum in buffer, tissues were incubated overnight at 4°C with the primary antibody, monoclonal anti-PAN sodium channel antibody (Sigma), at a dilution of 1:250 in Tris buffer containing 2% normal goat serum. The tissues were rinsed thoroughly in Tris buffer and reacted with a 1:100 dilution of goat anti-mouse Alexa 488 secondary antibody (Molecular Probes, Eugene, OR), in Tris buffer for 90 minutes prior to visualization.

For neurofilament staining, PFA-fixed whole tissue constructs (as above) were permeabilized by treatment with a detergent mix (150 mM NaCl, 1 mM ethylenediamine tetraacetic acid, 50 mM Tris, 1% Nonidet P-40, 0.5% sodium deoxycholate and 0.1% sodium dodecyl sulphate (Brugge and Erikson, 1977)) for 20 minutes. Constructs were rinsed in Tris buffered saline (TBS), and incubated with the primary antibody, anti-neurofilament 200 (Sigma; diluted 1:40 in TBS containing 0.6% carrageenan and 0.3% Triton-X 100 (TCT)) overnight at 4°C. The constructs were then rinsed in TBS and incubated with a Cy3-conjugated secondary antibody (1:200 in TCT; Amersham, Baie D'Urfé, Canada) for 150 minutes at room temperature (RT). Negative controls were incubated without the primary antibody. Positive controls included staining for DRG and neural tube explants. Nerves were visualized under fluorescence confocal microscopy.

For visualization of live nerve fibers, acetoxymethyl (AM) ester (Calcein AM, Molecular Probes) was used. Calcein AM, provided at a concentration of 1 mg/ml in dimethylsulfoxide (DMSO), was diluted into 0.1 M phosphate-buffered solution (PBS) to a 1

μM working concentration. The dye was loaded into whole tissue for 30 minutes at RT, and then the constructs were rinsed several times in PBS prior to visualization with the 2-photon laser-scanning microscope. Imaging was performed on a Nikon C1 laser scanning microscope custom-modified for 2-photon operation (Risdale et al., 2004). Fluorophores were excited by a 800 nm pulsed beam from a Ti:sapphire laser (Tsunami, Spectra Physics, Mountainview, CA), and fluorescence collected by a 60x 1.0NA immersion objective. Images were analyzed using ImageTrak software written by PKS (http://www.ohri.ca/stys/imagetrak).

Effects of innervation on the epithelium

To investigate the effects of innervation on stratification of the epithelium and the production of its protective mucin layer, constructs with and without DRG were cultured. TE corneas were fixed in 4% PFA (as above) at 2, 4, 6, and 10 days, and subsequently sectioned. For examination of epithelial thickness, sections were processed for routine hematoxylin and eosin (H&E) staining. The thickness of the epithelium was measured in six random sections for each sample, and the mean was calculated for each time point. For mucin staining, sections were rinsed in TBS and incubated with the primary antibody, anti-MUC16 (CA125; Dako) at a dilution of 1:50 in TCT overnight at 4°C. The constructs were then rinsed in TBS and incubated with a Cy2-conjugated secondary antibody (1:200 in TCT; Amersham) for 150 minutes at RT. Negative controls were incubated without the primary antibody. Nerves were visualized under fluorescence confocal microscopy.

Live/dead staining

Innervated and non-innervated constructs were exposed to either A) artificial tears (Alcon) for 1 hour; B) a mixture of 8.5% Tween-80 surfactant and 1.5% ethanol in SHEM medium for 1 hour; C) 500 μM ouabain for 30 minutes or D) 0.5 % sodium dodecyl sulfate (SDS) for 1 minute. Controls consisted of untreated constructs with and without nerves. Quantification of the viability of epithelial cells was done using the acridine orange/ethidium bromide method combined with Hoescht staining for nuclear labeling. The dye mix consisted of 0.1 M PBS containing 100 μg/ml of acridine orange, 100 μg/ml of ethidium bromide and 250 μg/ml of Hoescht dye. Following the surfactant treatment, a volume of 10 μl of the dye mix was added to the inside of each insert, which contained 500 μl of medium. The constructs were stained for 5 minutes and images were captured for epithelial cell counts. Dead cells (apoptotic or necrotic) stained red and live cells stained green. The numbers of live and dead epithelial cells were counted within 5 different areas per construct. Dividing the number of dead cells by the total number of cells, and multiplying by 100 determined the percentage of epithelial cells that were dead. A Two-way ANOVA was performed to determine statistical significance set at $P < 0.05$.

Sodium visualization

For these experiments, some modifications were made to the methods for cornea construction. In the experiments described above, the constructs were removed from their inserts for visualization by the 2-photon system. Due to the soft nature of the stromal matrix, there was a slow expansion of the tissue over time, which did not affect single image capture. However, for time series experiments, there is a requirement for tissue stability over time.

The dimensions of the inserts described above do not allow for observation by the 2-photon system, and for this reason, constructs were transferred to organ tissue culture dishes (Becton-Dickinson) and surrounded by a ring of collagen-CS mixture, prepared as described above. This insert has dimensions suitable for use with the 2-photon system apparatus and its use ensures that the field of interest is maintained over time. However, it cannot be used for long-term culture due to its lack of a membrane, essential for proper nutrient delivery within the corneal stroma.

Constructs within organ culture dishes were loaded with the Na^+-indicator dye, sodium-binding benzofuran-isophthalate (SBFI; 10 μM) and the solubilization facilitator Pluronic F-127 (both from Molecular Probes), at a ratio of 1:1, prepared just before use. Loading time was 4 hours and the tissues were rinsed in PBS several times after loading. The construct was transferred to a custom-built chamber and immersed in artificial cerebral spinal fluid (aCSF; in mM): NaCl, 126; KCl, 3.0; $MgSO_4$, 2.0; $NaHCO_3$, 26; NaH_2PO_4, 1.25; $CaCl_2$, 2.0; and dextrose, 10). Axons within the construct were imaged before and 10 minutes after application of the following treatments: aCSF, 14 μM dimethyl sulphoxide (DMSO), 50 μM veratridine, 500 μM ouabain or 50 μM veratridine + 500 μM ouabain at RT. Because DMSO is used at a final concentration of 14 μM to reconstitute veratridine and ouabain, its effect on Na^+ retention was also tested to examine the possibility that it contributes to any observed response in the treatment groups. The signal from the Na^+-insensitive background was subtracted from the Na^+-dependent signal to give the Na^+ fluorescence intensity. The subtraction of fluorescence intensity at time = 0 from the intensity at time = 10 minutes, and multiplication by 100, yielded the percent change of Na^+ fluorescence intensity over time.

Data were then normalized (relative percentage increase for each test group over the aCSF control).

Statistical Analyses

Statistical analysis of epithelial thickness was performed using two-way multivariate analysis of variance (2-way ANOVA) procedures. Independent samples (n = 3) were used for each time point. The endpoint included in the 2-way ANOVA was number of cell layers and significant differences between group means were analyzed using Tukey's Studentized Range Test (Tukey's test). For epithelial cell viability, a 2-way ANOVA was performed with independent samples for each treatment condition (n = 4). The endpoint consisted of the percentage of the epithelial cells that were dead and Tukey's Test was used to analyze significant differences between group means. For analysis of Na^+ concentration within the nerves (n = 4), a 1-way ANOVA was performed with the normalized relative change in SBFI fluorescence as the endpoint and with Tukey's Test to analyze significant differences between group means. For all comparisons, $P < 0.05$.

Results

Effects of Innervation on TE Corneal Properties

Innervation stimulated epithelial growth in TE corneas. After 2 days of culture, there was no difference in the thickness of the epithelium between innervated and non-innervated TE corneas. However, at 4, 6, and 10 days of culture, greater epithelial thickness (~twofold greater after 10 days) was observed in the epithelium of innervated TE corneas compared with non-innervated controls (Fig. 2A). The presence of the protective mucin layer, as determined by staining for MUC16, on the surface of the epithelium was greater in innervated TE corneas versus non-innervated controls. At 2 and 4 days of culture, mucin

staining was not observed in either innervated or non-innervated constructs (data not shown). However, at 6 and 10 days, mucin staining was more intense on the surface of the epithelium of innervated, compared to very little staining of non-innervated TE corneas (Fig. 2B-E). The mucin layer of the TE corneas from either group was not uniform, but instead displayed a patchy expression.

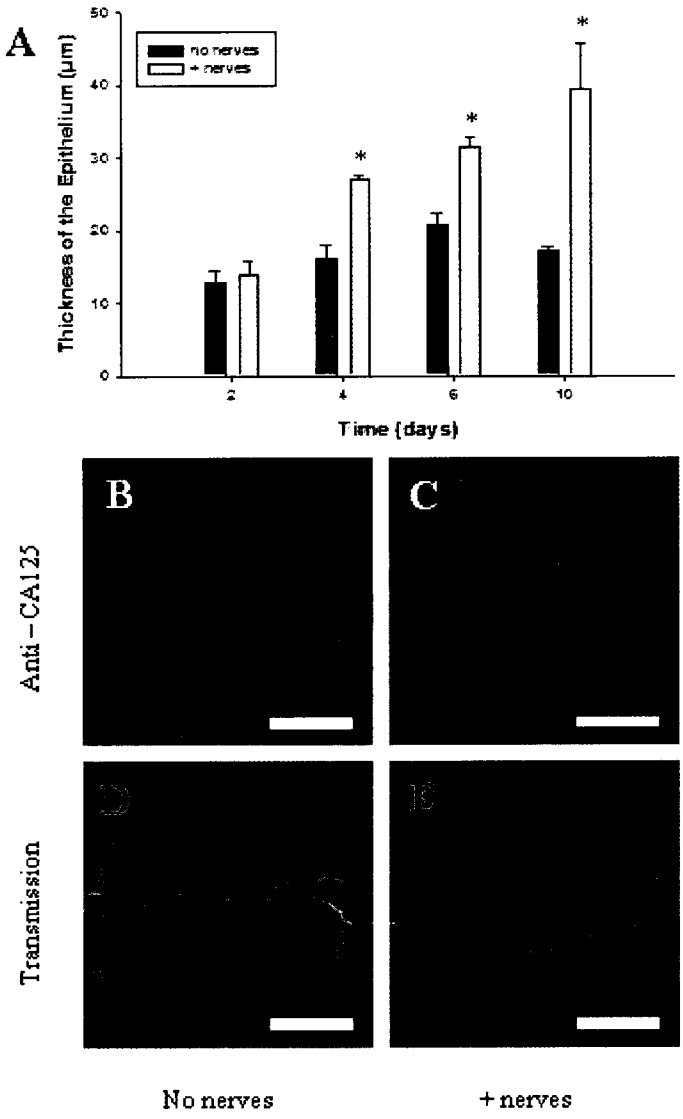

Fig. 2. Effects of innervation on properties of the epithelium. **(A)** The thickness of the epithelium (mean ± se, n=3) for innervated and non-innervated TE corneas over time. *Significantly different from non-innervated control at day 4, 6, and 10 (two-way ANOVA; P<0.05). **(B, C)** Mucin staining at 6 days in non-innervated **(B)** versus innervated **(C)** TE corneas. **(D, E)** Respective transmission images of overlying images. Scale bar = 60 µm.

Effects of Innervation on Epithelial Cell Viability

In untreated control and artificial tears-treated constructs, no difference in the percentage of dead cells was observed between innervated and non-innervated TE corneas (Fig. 3A). However, when treated with the three chemical irritants (surfactant/ethanol mix, ouabain and SDS), significantly greater cell death was observed in the epithelium of non-innervated TE corneas (Fig. 3A). The percentage of dead cells was approximately 4- and 2.5-times greater in non-innervated constructs compared to their innervated counterparts in the surfactant/ethanol- and SDS-treated groups, respectively. For the ouabain-treated group, cell death was approximately 2-times greater in non-innervated compared to innervated TE corneas (Fig. 3 B-G). In addition, within the innervated group, epithelial cell death was significantly greater in SDS-treated TE corneas versus all other treatments, and cell death in both the surfactant/ethanol and ouabain-treated TE corneas was significantly greater than in controls and those treated with artificial tears (Fig. 3A).

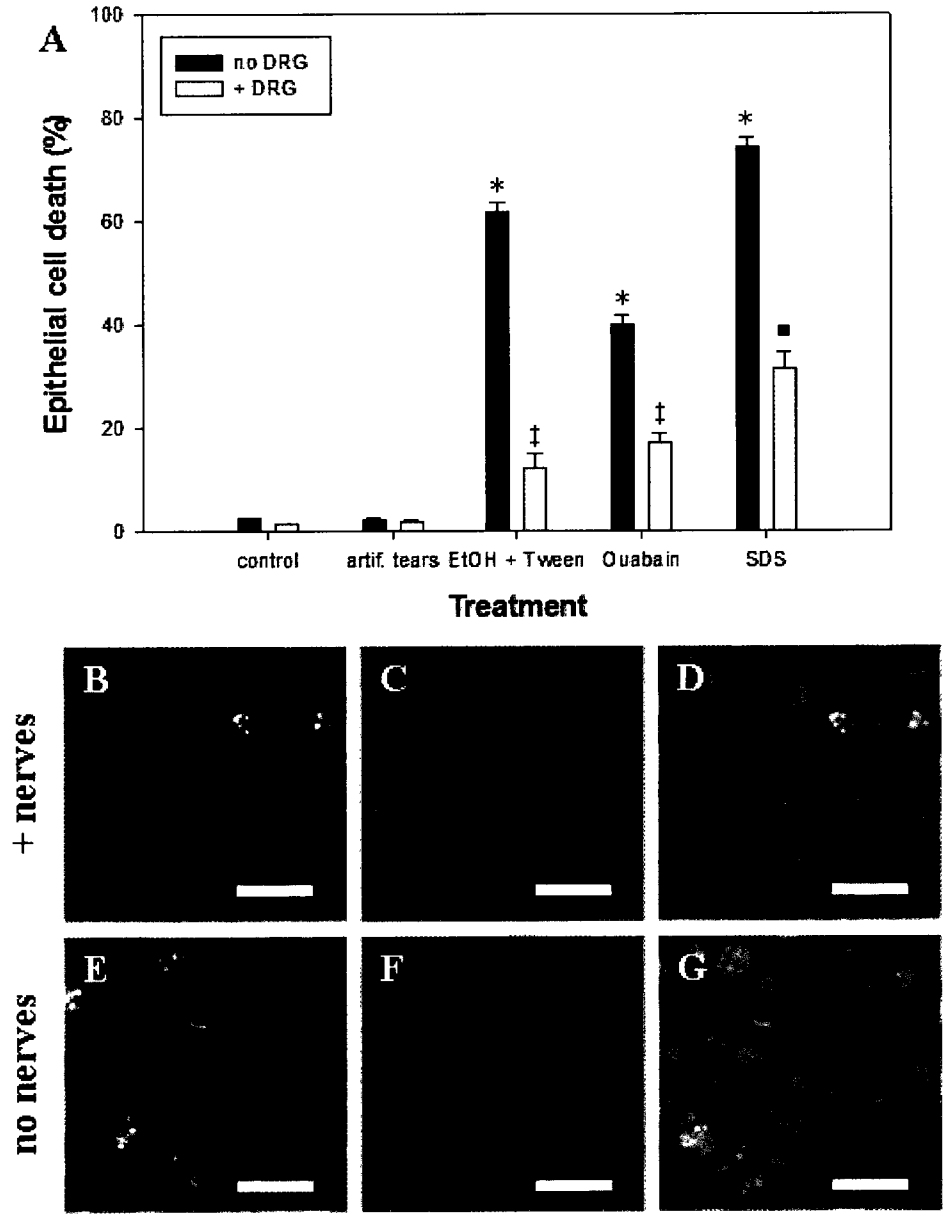

Fig. 3. Epithelial cell viability. (**A**) Epithelial cell death in innervated versus non-innervated TE corneas, with different treatment substances. *Significantly different from innervated group within treatment, ▪significantly different from other treatments within innervated group, and ‡significantly different from control and artificial tears-treated TE corneas within innervated group (two-way ANOVA; $P<0.05$). (**B-G**) Examples of live-dead stained constructs: Epithelium of innervated (**B-D**) and non-innervated (**E-G**) TE corneas after ethanol treatment. (**B** and **E**) live/dead stain, where red indicates dead cells; green indicates live cells; (**C** and **F**) Hoescht nuclear stain; and (**D** and **G**) combined images. Scale bar = 25 μm.

Nerve study using 2-photon confocal microscopy

Two-photon microscopy showed extensive nerve growth throughout the corneal construct (Fig. 4A), from the epithelium through to a depth of 200 μm into the stromal matrix of the tissue. Characteristic of human corneal nerves, both smooth and beaded nerve fibers were observed within the epithelial cell layers and the plexus network just below the epithelium (Fig. 4B). The feasibility of visualizing live TE corneas was also assessed. For this, constructs were loaded with the cell viability indicator, Calcein AM. This dye allowed for the observation of nerves within both the epithelium and the stroma (Fig. 4C and D), and its retention by both epithelial cells and nerve fibers indicated that these cells were alive and healthy.

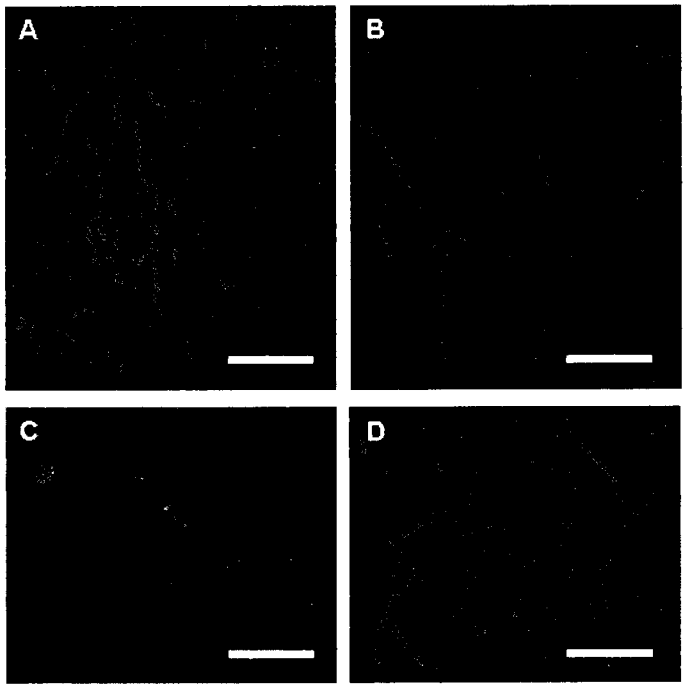

Fig. 4. Visualization with 2-photon microscopy. (**A**) NF-200 staining revealed extensive innervation throughout the TE cornea. (**B**) Both smooth and beaded fibres were observed in the anterior regions. (**C**, **D**) Calcein AM staining revealed healthy epithelial cells and nerve fibres within the epithelium (**C**) and stroma (**D**). All panels are composite images with the different colors representing different depths within the tissue. Scale bar = 200 μm (**A**); 50 μm (**B**); 20 μm (**C**); 150 μm (**D**).

Immunohistochemistry revealed the presence of Na^+ channels, co-localized with neurofilament staining and expressed ubiquitously along the length of the fibers in the TE cornea (Fig. 5A). This indicated that the nerves possessed the machinery necessary to mediate changes in $[Na^+]_i$. Differential changes in $[Na^+]_i$ were observed in TE corneas treated with DMSO, the Na channel opener veratridine, ouabain (an inhibitor of Na-K-ATPase), or veratridine and ouabain together (Fig. 5B). Changes in $[Na^+]_i$ were significantly different between veratridine and ouabain treatments and both elicited greater Na^+ accumulation within the fibers compared to DMSO treatment. In addition, simultaneous treatment with veratridine and ouabain resulted in a greater change in internal Na^+ than either treatment alone.

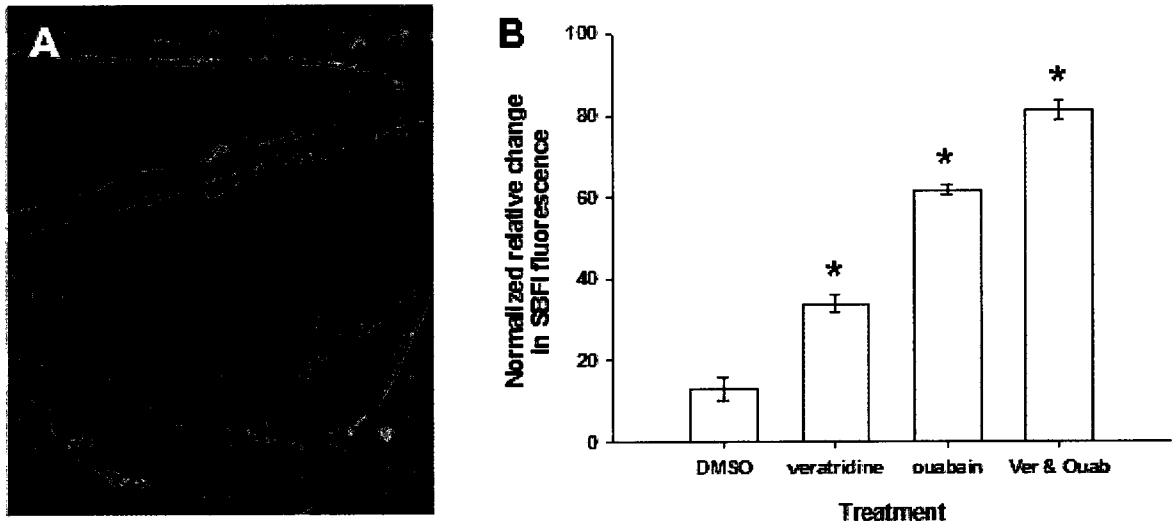

Fig. 5. Na^+ channels and internal Na^+ concentration in nerve fibres of the TE cornea. (A) Na^+ channels (green/yellow) were distributed uniformly along the length of the nerve fibres. Scale bar = 40 μm. **(B)** The normalized relative change in fluorescence of SBFI, a Na^+ indicator, in response to treatment with various chemicals. *Significantly different from all other treatment groups (one-way ANOVA; $P<0.05$), including the control (not shown; control normalized to 0).

Discussion

Currently, the standard for measuring the potential ocular toxicity of manufactured consumer products is the Draize or the low volume live rabbit ocular irritancy tests (Daston and Freeberg, 1991). However, the reliability and relevance of these methods obtained from non-human tissues remains questionable (Symposium Proceedings, technical committee on alternatives to animal testing, 1996). In addition, there is a push for a ban on the use of live animals for testing, which has already been implemented in Europe (European Union Directive 76/768/EEC). This has resulted in the need to develop alternatives for the safety and efficacy testing of consumer products. While several promising models have been developed, including organ culture systems (Gautheron et al., 1992; Xu et al., 2000), and cultures or tissue equivalents using immortalized cell lines (Griffith et al., 1999; Kruszewski et al., 1997), there still is no validated alternative method. These models all share a common factor that may contribute to their failure as absolute, suitable replacements for the rabbit eye tests: lack of innervation.

The tissue engineered *in vitro* human cornea model we developed addresses the issue of innervation. This is important, considering that the optimal function, maintenance and wound healing of many tissues are dependent, in part, on proper peripheral sensory innervation (Anand et al., 1996; Gover et al., 2003; Holzer, 1988). The effect of nerves on the properties of the epithelial and stromal cells in our model was previously demonstrated (Suuronen et al., 2004). Here, we provide evidence that these effects contribute to the overall function of the model and its response to chemical irritation. We showed that the presence of nerves in the TE cornea was able to protect the epithelium from chemical irritation. After

exposure to a surfactant/ethanol mixture, ouabain, or SDS epithelial cell death was approximately 4, 2 and 2.5 times greater, respectively, in non-innervated corneas compared to innervated constructs. This was consistent with the demonstrated role for nerves in the homeostasis of corneal epithelial cells in the human cornea (Araki-Sasaki et al., 2000). SDS, the harshest of the treatment conditions, elicited the greatest level of cell death within the constructs. In addition, both ouabain and surfactant/ethanol, considered more mild irritants, caused greater cell death in the epithelium compared to TE corneas after application of medium or artificial tears, both non-irritants. Therefore, these data demonstrated differential cell death to different treatment substances, showing evidence of sensitivity of the innervated TE cornea. The nerves affected several properties of the epithelium, which in turn may affect the response of the TE cornea to chemical irritation.

One property of the epithelium that can play a role in its protective function is its thickness. Differences in ocular irritancy are related to differences in the extent of initial injury (Maurer et al., 1999) and a thicker epithelium will provide greater protection from insult. The thickness of the epithelium in innervated TE corneas was greater compared to non-innervated constructs over a culture period of 10 days. Trigeminal denervation of the rabbit cornea has been previously observed to cause thinning of the epithelium (Araki et al., 1992) and increased permeability (Beuerman and Schimmelpfennig, 1980). Therefore, it is possible that the significantly greater epithelial cell death observed in non-innervated corneas upon chemical treatment could be due to greater permeation of the toxicant through the epithelium as a result of its compromised thickness. The thinning of the epithelium in denervated corneas has been associated with impairment of epithelial cell adhesion (Araki et al., 1994). We observed compromised adhesion in non-innervated TE corneas after

prolonged chemical assault (data not shown). These differential adhesive properties between innervated and non-innervated constructs may also have been a factor in the response of the cornea to chemical insult. Overall, the presence of nerves in the TE cornea model promoted an increase in epithelial thickness, which can potentially reduce permeability and enhance the resistance to chemical irritation.

The production of the mucin layer is another protective mechanism of the epithelium of several tissues including the cornea. Mucins are glycoproteins produced by the surface epithelia (Gipson et al., 1995) that lubricate the surface to provide a barrier for the cell membrane and protect the cornea from desiccation (Argueso and Gipson, 2001). Mucin 16, in particular, is expressed by corneal surface epithelia (Argueso et al., 2003) and its expression is altered in the conjunctival epithelia of patients who suffer from dry eye syndrome (Danjo et al., 1998), a condition related to compromised innervation (Stern et al., 1998). In the TE cornea model, innervation promoted greater production of the mucin layer by the surface epithelia, as determined by MUC16 staining. This demonstrated that innervation plays a role in the expression of mucin in the cornea, as had already been observed in the surrounding conjunctiva (Danjo et al., 1998), and that this model could be used to study the pathology of dry eye syndrome. In addition, the lessened mucin production in non-innervated TE corneas may contribute to the observed increase in epithelial cell death. Without a protective surface layer of mucin, the permeation of the chemical assault may be deeper and cause greater damage to the epithelial tissue of the cornea. Although not investigated, deep chemical penetration could also affect stromal cell viability and alter its interaction with the epithelium, itself important for the health of the epithelial cells (Wilson et al., 1999).

Overall, the presence of nerves within the TE cornea promoted greater epithelial thickness, improved production of the protective mucin layer, and as was shown previously, increased epithelial and stromal cell proliferation, and had an effect on epithelial wound healing (Suuronen et al., 2004). These are important considerations in the development of tissue-engineered models for toxicology testing, as they have an effect on the resistance and protective qualities of the epithelial surface, and hence can alter sensitivity of the model. The lack of innervation may be responsible, in part, for the failure of the current alternative toxicology models to provide undisputed, suitable, replacements for rabbit eye tests.

While innervation affected the protective quality and function of the engineered tissue, we also investigated the effects of irritation on the nerves themselves. Upon stimulation, the nerve transmits its message by the generation of action potentials (APs), which propagate via the axon to the central nervous system to cause the sensation of pain (Brock et al., 1998), and to the nerve terminals to cause the release of neuropeptides (Unger, 1990). AP generation occurs by the opening of Na^+ channels, and the subsequent Na^+ current and depolarization of the membrane. Variability of the Na^+ current has been correlated with the amplitude of the nerve response (Johansson, 1994). In the TE cornea, differential changes in internal Na^+ concentration $[Na^+]_i$ were observed within the nerve fibers when treated with different chemicals, including veratridine and ouabain. While veratridine operates by a Na^+ channel-dependent mechanism, ouabain does not, yet both elicited responses that can be detected by changes in $[Na^+]_i$. Ouabain, in addition to its role as a Na^+ regulator, has been shown to induce cell death of epithelial cells, including those of renal and lens origin (Lichtstein et al., 1999; Pchejetski et al., 2003) and of neuronal cells (Xiao et al., 2002). Although further study of the relationship between sensory neuronal toxicity and tissue

irritancy is needed, these results provide proof of concept that this technique could be used to detect the effects of irritants that do and don't act via Na^+ channels. As discussed, the health of the epithelium is dependent on innervation, therefore, differential $[Na^+]_i$ responses within nerves could be used as indicators of the severity of an insult in this model, by both the assessment of intensity and depth of permeation.

One mechanism by which sensory nerves exert their influence on their environment is by the release of neuropeptides. This may include the release of substance P (SP) neuropeptide (Maggi, 1991), which can be regulated by Na^+ channel-dependent mechanisms. The differential changes in $[Na^+]_i$ observed in nerves of the TE cornea could translate to differential responses of the nerve (Johansson, 1994), including release of SP. Therefore, the release of SP can be correlated to $[Na^+]_i$, which can be regulated by the influx of Na^+ into the fibers through the Na^+ channels of the axonal membrane. Unlike the highly focal distribution of Na^+ channels in myelinated axons, Na^+ channels present in the TE cornea were distributed continuously along the membrane of the nerve. This pattern is typical of nonmyelinated sensory axons (Black et al., 2002), the type of axons found in the cornea, and supports continuous (as opposed to saltatory) conduction along these axons. We previously observed differential release of SP upon treatment with various chemicals, including veratridine (Suuronen et al., 2004). Veratridine causes the release of SP by opening Na^+ channels and depolarizing the membrane (Neubert et al., 2000). Therefore, it appeared as though the nerves within the TE corneal model behaved in a manner typical of native corneal nerves. Described simply, the application of a chemical irritant to the innervated TE cornea caused changes in $[Na^+]_i$, and through the depolarizing effects, SP neuropeptide is released, which then can affect epithelial properties (Gallar et al., 1990; Nishida et al., 1996). The magnitude

of the response would depend on the level of irritation. As mentioned above, some chemicals operate by Na^+ channel-independent mechanisms, but can still result in the release of neuropeptides, including SP (Keen et al., 1982). This mechanism of SP release was also observed in the TE cornea in previous work (Suuronen et al., 2004). Therefore, our innervated TE cornea model could be developed for use as an alternative to animals in ocular toxicity testing. The degree of cell death, the levels of neurotransmitter release and the response of the nerves themselves could all be used to ascertain the toxicity of potential ocular irritants.

Knowledge of sensory nerve function has come largely from monolayer or thin tissue slice culture systems that do not fully replicate the *in vivo* environment. The emergence of tissue engineering is providing new, more relevant models for the study of tissues and the function of their constituent cells. The re-creation of both the natural environment and the appropriate interactions between nerves and their target tissues make tissue-engineered systems superior to traditional cell culture, and more accessible and easier to manipulate than *in vivo* models for the study of innervation. However, the investigation of sensory nerve fibers, in particular, and their terminals and interactions with their target tissue is difficult in whole, 3-dimensional tissue due to their miniature size. As such, their study has been limited and many of their functional properties remain unclear. Two-photon microscopy has significantly enhanced the visualization and study of fine nerve fibers (Malone et al., 2002; Rose et al., 1999). Two-photon imaging has the advantage of high resolution imaging at substantial depths in intact tissue, despite the scattering effects of thick tissues (Denk and Svoboda, 1997), and it minimizes the effects of photobleaching and photodamage (Denk et al., 1995). Combining the technologies of tissue engineering and 2-photon microscopy

presents methodologies that can improve our current knowledge of nerve behavior and function, using more accurate, 3-dimensional models.

Nerves within the TE cornea, stained with anti-NF 200 (fixed tissue) or Calcein AM (live tissue), were easily visualized in the epithelium and the stroma using the 2-photon system. Typical of corneal nerves (Müller et al., 1997), both smooth and beaded fibers migrated within the epithelium. The 2-photon system allowed observation of the nerves from just below the epithelial surface to a depth of 200 μm within the stroma. The retention of the Calcein AM dye, an indicator of cell viability, provided evidence that both the nerve and epithelial cells were alive and healthy. Therefore, 2-photon microscopy enables the study of the fine sensory structures within the TE cornea and their interactions with their target tissue. These results emphasize the potential of combining the technologies of tissue engineering and 2-photon microscopy to improve our current knowledge of nerve behavior and function.

In summary, we demonstrate the importance of nerves in an engineered tissue with respect to its function. The presence of nerves affects several properties of the TE cornea, including its epithelial thickness, its production of the protective mucin layer, and its proliferation of epithelial and stromal cells, all of which can affect both its maintenance and its sensitivity. These are important considerations for the development of any optimized, TE substitutes for transplantation that promote the growth of nerves from the host tissue, or for *in vitro* use, either as toxicology models or the study of innervation.

Acknowledgements

We thank E. Codèrre for technical assistance; and Drs. R. Beuerman, D. Carlsson and I. Micu for helpful insights. Supported by grants (227212-1999; 227951-01) and studentship

from NSERC Canada, and extramural grant from Santen Pharmaceutical Co. EJS is a Fellow of the International Foundation for Ethical Research (IFER). PKS is supported by a Career Investigator Award from the Heart and Stroke Foundation of Ontario.

Chapter 3

3.1 Manuscript 2

Regeneration of Corneal Cells and Nerves in an Implanted Collagen Corneal Substitute.

Cornea. 2008 Jun;27(5):580-9.

The previous manuscript detailed that an artificial cornea constructed from type I collagen was an excellent *in vitro* alternative to normal corneal tissue. It provided the basis for the development of stronger and tougher cornea substitutes for transplantation which promoted nerve in-growth. This manuscript showed that carbodiimide crosslinked type 1 porcine collagen implanted through partial thickness keratoplasty model in mini pigs allowed for regeneration of corneal cell types and nerves, and the implants retained optical clarity after 12 months. Mechanical testing showed that after 12 months implantation, the corneal substitute had seamlessly integrated with the host tissue, showing comparable mechanical properties to unoperated control corneas. *In vivo* confocal microscopy showed the regeneration of sub-epithelial nerves at comparable densities to control eyes.

Regeneration of Corneal Cells and Nerves in an Implanted Collagen Corneal Substitute

C.R. McLaughlin[1,2], B.Sc., P. Fagerholm[3], M.D., PhD., L. Muzakare[1], M.Sc. N. Lagali[1], Ph.D., J.V. Forrester[4], M.D., L. Kuffova[4], M.D., M.A. Rafat[1], M.Sc. Y. Liu[5], Ph.D., N. Shinozaki[6], Ph.D., S.G. Vascotto[1],Ph.D., R. Munger[1], Ph.D., and M. Griffith[1,2] Ph.D.,

[1]University of Ottawa Eye Institute, 501 Smyth Road, Ottawa, ON, Canada K1H 8L6

[2]Dept. of Cellular and Molecular Medicine, Univ. of Ottawa, 451 Smyth Road, Ottawa, ON, Canada K1H 8M5

[3]Linköping University Hospital, Dept. of Ophthalmology, Se-58185 Linköping, Sweden.

[4]Department of Ophthalmology, University of Aberdeen, Aberdeen, AB25 2ZD, Scotland, UK

[5]National Research Council Canada, 1200 Montreal Road, Ottawa, ON,Canada, K1A 0R6

[6]Tokyo Dental College-Ichikawa General Hospital Cornea Centre, Ichikawa, Chiba, Japan

Grant Information:

NSERC Canada Grant STPGP 246418-01 and Canadian Stem Cell Network grant to MG, NSERC studentship to CRM, NSERC Visiting Fellowship to YL and CIHR Canada post-doctoral fellowship to NL.

Corresponding Author:

May Griffith, PhD

University of Ottawa Eye Institute

The Ottawa Hospital – General Campus

501 Smyth Road

Ottawa, ON K1H 8L6, Canada

Phone: (613) 737-8899, ext. 74011

Fax: (613) 739-6070

E-mail: mgriffith@ohri.ca

Co-author Contributions to Manuscript

Fagerholm, Per

Dr. Fagerholm, an ophthalmologist at Linköping University Hospital in Sweden, was responsible for the implantation of the artificial corneas into the pigs.

Muzakare, Lea

Lea Muzakare was a research technician in the Griffith Laboratory who aided in the tissue processing of the pig implants.

Lagali, Neil

Dr. Lagali, was a post doctoral fellow in the Munger Lab who was mainly responsible for the *in vivo* confocal microscopy images.

Forrester, John and Kuffova, Lucia

Drs. Forrester and Kuffova are ophthalmologists at the University of Aberdeen in Scotland. They trained me to perform corneal transplants in mice and how to harvest samples for analyses.

Rafat, Mehrdad

Dr. Rafat, was at the time a PhD student in the laboratory who performed the mechanical testing of the corneal substitutes.

Liu, Yuwen

Dr. Liu, was at the time, a post doctoral fellow in the laboratory who developed the formulation for the artificial cornea.

Shinozaki, Naoshi

Dr. Shinozaki, Director of the Ichikawa General Hospital Cornea Center in Japan, provided some of the electron microscopy images of the implanted corneas

Vascotto, Sandy

Dr. Vascotto, at the time, was a post doctoral fellow, who helped contribute to the development of the biotin staining method for labelling the implants.

Munger, Rejean

Dr. Munger, an optical physicist at the University of Ottawa Eye Institute, aided in analysis of the in vivo confocal microscopy images of the artificial cornea.

Griffith, May

Dr. Griffith was my supervisor, and helped guide me in designing the study, arranged for my surgical training and helped me with the manuscript preparation.

Abstract

Purpose: Our objective was to evaluate promotion of tissue regeneration by extracellular matrix (ECM) mimics, using corneal implantation as a model system.

Methods: Carbodiimide crosslinked porcine type I collagen was moulded into appropriate corneal dimensions to serve as substitutes for natural corneal ECM. These were implanted into corneas of mini-pigs after removal of the host tissue, and tracked over 12 months, by clinical examination, slit-lamp biomicroscopy, *in vivo* confocal microscopy, topography and aesthesiometry. Histopathology and tensile strength testing were performed at the end of 12 months. Other samples were biotin-labeled and implanted into mice to evaluate matrix remodeling.

Results: The implants promoted regeneration of corneal cells, nerves and the tear film, while retaining optical clarity. Mechanical testing data was consistent with stable, seamless host-graft integration in regenerated corneas, that were as robust as the untreated contralateral corneas. Biotin conjugation is an effective method for tracking the implant within the host tissue.

Conclusions: We show that a simple ECM mimetic can promote regeneration of corneal cells and nerves. Gradual turnover of matrix material as part of the natural remodeling process, allowed for stable integration with host tissue and restoration of mechanical properties of the organ. The simplicity in fabrication and demonstrated functionality shows potential for ECM substitutes in future clinical applications.

Key words: Cornea, ECM (extracellular matrix), collagen, nerve regeneration, mechanical properties, hydrogel

Introduction

The extracellular matrix (ECM) has been considered to be a biologically active scaffold that provides the appropriate microenvironment for stem or precursor cells to differentiate during embryonic development of an organ. During wound healing, ECM macromolecules help provide cues for repair and regeneration, serving as "regeneration templates". [1]

The human cornea is the optically clear, tough covering in front of the eye that is responsible for majority of light transmission and refraction to the retina for vision. It is avascular and has three main cellular layers. It can be viewed as a hydrated ECM containing stromal cells that is sandwiched by an outer stratified, non-keratinizing epithelium and inner single-layered endothelium. [2] The ECM is composed mainly of collagen, being over 70% dry weight of the cornea. [2] Due to its superficial location, the cornea is prone to disease or trauma that may result in the loss of transparency, and, where irreversible, permanent vision loss occurs. Corneal opacification from disease or trauma is estimated to affect over 10 million people worldwide [3] and is generally treated by transplantation with grafts from donor human corneas. A variety of materials, both synthetic, such as poly(2-hydroxyethyl methacrylate) [4], as well as naturally derived materials, have been utilized for the production of artificial hydrogels for developing tissue engineered scaffolds. [5, 6] The need to develop viable alternatives to human donor tissue results from the current and projected shortage of acceptable corneas for transplantation worldwide driven by age demographics, increases in incidence of transmissible diseases (like HIV, hepatitis and CJD) and the increasing use of laser vision corrective surgery (which renders corneas unsuitable for grafting).

The relative structural simplicity and the medical need, makes the cornea an ideal model for the development of a simple, single component ECM mimic. Collagen has previously been utilized by other groups for uses in the cornea, such as intracorneal lamellar implants [7], and as contact lens for wound healing and drug delivery. [8] We recently reported the development of a corneal substitute that comprised a matrix of crosslinked type I collagen that promoted corneal cell and nerve repair over 6 months. [9] The hydrated matrix (hydrogel) was stabilized by cross-linking through chemical reactions mediated by water soluble carbodiimides (WSCs). The WSCs themselves do not become incorporated as part of the final cross-links in these collagen hydrogels, so there is no possibility of toxic substance release into tissues from subsequent cross-link break down after hydrogel implantation. [10] The aim of the present study was to examine the effectiveness of collagen hydrogels as ECM substitutes in promoting stable, tissue regeneration over 12 months in pigs, and to determine the mechanisms involved. We show that the gradual remodeling of the implanted matrix allowed for seamless host-graft integration, in restoration of both optical and mechanical properties, as well as restoration of innervation patterns.

Materials and Methods

Fabrication of Corneal Implants

Corneal implants were fabricated as previously described. [9] Briefly, 0.5 to 1 ml aliquots of 10 % wt/wt solutions of acid freeze dried, porcine type I atelocollagen (Nippon Ham, Tskuba, Japan; Koken, Japan) were adjusted to pH 5 by titration with 1.0 M aqueous NaOH, followed by thorough mixing. A 10% (wt/vol%) aqueous solution of 1-ethyl-3-(3-dimethylaminopropyl) carbodiimide (EDC) and its co-reactant N-hydroxysuccinimide (NHS) (both from Sigma Aldrich, Oakville, Canada) at a 2:1 molar ratio of EDC to NHS, was rapidly and completely mixed into the collagen solution to crosslink the collagen. The final homogenous solution was dispensed into contact lens moulds and cured at 100% humidity. After curing (21°C for 24 h and then at 37°C for 24 h), cross-linked, cornea-shaped hydrogels (12 mm diameter, 500 μm thickness) were removed from each mould and washed with 0.1 M phosphate buffered saline (PBS) (Sigma Aldrich, Oakville, Canada) at 4°C. Each implant was individually stored in PBS containing 1% chloroform to maintain sterility. For pig implantation, a 6 mm disc was trephined from the center of each cornea shaped matrix. For mouse implants, flat sheets (100 μm thickness) were made using the above procedure and 2.0 mm discs were trephined out of the hydrogel sheets for implantation.

Biotin Labelling

Corneal implants intended for mouse implantation were incubated in a 25 μg/mL solution of biotinamidohexanoic acid 3-sulfo-N-hydroxysuccinimide ester, sodium salt in PBS, for 1.5 hours at 37°C. The ratio of the biotin reagent to free primary amine groups (on lysine repeats) in collagen was 1 to 3 equivalents. Any unreacted biotin was chemically

neutralized by incubating implants for 30 min in Dulbecco's Modified Eagle Medium (DMEM, Sigma Aldrich) plus 10% fetal bovine serum (FBS), after which samples were thoroughly washed and stored in PBS at 4°C.

Implantation Method

Implants into animals were performed with ethics approval from the University of Ottawa (Protocol EI-5), and in accordance to the Animal Licence Act (UK) and in accordance with ARVO guidelines for the treatment of animals. Corneal matrices (500 μm thick and 6 mm diameter) were implanted into one cornea each of eight Göttingen mini-pigs by deep lamellar keratoplasty (DLKP), with overlying sutures (Zirm retention bridge suturing). [11] This involved trephining to a depth of 500 μm, and removing this tissue, which left 190 μm of the host stroma. Prior to surgery and at all follow up examinations, animals were anaesthetized with i.m xylazine (5 mg/kg; Rompun®, Bayer Leverkusen, Germany) and ketamine (30 mg/kg; Ketalar®, Parke-Davis, Barcelona, Spain). The non-operated, contralateral eyes served as controls. The penetrating keratoplasty technique for Balb/C mice was modified by the authors from previously published procedures. [12] Briefly, a biotin labeled collagen hydrogel was implanted into each cornea of a mouse, after removal of the host cornea, and sutured in place with a continuous 11-0 suture (Ethicon™, Edinburgh, UK) that was retained for the duration of the experiment. Animals were given antibiotics and analgesics over the first week postoperatively, with no steroids administered. Sutures were removed three weeks postoperatively for the pigs, and remained in place for the mice.

Clinical Evaluation

In pigs, follow-up examinations were performed on a daily basis for the first week following surgery, and then weekly. Slit-lamp examinations were performed to verify corneas were optically clear, followed by Schirmers' test to assess tear film, and sodium fluorescein staining to determine epithelial integrity and barrier function. Intraocular pressure measurements were measured with a Tono-Pen XL Tonometer (Medtronic Solan, Minneapolis, MN) also taken to show that proper aqueous humour flow was occurring, and not being blocked by the implants. Aesthesiometry was used to test for nerve touch sensitivity in the control and surgically operated eye using a Cochet-Bonnet aesthesiometer (Handaya Co., Tokyo, Japan), as previously described.[13]

Using a fluorescence profilometer (Par Vision Systems, New Hartford NY), corneal topographies were measured *in situ* on both control and operated eyes in the pigs preoperatively and at twelve months postoperatively. Average refractive powers were derived from the measured topographies of each cornea. The average power (P_{ave}) was calculated by transforming the radius of curvature (R in meters) of the best-fit sphere from the topography into dioptric power with $P_{ave} = (n-1)/R$ using a refractive index (n) of 1.337. *In vivo* confocal microscopy (IVCM) examination (ConfoScan3, Nidek, Japan) was utilized to assess nerve in-growth, and to determine total corneal thickness in live animals (depth difference between epithelial and endothelial images.[14] IVCM was used to obtain full-thickness corneal scans of control and operated eyes from all 8 pigs at three examination periods: preoperatively, and then at 6, and 12 months postoperatively. For the mice, corneas were examined *in vivo* three times per week under the operating microscope for signs of rejection, including increased corneal opacity and thickness. [15]

Assessment of Nerve Regeneration and Remodelling

Serial IVCM images of the central area of each cornea were acquired at 10μm depth intervals (image size: 440 × 330μm, w × h) through the entire thickness of the cornea and several scans were made through each cornea. All images containing at least one nerve fiber bundle (NFB) were identified and indexed according to depth from the corneal epithelial surface. Nerve tracing software, Image J and Neuron J (NIH) [16] were used to determine the total length of all NFBs (including branches) in each image. The NFB density for each image was calculated as the total NFB length divided by the image volume (image area × confocal depth of field) and expressed as $\mu m/mm^3$. The NFB density has been used as a method by other groups [17] to evaluate normal and postoperative human corneal innervation *in vitro*. For statistical analysis, IVCM images were grouped by image depth from the epithelial surface into three corneal regions: sub-basal (20-50μm), representing the nerves of the subbasal nerve plexus found at the basal epithelium and sub epithelial regions, anterior stroma zone 1 (60-100μm) and anterior stroma zone 2 (110-150μm). Below a depth of 150 μm, there was a marked infrequency of nerves in the control cornea to allow for a proper comparison to be made. However, the scarcity of innervation in the mid and deep stroma is consistent with findings for normal human corneas.[18] The total length of NFBs from all image depths within each region was calculated and divided by the sample volume of the region to determine the NFB density in a region, expressed in $\mu m/mm^3$. This metric has been used by Calvillo et al. [18] to assess postoperative NFB length changes in three-dimensional corneal volumes. NFB densities in control and operated eyes were compared at each examination period in each corneal region using the Mann-Whitney rank sum test for non-normally distributed data. A P-value of less than 0.05 was considered statistically

significant. Differences in NFB density with time were determined by Friedman's repeated measures analysis of variance on ranks. Pairwise differences adjusted for multiple comparisons were determined using the Student-Newman-Keuls procedure. All statistics were calculated using SigmaStat v3.1 software for Windows (Systat Software Inc., Point Richmond, CA). This method of image analysis has recently been described in further detail by our group. [19].

Histopathological Evaluation

The pigs were sacrificed 12 months postoperatively. Corneas with implants, and control unoperated corneas were processed for routine histopathological examination after H&E staining. Mice were sacrificed at one, two, four and eight weeks postoperatively (n=3 at each time point). Eyes were fixed in 4% paraformaldehyde in 0.1M PBS and then processed for routine cryosectioning.

Immunohistochemistry

For visualization of biotin tag, 10 μm sagittal sections through whole mouse eyes were pre-treated with 0.1% H_2O_2 in PBS for 30 minutes to block endogenous peroxidase activity. They were then washed in PBS and blocked for 1 hour in 3% BSA in PBS prior to application of a 1:1000 dilution (in blocking solution) of streptavidin-horseradish peroxidase (HRP, Amersham Biosciences) for 3 hours at room temperature. Following washing, sections were reacted with diaminobenzidine (DAB; Roche) for visualization of the resulting dark brown biotin-HRP-DAB complexes. Sections were examined using differential interference contrast microscopy.

To visualize the epithelium for the pig and mouse sections, slides were blocked in 4% FBS in 0.2% Triton X-100 in TBS pH 8.0, with 50 mM NH_4Cl to reduce background

fluorescence. An antibody towards pan-cytokeratin (Z0622, DAKO, Mississauga, Canada) was applied at 1:400 in 0.2% Triton X-100 in TBS overnight at 4°C, washed with TBS, and visualized with a 1:600 dilution of CY2 conjugated anti-rabbit secondary and 1:10000 of DAPI to stain the nucleus and visualized using a Zeiss Axioscop 2. Macrophages were visualized using a 1:5000 dilution of F4/80 antibody (MCAP497, Serotec, Raleigh, NC, USA) . Other samples were stained with antibodies against collagen VII (Sigma C6805), smooth muscle actin (CMC533, Cell Marque, Hot Springs, AR), and procollagen (M38, Developmental Studies Hybridoma Bank, Iowa City, Iowa). They were first blocked in 5% FBS in PBS. Antibodies to Smooth Muscle Actin (1:100), Collagen VII (1:50) and Procollagen (1:20) were then applied overnight at 4°C in blocking solution plus 0.3% Triton X-100, washed with PBS, and visualized with a 1:400 dilution of CY2 conjugated anti-rabbit secondary.

For transmission electron microscopy (TEM), all samples were fixed in Karnovsky's fixative and osmium tetroxide, en bloc stained with uranyl acetate and embedded in epoxy resin. Thin sections were cut and stained to visualize corneal nerves.

Physical and Optical Characterization

The hydrogels utilized for implantation were tested for optical properties, permeability, water content and biocompatibility. Results were published in Liu et al. [9]

Mechanical Testing

After 12 months post-surgery, corneas with implants were harvested from three pigs and cut into dumbbell shapes with a 4 x 10 mm waist, which included the central implant area to ensure that the central gauge length of each tensile sample contained the maximum

area of the implanted gel. Tensile measurements were performed on the samples using an Instron Materials Testing System (model 5565) with a load cell of 500N capacity and pneumatic, rubber faced grips (model 2712, jaw pressure 5 bar), at a crosshead speed of 10 mm/min and an initial grip separation of 13 mm. To avoid breakage and slippage of the sample in the pneumatic jaws, the 6 mm wide tabs on the end of each dumb bell sample (mainly scleral tissue) were compressed with forceps, tamped dry to remove exuded medium, then coated with Dermabond™ (Ethicon, Somerville, USA), a fast curing, cyanoacrylate-based skin adhesive, and reinforced with tape on both sides. This method of sample mounting completely prevented jaw breaks and sample slippage. Samples were not stress preconditioned prior to testing to failure. Controls consisted of unoperated contralateral corneas.

The maximum tensile strength, elongation at this tensile maximum and Young's modulus for each sample were calculated from the raw stress-strain data, using the Instron's Bluehill software, and the initial cross-sectional area. Elastic (tangent) moduli were calculated from the quite linear part of the stress/strain curves found for all samples over the 0.15 to 0.30 strain range. This linearity has been reported previously for human corneas. [20] Tensile properties of the collagen hydrogel alone were similarily measured, on flat film cast from the cross-linking gel (500 μm thickness).

Results

Biotin Labelled Collagen Implants in Mice

Homogenous biotin labeling of collagen implants was confirmed by visualization of dark brown staining of serial sections through samples after chromophore development. The

covalent conjugation of biotin to the gels had no effect on optical clarity, and biotinylated matrices were found to be non-cytotoxic by *in vitro* testing (results not shown here). Non-implanted gels retained their biotin tag after 60 days at 37°C in culture media (data not shown). At one week postoperative, the biotinylated implant was largely intact, showing a distinct continuous edge between the implant and the epithelium (Fig. 1A) and between the implant and adjacent host stromal bed (not shown). The implant was completely covered by cytokeratin-positive epithelium (Fig. 1B). Several scattered macrophages were observed within the implant area (Fig. 1C). At two weeks postoperative, the overlying epithelium was further stratified (Fig 1D, E). In addition to macrophages (Fig 1F), biotin-labeled stromal cells were found around the implant (Fig. 1D). At four weeks and eight weeks post-operative, the implant showed evidence of initiation of remodelling as the implant edge was no longer continuous (Fig. 1G, J) and macrophages were still present (Fig. 1L). There were no macrophages in any of the unoperated control corneas (Fig 1O).

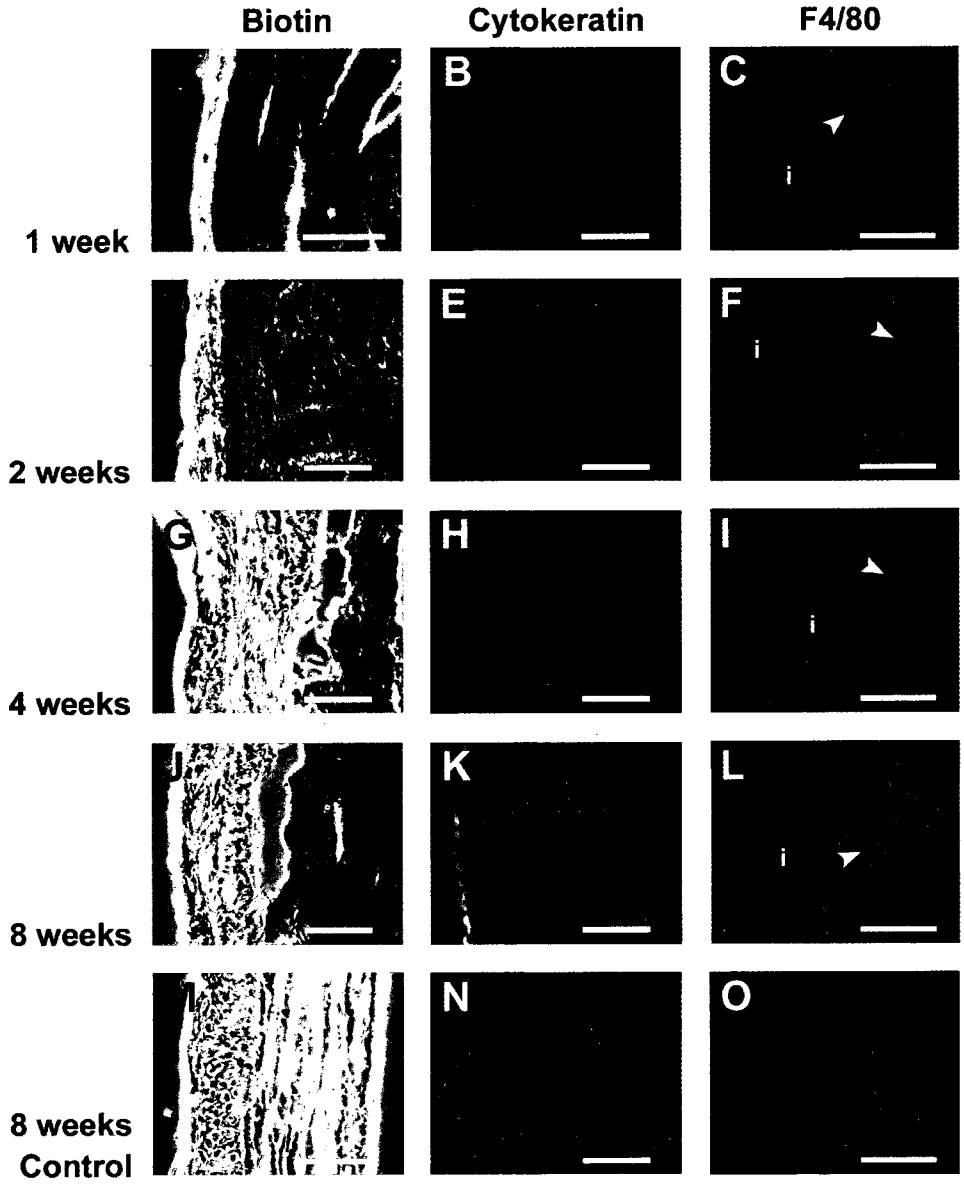

Fig. 1. Sections through biotinylated cornea substitutes implanted by penetrating keratoplasty into corneas of mice. (A-O) DIC images (A, D, G, J, M) and fluorescent staining for cytokeratin (red) and DAPI (blue) (B, E, H, K, N), and macrophages (C, F, I, L, O). (A-C) 1 week post implantation, showing biotin stained intact implant (A) covered by epithelium (B). Several macrophages are seen (arrowhead) (C). (D-F) 2 weeks post implantation, showing a further stratified epithelium (D,E), and the presence of macrophages (F), as well as biotin labelled stromal cells around the implant (D). (G-I) 4 weeks post implantation and (J-L) 8 weeks post implantation the edge of the implant is no longer continuous showing initiation of possible remodeling. (M-O) 2 month control cornea showing lack of DAB staining in the epithelium or stroma, and normal epithelial staining for cytokeratin (N), and lack of macrophages (O). Bars, 50 μm.

Implantation in Pigs and Clinical Evaluation

Implants in animals remained optically clear (Fig. 2B) which was confirmed clinically through slit lamp biomicroscopy. One animal had some very mild haze (+0.5 by slit lamp biomicroscopy) and a second animal had a discrete opacity at one of the suture points on the periphery. As previously published, slit lamp examination on non-labelled, implanted corneas of pigs showed re-epithelialization within the first postoperative week. [9] The absence of sodium fluorescein staining indicated that an intact epithelial barrier was restored and remained stable over 12 months. The Schirmer's test indicated the presence of a tear film comparable to the contralateral unoperated eyes as measured at 12 months. From preoperative topographical measurements, the refractive powers (P_{ave}) of the control and surgical eyes were not significantly different whereas postoperatively, the calculated P_{ave} of both the control and implanted eyes had significantly decreased, but the postoperative P_{ave} values of each control and its corresponding implanted eye were not significantly different. Touch sensitivity indicating nerve function was observed in operated corneas after 6 months postoperative [9, 21] and remained at 12 months.

Histopathological examination of sections through corneas with implants resembled those of unoperated controls, with a stratified epithelium and stroma with keratocytes arranged in lamellae (Fig. 2D) The epithelium was positively stained for pan-cytokeratin marker (Fig. 2F), similar to the epithelium of the unoperated contralateral controls (Fig. 2E). In addition, positive staining for type VII collagen, a marker for anchoring fibrils, was found in both unoperated control corneas (Fig. 2G) and corneas with implants (Fig. 2H). Insets (Fig. 2G, H) show corresponding TEM images of hemidesmosomes in the basal epithelial cells of control and operated corneas. Samples were negative for pro-collagen and anti-

smooth muscle actin, as with the controls, suggesting that stromal cells are not activated and no active collagen production was seen at this time-point. However, both H&E and TEMs reveal stromal cells within implant areas that were arranged in lamellae, similar to unoperated corneas. As well, H&E images did not show any fibrosis in the cornea after 12 months of implantation.

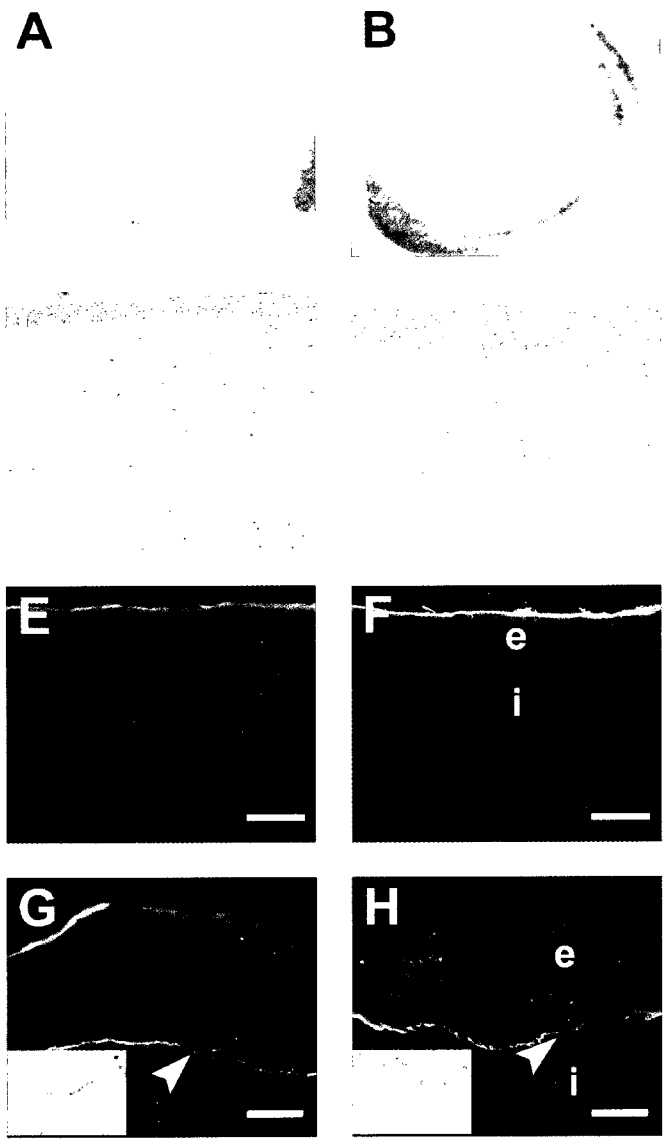

Fig. 2. Corneal implantation by lamellar keratoplasty in pigs at 12 months. (A): unoperated, contralateral cornea (B): optically clear operated cornea. (C-D): H&E staining of unoperated (C) and operated cornea (D), both showing a stratified epithelium over a stroma. (E-F) Cytokeratin staining showing the presence of a normal, differentiated, stratified, non-keratinizing epithelium on the unoperated (E) and operated cornea (F). (G-H) Collagen VII staining at the epithelial/stromal junction in the operated cornea (arrows) indicate the presence of anchoring fibrils in both operated (H) and control (G) corneas. Insets show TEM images of hemidesmosomes (arrowheads). Scale bars for C-F are 50 μm, scale bars for G-H are 40 μm. (e) denotes epithelium, (i) denotes implant.

In-growth of nerves into the implants was confirmed by IVCM (Fig. 3B,D) followed by immunohistochemical staining with an anti-neurofilament antibody (results not shown) and TEM. TEM images through the sub-epithelial region of the implanted site showed the presence of nerves containing both light and dense core vesicles typical of an axon (Fig. 3F,H). Similar nerve fibres were seen in unoperated control corneas (Fig. 3E,G).

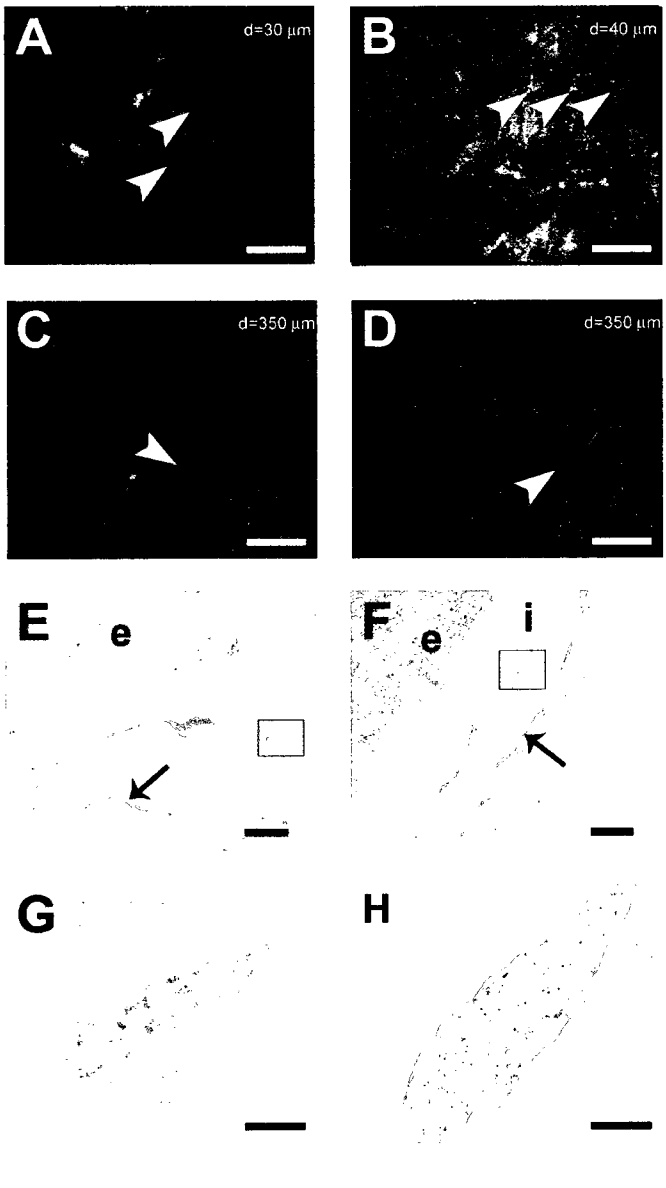

Fig. 3. IVCM and TEM images at 12 months from pigs. (A-D) *in vivo* confocal images. Regenerated nerves (arrowheads) can be seen sub-basally in both non-surgical (A) and operated cornea (B). In the deep stromal layer, deep nerves observed in the contralateral control (C) are also observed (arrowheads) in the operated cornea (D). (E-H) Postoperative regeneration of nerves in the tissue engineered cross sections of control and implanted corneas by TEM. (E) Unoperated cornea visualized using transmission electron microscopy showing normal epithelial stromal boundary and nerve fibre (boxed). The operated eye shows similar epithelial/stromal boundary (F), as well as re-innervation at 12 months (boxed). (G) Magnification of boxed inset from the control eye showing intact nerve. (H) Magnification of boxed inset from the operated eye showing a regenerated nerve, show the staining of light and dense vesicles. (A-D) Scale bars are 50 µm. (E-F) Scale bars are 5 µm. (G-H) Scale bars are 1 µm. (e) denotes epithelium, (i) denotes implant.

From IVCM images, nerve density in the sub-basal epithelial and stromal regions of the unoperated porcine corneas agrees well with values observed in normal human corneas. [17, 18] IVCM analysis of nerve density within the central implant region (Table 1 and Fig. 4) indicated a significant decline in sub-basal nerve density at 6 months relative to both the untreated contralateral cornea ($P<0.001$) and preoperative ($P=0.04$) levels, as no sub-epithelial nerves were detected in any operated eye at 6 months following surgery (Table 1 and Fig. 4D). Sub-epithelial nerves, however, recovered to preoperative ($P>0.05$) and control ($P=0.69$) densities at 12 months (Table 1 and Fig. 4F). Similarly, anterior stromal zone 1 nerve density had declined significantly in implants relative to controls by 6 months ($P=0.004$, Table 1 and Fig. 4D), with recovery to preoperative ($P>0.05$) and control ($P=0.9$) levels at 12 months (Table 1 and Fig. 4F). Contrary to declines in sub-basal and anterior stromal zone 1 nerve density, in the anterior stromal zone 2, nerve density in implants had increased significantly by 6 months (Fig 4D) relative to controls ($P=0.01$). This significant increase relative to controls persisted to 12 months ($P=0.04$), while nerve presence in the anterior stroma zone 2 of control corneas remained sparse (Fig. 4F).

Table 1. Nerve Density ($n = 8$)*

Location	Cornea	Months after surgery: Preoperative	6	12	Friedman's P-value†
Sub-basal epithelium	Operated	4.07 (2.68, 6.65) [4.73 ± 2.39]†	0 (0, 0)†	0.96 (0, 2.81) [1.36 ± 1.48]	0.04
	Control	3.58 (1.91, 5.26) [3.92 ± 2.51]	3.17 (1.63, 4.30)	1.51 (0.72, 2.98) [1.91 ± 1.77]	0.37
	Mann-Whitney P-value	0.57	< 0.001	0.69	
Anterior stroma zone 1	Operated	2.00 (1.15, 2.29) [1.84 ± 0.81]	0 (0, 0.72) [0.40 ± 0.58]	1.28 (0, 3.63) [1.89 ± 2.32]	0.052
	Control	1.19 (0.53, 1.81) [1.22 ± 0.77]	1.54 (0.84, 2.50) [1.70 ± 0.90]	2.33 (1.01, 3.03) [1.74 ± 1.57]	0.96
	Mann-Whitney P-value	0.11	0.004	0.9	
Anterior stroma zone 2	Operated	0.40 (0.22, 1.07)	5.33 (1.34, 6.48) [4.92 ± 3.94]	2.26 (1.21, 4.61) [3.02 ± 2.42]	0.12
	Control	0.79 (0.59, 1.14)	0 (0, 0.81) [0.65 ± 1.31]	0.20 (0, 0.85) [0.70 ± 1.14]	0.95
	Mann-Whitney P-value	0.22	0.01	0.04	

Data represents the nerve density (x 10^5 μm/mm^3) for each time point

* Median (interquartile range: Q25, Q75). Means and standard deviations are given in square brackets where data was normally distributed.

† Medians with the same symbol were significantly different from each other (Student-Newman-Keuls test).

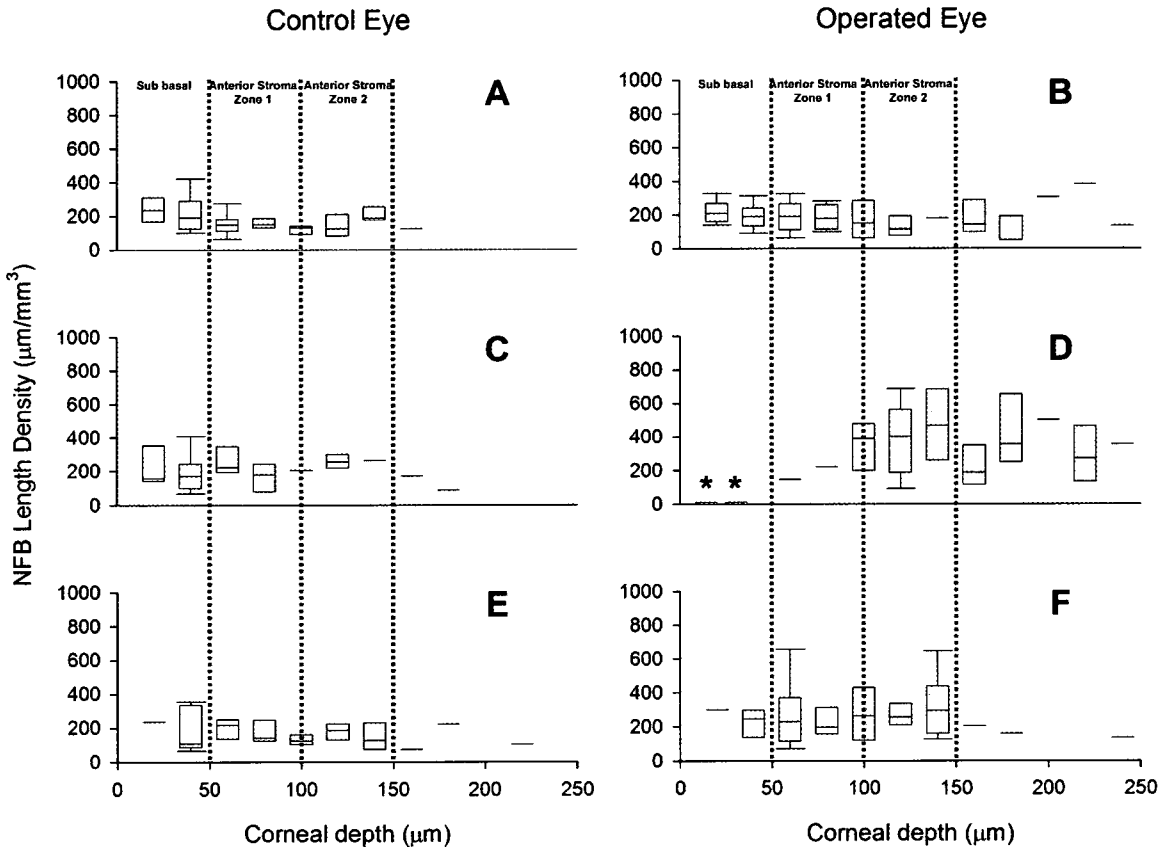

Fig. 4. Nerve fibre bundle length density calculated by analysis of serial *in vitro* confocal micrographs. (A-B) Preoperative densities showing similar NFB length density for control eye and operated eye. (C-D) 6 months post-surgery reveals the lack of innervation in the sub-epithelium following lamellar keratoplasty; asterisk (*) denotes significance of density from operated eye versus control. (E-F) 12 months post surgery shows NFB length density in the implanted returns to levels comparable to unoperated eye. Box plots are presented as medians, representing nerve density averaged over two adjacent microscopic images, showing the interquartile ranges (Q25, Q75), and whisker plots representing 10^{th} and 90^{th} percentiles.

In vivo measurements of corneal thickness with or without implants by IVCM (depth difference between the epithelial and endothelial images) showed no statistical significance ($P<0.05$) between the operated and unoperated corneas, indicating that the implants were not thinning or swelling within the 12 month test period, and were all 690±40μm.

Mechanical Tensile Properties

Tensile data showed that the corneas harvested from implanted eyes were similar to normal pig corneas in key mechanical properties (Table 2). However some animal to animal variation is to be expected and was found between the tensile properties of control cornea samples harvested from pigs at 12 month postoperation. Consequently, we believe that it is more statistically meaningful to compare the ratio of each specific tensile property of the cornea sample harvested from an implanted eye to that from the corresponding, contralateral control eye. These ratios are shown in Table 2. The maximum tensile stress ratio is very close to unity, which is the relative strength of each implant was very similar to its corresponding control. The average value of the elongation ratio was significantly greater than unity, whereas the elastic moduli ratio was below unity, both indicating that implants were less stiff and could be stretched more before failure as compared to the controls.

Table 2. Averaged tensile properties of pig corneas harvested from control and implanted eyes and of the cross-linked collagen hydrogel alone.

TABLE 2. Averaged Tensile Properties of Pig Corneas Harvested from Control and Implanted Eyes and of the Cross-linked Collagen Hydrogel Alone

Sample	Maximum Recorded Tensile Stress (MPa)*	Elongation at Maximum Tensile Stress (%)*	Elastic Modulus (MPa)*
Twelve-mo postoperation control corneas	7.0 ± 0.2	27 ± 7	27 ± 2
Twelve-mo postoperation implanted corneas	7.6 ± 0.8	38 ± 8	21 ± 2
Cross-linked collagen hydrogel alone	0.4 ± 0.1	28 ± 7	1.5 ± 0.1
Ave ratios of tensile properties for each implanted cornea to its fellow control cornea after 12-mo implantation	1.00 ± 0.02	1.4 ± 0.1	0.78 ± 0.04

*Values ± SD for n = 3, using the in vivo corneal thickness of 690 μm.

Discussion

Desired outcomes of cornea transplantation include restoration of normal function, and the ultimate goal is to regenerate both natural architecture and cell function. To be a functional template for regeneration, an implanted ECM substitute or mimic should ideally allow in-growth of precursor cells to repopulate the matrix, and then biodegrade gradually to allow replacement by natural macromolecules elaborated by the newly established cells. In the cornea, this replacement must occur without unnatural changes in thickness or optical properties, and should also allow the cornea to recover its full tensile properties.

In this study, we directly labeled our collagen implants and showed that this method was effective for tracking the fate of the implants. The water soluble, biotin moiety chemically bound to a NHS ester, spontaneously reacted at a neutral pH with primary amine groups on lysine residues found in the fabricated corneal substitute. Covalently conjugating biotin to only 33% of the lysine amine groups (~24 equiv./1000 amino acid residues) [22] remaining after carbodiimide cross-linking of the collagen in the implant hydrogel was not expected to affect the enzymatic biodegradation rate of the collagen constituting the implant. This was confirmed *in vitro* (data not shown).

Our carbodiimide stabilized collagen implants showed biodegradation after 2 weeks in mice, as evidenced by the presence of macrophages and the loss of the continuous, smooth implant edge, but the degradation was not pronounced until 4 weeks postoperatively. It has been shown that the implantation of an allogeneic cornea will trigger an innate immune response by neutrophils, macrophages, natural killer cells, and dendritic cells, in which macrophages move into the implant area. [23] However, an adaptive response will also be initiated, that contributes to stable engraftment. [11] In our case, the macrophages observed

were most likely contributing to implant breakdown but, there was no adverse impact on host-graft integration. The remodeling of the collagen implant was expected as enzymes such as matrix metalloproteinases, collagenases, and stromelysins are expressed in the cornea following wounding to remodel any scar tissue that may be formed [24], in addition to the innate immune and adaptive responses to surgery discussed above. Preliminary studies, have shown that initially a low grade, self-limiting inflammatory response occurs when these EDC/NHS crosslinked gels are implanted via full thickness penetrating into mice. [25] The main obstacle encountered in these full thickness grafts were the formation of a retro corneal membrane. However, because the mouse corneas were very small, the implants overlapped the adjacent, surrounding host tissue, making it very possible for host stromal cells to grow onto the overlying implants and thus give rise to a retroprosthetic membrane. Nevertheless, we show that with lamellar grafts, the implants were very well-tolerated and retained clarity over the 12 months. Unlike the more aggressive wound repair process that would occur in large wounds to the stroma, there was little fibrosis or scarring over time, although remodeling was clearly observed. The engineered ECM having its collagen microstructure chemically locked in a transparent form appeared to have functioned as a regeneration template, allowing for a more gradual remodeling process. The presence of a scaffold versus a gaping wound appears to have tempered the wound healing response.

In the pigs, at 12 months postoperative, both operated and control corneas remained optically clear as evidenced clinically through slit lamp biomicroscopy and topography showed retention of cornea shape and refractive power over time (not shown). Type VII collagen staining of anchoring fibrils in the basement membrane between the epithelium and stroma, along with TEM confirmation of hemidesmosomes confirm the stability of both the

graft and the anchorage of the epithelial layer to the implant. Histological analysis through H&E staining did not show the presence of any fibrosis in the cornea after 12 months.

TEMs of operated corneas show stromal cells oriented in parallel striations, as well as cross-plied collagen fibril lamellae, even though the architecture of our implants initially comprises randomly oriented, cross-linked fibrils [26], not the highly organized, cross-plied lamellae of parallel fibrils found in mammalian corneas. [27] This regeneration of the ordered structure of a natural cornea in our implants at 12 months supports the biotin evidence and the contention that the gradual remodeling observed was the mechanism by which stable engraftment of the implant had occurred.

Reported elastic moduli for porcine and human corneas ranged from 0.3-60 MPa, depending on test conditions. [28] Kampmeier et al. reported a tangent modulus of 3.5 MPa for porcine corneas, but at a much lower strain (0.1 strain) than we have used. [29] Simonsen et al. [30] have followed restoration of strength in human corneas for up to 12 years following cataract surgery, requiring corneal incisions. Over the 4-5 years after the incisions were made, tensile properties of human corneal tissue that encompassed the incision were found to plateau at the strength of the nonoperated, control corneas (~5.5 MPa). In our study, restoration of tensile strengths was observed in operated pig corneas (Table 1). Our maximum tensile stress range is greater than the value reported by Zeng et al. [31] of 3.7±0.2 MPa for swollen pig corneas which is also close to reported values for swollen human corneas [~5.5 and 3.8±0.4 Mpa] [30, 31].

While direct experimental measurement of the maximum tensile strength of the implanted corneas immediately after implantation was not practical, the initial tensile strength can be calculated, based on the thickness of each layer in the implanted cornea (500

μm of implanted gel and 190 μm of pig tissue remaining after DLKP) and on the assumption of linear additivity of properties. From the average properties of cornea controls and gel properties (Table 1), the estimated value of the maximum tensile strength of the cornea immediately upon implantation is then

$[(7.7\pm0.2)x190/690 + (0.4\pm0.1)x500/690] = 2.2\pm0.1$ MPa

if no remodeling and/or regeneration had occurred. This calculated, initial tensile strength is much lower than the average value (7.6 ±0.8 MPa) found for the 12 month implanted corneas and is consistent with extensive remodeling over this time frame.

While we were not able to directly measure in any detail the implant breakdown process because an absolute measure of molecular scission would require an elaborate recovery and fractionation of the collagen and its breakdown products, which is beyond the scope of this study, we were nevertheless able to provide evidence for remodeling. The loss of implanted biotin-labelled collagen matrices in the mice coupled with the infiltration of macrophages and stromal cells, the presence of unlabelled matrix and restoration of overall mechanical properties to the operated corneas confirm turnover of the implanted collagen matrix.

We have therefore confirmed our prior *in vitro* study conclusions [9, 22] that simple ECM substitutes such as collagen crosslinked through EDC/NHS chemistry allowed for stable implantation and for integration of the implant into the adjacent host tissue by providing a conducive template for cell in-growth or overgrowth. These corneal substitutes allowed cell recruitment and nerve regrowth over the 12 month postoperative period for regeneration of proper architecture and function of the cornea. The integration with host tissue was seamless and stable. From biomechanical studies, remodeling of the pig cornea

occurred to restore the mechanical properties to the implanted cornea, with an elastic modulus and tensile strength fairly similar to those of the native cornea. Use of biotin tagged corneal implants in mice strongly suggests remodeling of the matrix as a mechanism by which stable host-graft integration occurred in the present study. However, it is pertinent to note that the mice received full-thickness grafts by penetrating keratoplasty (penetrating the anterior chamber of the eye), while the pigs received lamellar implants in which the posterior stroma and endothelial layers were intact (and anterior chamber was undisturbed). In a previous longer term mouse study (Liu et al. [25]), a low grade inflammatory innate immune response was induced, with retrograft membrane formation that may be related to the xenogeneic pairing, or migration of stromal cells from the underlying lip of the host cornea onto which the thin mouse implants were secured for suturing. However, all corneal implants in pigs remained free of inflammation even without steroid treatment. While further studies are investigating this effect, it is clear that lamellar grafts in pigs are fully integrated and show considerable potential for use in humans particularly if the endothelial cells are still functional since this implant did not seem to impair host endothelial function in any way. It is likely that integration of similar collagen-based lamellar implants into human eyes would also occur through similar mechanisms. Indeed, initial implants of small lenticules into blind human eyes in a limited clinical study with crosslinked collagen [5] have shown that the implants did not cause any inflammation nor irritation to the subjects. ECM substitutes such as this simple crosslinked collagen model therefore has the potential for future use in cornea replacements as implants, or temporary patches for promoting regeneration.

Acknowledgements

Supported by NSERC Canada STPGP 246418 to MG. Thanks to CooperVision for the pigs. The authors thank David Priest, Dr. David Carlsson, Dr. Mitchell Watsky, Dr. Lisha Gan and Dr. Lei Liu for technical expertise and advice. We also thank Dr. Yasuhiro Kato and Minoru Fukuda for TEM images, and Dr. Marilyn Keaney and her team at the University of Ottawa Animal Care and Veterinary Services for their contribution to our research efforts.

Chapter 4

4.1 Manuscript 3

Collagen-phosphorylcholine Interpenetrating Network Hydrogels as Corneal Substitutes.

***Biomaterials*. 2009 Mar;30(8):1551-9. Epub 2008 Dec 20.**

This manuscript investigated the use of an improved corneal substitute consisting of type 1 porcine collagen and 2-methacryloyloxyethyl phosphorylcholine (MPC) which is a phosphobetaine monomer that mimics the phospholipids found in plasma membranes of cells. Polymeric MPC was developed initially as a biocompatible, anti-fouling material with a unique, high water-holding capacity. The incorporation of MPC into the corneal substitute resulted in improved mechanical properties, which is important for transplantation and suture retention. Following 12 months implantation through partial thickness keratoplasty into mini pigs, it was found that all corneal cell types and sensory nerves had entered the implant.

Collagen-phosphorylcholine Interpenetrating Network Hydrogels as Corneal Substitutes.

Wenguang Liu[a,1], Chao Deng[a,1], Christopher R. McLaughlin[a,b], Per Fagerholm[c], Neil S. Lagali[b,c], Belinda Heyne[d], Juan C. Scaiano[d], Mitchell A. Watsky[e], Yasuhiro Kato[f] Rejean Munger[b], Naoshi Shinozaki[f], Fengfu Li[b,2] and May Griffith[a,b,2,*]

[a]Department of Cellular and Molecular Medicine, University of Ottawa, Ottawa, Ontario, Canada

[b]University of Ottawa Eye Institute, 501 Smyth Road, Ottawa, Ontario, Canada

[c]Department of Ophthalmology, Linköping University, Linköping, Sweden

[d]Department of Chemistry, University of Ottawa, Ottawa, Ontario, Canada

[e]Department of Physiology, University of Tennessee Health Science Centre, Memphis, TN 38163

[f]Department of Ophthalmology and Cornea Centre, Tokyo Dental College, Chiba, Japan

[1, 2] Equivalent contributions

*Corresponding Author

E-mail: mgriffith@ohri.ca

Tel: 613 737 8899 exit 74011

Co-author Contributions to Manucript

Liu, Wenguang

Dr. Liu was a post doctoral fellow who developed the chemically crosslinked collagen MPC formulation, and performed the mechanical testing of the artificial corneas.

Deng, Chao

Dr. Deng, was a post doctoral fellow who created the UV light crosslinked collagen MPC formulation and performed the in vitro degradation, and mechanical testing.

Fagerholm, Per

Dr. Fagerholm, an ophthalmologist at Linköping University Hospital in Sweden, was responsible for the implantation of the artificial corneas into the pigs.

Lagali, Neil

Dr. Lagali, was a post doctoral fellow in the Munger Lab who was mainly responsible for the *in vivo* confocal microscopy images.

Heyne, Belinda

Dr. Heyne is a post doctoral fellow in the Department of Chemistry at the University of Ottawa, who performed the UV biodegradation testing of the artificial corneas.

Scaiano, Juan

Dr. Scaiano is a professor of Chemistry at the University of Ottawa, who provided guidance for the UV crosslinking of the artificial corneas, and chemical analysis.

Watsky, Mitchell

Dr. Watsky is a corneal physiologist at the University of Tennessee. He performed the glucose and albumin permeability assays.

Kato, Yasuhiro

Dr. Yasuhiro is a post doctoral fellow at the Ichikawa General Hospital Cornea Center in Japan, and provided the electron microscopy images of the implanted corneas.

Munger, Rejean

Dr. Munger, an optical physicist at the University of Ottawa Eye Institute, aided in analysis of the in vivo confocal microscopy images of the artificial cornea.

Shinozaki, Naoshi

Dr. Shinozaki, Director of the Ichikawa General Hospital Cornea Center in Japan, provided guidance in interpretation of the electron microscopy images of the implanted corneas.

Li, Fengfu

Dr. Li is research fellow at the University of Ottawa who helped to direct the mechanical characterizations of the artificial corneas and prepare the manuscript.

Griffith, May

Dr. Griffith was my supervisor, and was responsible for the overall study design, management of the project and revision of the manuscript.

My role in this manuscript was to perform all the *in vitro* biocompatibility assays on the various formulations to select the formulations that were suitable for implantation. I was also responsible for the histopathological analysis of the implants. I assembled all the figures and wrote up all the biological portions of the manuscript.

Abstract

A biointeractive collagen-phospholipid corneal substitute was fabricated from interpenetrating polymeric networks comprising 1-ethyl-3-(3-dimethyl aminopropyl) carbodiimide and *N*-hydroxysuccinimide crosslinked porcine atelocollagen, and poly(ethylene glycol) diacrylate crosslinked 2-methacryloyloxyethyl phosphorylcholine (MPC). The resulting hydrogels showed an overall increase in mechanical strength beyond that of either original component and enhanced stability against enzymatic digestion (by collagenase) or UV degradation. More strikingly, these hydrogels retained the full bio-interactive, cell friendly properties of collagen in promoting corneal cell and nerve in-growth and regeneration (despite MPC's known anti-adhesive properties). Measurements of refractive indices, white light transmission and backscatter showed the optical properties of collagen-MPC are comparable or superior to those of the human cornea. In addition, the glucose and albumin permeability were comparable to those of human corneas. Twelve-month post-implantation results of collagen-MPC hydrogels into mini-pigs showed regeneration of corneal tissue (epithelium, stroma) as well as the tear film and sensory nerves. We also show that porcine collagen can be substituted with recombinant human collagen, resulting in a fully-synthetic implant that is free from the potential risks of disease transmission (e.g. prions) present in animal source materials.

Keywords: Recombinant collagen, phospholipid, cornea substitute, tissue engineering, biomedical regeneration

Introduction

The extracellular matrix (ECM) of tissues and organs is secreted by cells during development, providing templates upon which organogenesis proceeds. The ECM also serves as a regeneration template during wound healing [1]. As such, ECM macromolecules are excellent candidates for tissue scaffolds. One such macromolecule that has been widely used for tissue engineering applications is collagen.

The human cornea is the transparent window to the eye and is the main refractive element that is responsible for transmission of light to the retina for vision. It can be thought of as a largely optically clear, collagenous hydrogel containing fibroblastic cells (stroma) that is sandwiched between an outermost, stratified epithelium and an innermost single-layered endothelium. It is also avascular and immune privileged. Corneal diseases leading to loss of corneal transparency and hence vision loss or blindness, when irreversible, are a major cause of blindness worldwide. The only widely accepted treatment for corneal blindness is transplantation with human donor corneas. However, the demand exceeds supply in many countries, especially in the developing world. The short supply and conditions that are not amenable to donor grafting have led to many efforts to develop corneal substitutes [reviewed recently in 2]. To date, the corneal substitutes tested clinically have been prostheses designed to restore minimal function [2] and the lack of seamless host-graft integration has restricted their use to cases that are not amenable to donor tissue grafting [3]. The prostheses therefore do not alleviate the need for donor corneas. Our goal therefore was to develop corneal substitutes that would restore vision in a manner that was comparable to donor allografts, by promoting repair and regeneration of the damaged structures with the aid of bio-interactive ECM-based scaffolds.

We previously fabricated corneal regeneration templates based on collagen, the predominant ECM component of the cornea. This included simple carbodiimide crosslinked collagens that could be fabricated into corneal substitutes in non-chemistry labs, or in developing countries with basic lab equipment for use as implants or temporary patches in emergencies [4,5]. These implants, when implanted into mini-pig models, successfully promoted regeneration of host tissues and nerves [4-6], however, they only had a fraction of the mechanical strength of the human cornea and collagen turnover was rapid [7]. Therefore, in clinical conditions requiring transplantation where excess collagenases or matrix metalloproteinases (MMPs) are being produced, e.g. keratoconus or alkali burns, these carbodiimide crosslinked collagens would require reinforcement.

2-Methacryloyloxyethyl phosphorylcholine (MPC) is a phosphobetaine monomer that mimics the phospholipids found in plasma membranes of cells [8,9]. Polymeric MPC was initially developed as a biocompatible, anti-fouling material with a unique, high water-holding capacity. More importantly, recent reports of hydrogels created by immobilization of MPC onto collagen hydrogel substrates showed that the presence of MPC conferred the hybrid hydrogels with increased mechanical strength and resistance to enzymatic degradation by collagenase [10,11]. While these properties were desirable, the anti-adhesive property of MPC is not conducive to supporting cell attachment and therefore proliferation and/or differentiation on its own. In order to retain the enzymatic resistance, increased mechanical strength and hydrophilicity of MPC without the anti-adhesiveness, an interpenetrating polymeric network (IPN) combining collagen and MPC was therefore developed to exploit the properties of both macromolecules.

In this study, the collagen network was fabricated by crosslinking with 1-ethyl-3-(3-dimethyl aminopropyl) carbodiimide (EDC) and *N*-hydroxysuccinimide (NHS), while the MPC network was crosslinked by poly(ethylene glycol) diacrylate (PEGDA) initiated by ammonium persulphate (APS) or a photoinitiator, Irgacure 2959. The resistance to collagenase as well as the optical and mechanical properties of the resulting collagen-MPC IPN hydrogels were measured. The *in vitro* biocompatibility of the IPN hydrogel to corneal epithelial cells and nerves were also evaluated. Postoperative results from implantation of the IPN hydrogels into mini-pigs are reported.

2. Materials and Methods

2.1. Materials

Type I porcine atelocollagen was purchased from Nippon Meat Packers Inc. (Tokyo, Japan), while recombinant human type III collagen (RHCIII) produced in yeast cells (*Pichia pastoris*) were obtained from FibroGen Inc. (South San Francisco, CA). MPC was purchased from Biocompatibles (UK). PEGDA (Mn=575), collagenase (type I clostridium histolyticum, EC 3.4.24.3), EDC, APS and N,N,N',N'- tetramethyl ethylene diamine (TMEDA) were supplied by Sigma-Aldrich Canada Ltd (Oakville, Ontario, Canada). NHS was purchased from Fluka (Buchs, Switzerland). Irgacure 2959 was a gift from Ciba Specialty Chemicals Canada Inc (Canada). Morpholinoethanesulfonic acid (MES) was provided by EMD chemicals Inc, USA. All other reagents were of analytical grade and used as received.

2.2 Preparation of Collagen-MPC hydrogels with chemical initiator–APS/TMEDA.

400 mg of 20 % (w/w) porcine type I acidic atelocollagen solution was buffered with 150 µl of 0.63M MES buffer in a syringe mixing system that we previously described [4,12] and thoroughly mixed with calculated volumes of MPC solution and PEGDA solution in MES buffer with the mixing system immersed in an ice-water bath. The collagen:MPC ratio was 4:1 (w/w). The MPC:PEGDA ratio was 3:1 (w/w). 25µl of 4% (w/v) APS solution in MES buffer containing TMEDA (APS:TMEDA=1:0.78,w/w) was added into the collagen-MPC-PEGDA solution and thoroughly mixed at 0 °C. Calculated volumes of EDC and NHS solution (both at 20% wt/vol, molar equivalent ratio EDC:NHS:collagen-NH_2=1.5:1.5:1) were then added to crosslink the collagen and again thoroughly mixed at 0°C. The final mixed solution was immediately dispensed onto a glass plate or alternatively into cornea shaped moulds. The hydrogels were cured at 100% humidity under nitrogen at room temperature for 16 h and then at 37 °C for 5 h. After demoulding, they were washed thoroughly with 10mM phosphate buffered saline (PBS) and then stored in PBS containing 1 % chloroform to maintain sterility. Hydrogels with different collagen to MPC ratios, 2:1 or 1:1 were similarly prepared.

For recombinant human collagen hydrogels, 400 mg of 13.7% (w/w) RHCIII with the ratios of collagen:MPC=2:1, MPC:PEGDA=3:1, EDC:NHS: collagen-NH_2=0.3:0.3:1 were examined.

Control porcine and RHCIII only hydrogels were prepared by omitting MPC and PEGDA.

2.3. Preparation of Collagen-MPC hydrogels by photopolymerization.

500mg of 15% RHCIII solution buffered with 150 µl of MES (0.63M) was thoroughly mixed with 25mg of PEGDA, 100µl of 75% (w/v) MPC, and 200µl 0.5% (w/v) Irgacure 2959 aqueous solution in the mixing system as mentioned above. Calculated volumes of NHS and EDC (both at 10% wt/vol, EDC:NHS:collagen-NH_2=0.4:0.4:1) were injected into the above mixture sequentially and mixed thoroughly. The homogenous mixture was dispensed into moulds, UV irradiated in a crosslinking oven (model LZC-1, Luzchem Research Inc, Ottawa, Canada) at a wavelength of 313-406nm and intensity of 5.27 mW/cm^2) for 15 min. They were then post-cured as described above for chemically crosslinked hydrogels. Ratios of RHCIII:MPC of 1:1, 2:1 and 4:1 (w/w) were prepared for comparison with chemically crosslinked samples.

2.4. Chemical Characterization

To confirm the incorporation of MPC into the collagen-MPC IPNs, ^{13}C NMR and ^{31}P NMR spectra were measured using a Bruker AVANCE 500 MHz spectrometer at room temperature. The C, N, O and P content on freeze-dried hydrogel surfaces were further examined using the Kratos AXIS Ultra XPS (X-ray photoelectron spectroscopy) with a monochromated Al Kα X-ray source (Manchester, England). Crosslinked collagen-only hydrogels served as negative controls.

2.5. Physical and mechanical characterization

Optical properties (white light transmission, backscatter and refractive index), equilibrium water content, thermal properties and glucose and albumin permeability were

carried out as previously described [6]. Briefly, The refractive indices of flat and fully hydrated hydrogels equilibrated in PBS were recorded using an Abbe refractometer (Model C10, VEE GEE Scientific Inc., Kirkland, Washington) at 21 °C with bromonaphthalene as the calibration agent. White light transmission of hydrogels was determined at 21 °C on a custom-built instrument. The mechanical properties of flat hydrogels with 12 mm × 5 mm × 0.44 mm dimensions were measured using an Instron electromechanical universal tester (Model 3342, Instron, Canton, MA) [6]. The denaturation temperature (T_d) of hydrogels was determined on a Perkin–Elmer DSC-2C differential scanning calorimeter in the range 8–70 °C at a scan rate of 5 °C min^{-1}. In addition, the ability of the implants to tolerate the placement of interrupted and continuous sutures was also examined.

2.6. In vitro biodegradation

As previously described [6], three hydrated hydrogels of each formulation were placed in vials containing 5 ml of 10mM PBS, pH 7.4. Sixty microliters of 1 mg/ml collagenase was added and the vials were incubated at 37°C. At different time intervals, each sample was weighed after all surface water was carefully blotted off. The percent residual mass of hydrogels was calculated according to the following equation:

Residual mass % = W_t/W_0

where W_0 is the initial weight of the hydrogel; W_t is the weight of the hydrogel at each time point.

2.7. UV and sunlight exposure effects

In order to test the effects of UV exposure on the hydrogels, as per ISO standard 11985: 1998 (*in vitro* method for ageing of ophthalmic optics and contact lenses by exposure to UV and visible radiation), collagen-MPC and collagen only hydrogels (n=3 each) were placed in a sterile PBS solution (1x, pH 7.4; Invitrogen, Burlington, Ontario) and irradiated in a solar simulator (LZC-SSR, Luzchem Research Inc, Ottawa, Canada). As previously described [6], the simulator delivered 26.9 W/m^2 UVA, 4.9 W/m^2 UVB and 143 W/m^2 visible light with a color temperature of 6000K for 20h. As required, a specific cutoff filter (Schott) was used in order to avoid irradiation of samples below 300nm. An absorption spectrum of the different corneas was recorded before and after exposure on a UV-Vis spectrophotometer (Carry 50, Virian, Palo Alto, CA). Human eye bank corneas and contact lenses made of poly (2-hydroxyethyl methacrylate (pHEMA) without UV blockers (also n=3 each) served as benchmarks.

2.8. In vitro biocompatibility and performance

Epithelial coverage and nerve surface growth on collagen-MPC gels and crosslinked collagen controls were evaluated as previously described using an immortalized human corneal epithelial cell line and dorsal root ganglia isolated from E8 chick embryos [4-6]. Very briefly, cells were seeded onto hydrogels and supplemented with a serum-free medium (Keratonocyte Serum-Free Medium, Life Technologies, Burlington, Ontario) and growth rates were measured daily. Isolated ganglia were explanted onto the hydrogels and neurite outgrowth was followed. Tissue culture polystyrene plates served as further controls.

2.9. Implantation and clinical evaluation

With ethics approval from both the Univ. of Ottawa (Protocol EI-5) and Linköping University (Protocol 41-05), porcine collagen-MPC hydrogels, 500 μm thick and 6.25 mm diameter, and RHCIII-MPC hydrogels prepared with chemical initiator, 350 μm thick, 5.25 mm in diameter were implanted into the corneas of four Yucatan mini-pigs and New Zealand white rabbits, respectively. Deep lamellar keratoplasty (DLKP) with overlying sutures was used for surgical implantation [4, 6]. Animals were only given antibiotics and analgesics during the first week of surgery. They were given steroids (Prednisolone, Sandoz) 4 times daily to resolve neovascularization as needed (3-4 weeks). Sutures were removed at 3 weeks post-operative.

Follow-ups were performed daily on each animal for up to 7 days post-operative, and then weekly. Slit-lamp biomicroscopy was used to examine the corneas for optical clarity as well as to look for any inflammation (as indicated by excessive redness or swelling compared to the unoperated contralateral control cornea) or neovascularization (in-growth of blood vessels). Other tests included sodium fluorescein staining to assess epithelial integrity and barrier function, Schirmers to assess tear film regeneration, measurements of intraocular pressure to ensure that corneas were not blocking aqueous humour flow, and *in vivo* confocal microscopic examination (ConfoScan3, Nidek, Aichi, Japan used for pigs; Heidelberg Retinal Tomograph 3, Heidelberg Engineering, Heidelberg, Germany used for rabbits) to assess cell and nerve in-growth and to measure corneal thickness in live animals. The *in vitro* confocal microscopy also provided an additional means for imaging any neovascularization. Corneal touch sensitivity was measured using a Cochet-Bonnet aesthesiometer (Handaya

Co., Tokyo, Japan). Lidocaine was applied as a control for sensitivity, as topical application should extinguish reaction.

2.10. Histopathological Evaluation

Pigs were sacrificed after 12 months post-implantation. Corneas with implants, allografts and control unoperated corneas were processed for histopathological examination by both light and transmission electron microscopy (TEM) as previously described [6,13]. Sections were stained with H&E for routine histopathological examination. Frozen sections were stained with *Ulex europaeus* agglutinin (UEA) and AE-5, by standard immunohistochemistry. Briefly, sections were blocked with 4% foetal bovine serum (FBS) + 1% bovine serum albumin (BSA) in 0.1 M PBS, pH 7.2-7.4, and incubated in primary antibody overnight at 4°C. They were then incubated with 1:400 FITC conjugated secondary antibody (Sigma) and visualized on a Zeiss Axioskop 2. Paraffin sections were deparaffinized for procollagen I and SMA staining. They were treated with proteinase K (2 mg/ml) for 8 min for antigen retrieval, followed by 3% H_2O_2 and blocked for non-specific staining with 4% FBS + 1% BSA in PBS. Primary antibody incubation was carried out overnight at 4°C. After equilibration to room temperature and washing, they were incubated with 1:400 dilution of the biotinylated anti-mouse IgG antibody (Amersham). After rinsing off unbound IgG, sections were incubated in a 1:400 dilution of avidin-horseradish peroxidase (Amersham) and visualized with diaminobenzidine (Roche, Mannheim, Germany). For ultrastructural examination, samples were fixed in Karnovsky's fixative, post-fixed in osmium tetroxide and processed for TEM.

Rabbits were sacrificed at nine months post-operative and corneas were processed as for pigs.

3. Results

3.1. Fabrication of hydrogels and chemical characterization

Collagen-MPC IPN hydrogels were successfully fabricated by using either a chemical initiator, or by UV crosslinking using a photoinitiator, Irgacure 2959. Both methods gave strong hydrogels with comparable properties, although ratios of collagen to MPC for optimal performance differed. In addition, several differences in properties were observed, as detailed below.

^{13}C NMR and ^{31}P NMR spectra (Fig.1 and 2) confirmed the incorporation of MPC into the IPNs. Peaks at 54.6 ppm and 59.6-66.5 ppm (Fig.1), attributed to $-N(\mathbf{C}H_3)_3$ and methylene ($-OCH_2CH_2O-$, $-OCH_2CH_2N-$) of MPC, respectively[14], were seen. A peak at 71 ppm indicated PEG was also incorporated into the IPNs[15]. The peak at -1.05ppm (Fig.2) further indicates the presence of MPC in the IPN. XPS analysis showed the increase of P atom contents in IPN from 0.6% to 1.3% when the ratio of MPC to collagen was raised from 0.25 to 1 (w/w).

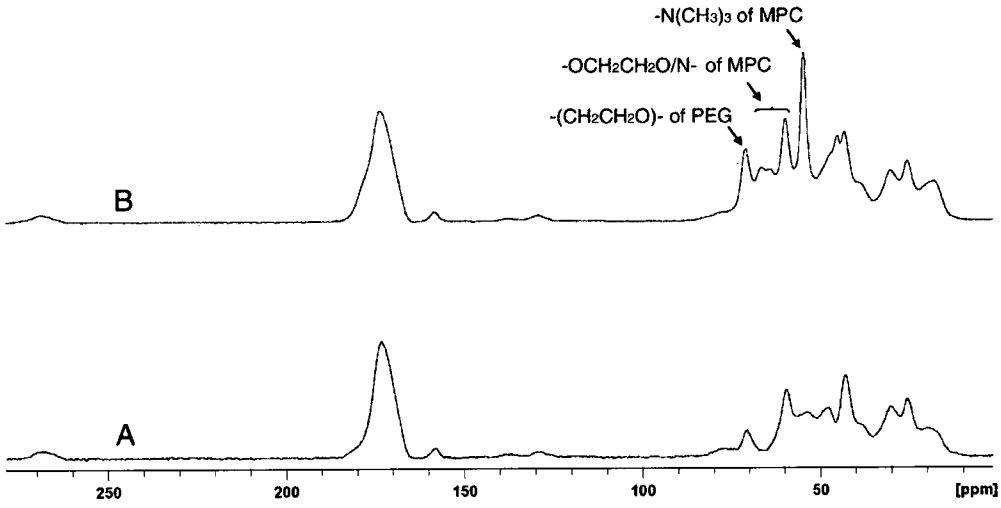

Fig. 1. The solid state ^{13}CNMR spectra of freeze-dried (A) pure porcine collagen hydrogel and (B) APS-initiated porcine collagen-MPC hydrogel (collagen:MPC=1:1,w/w)

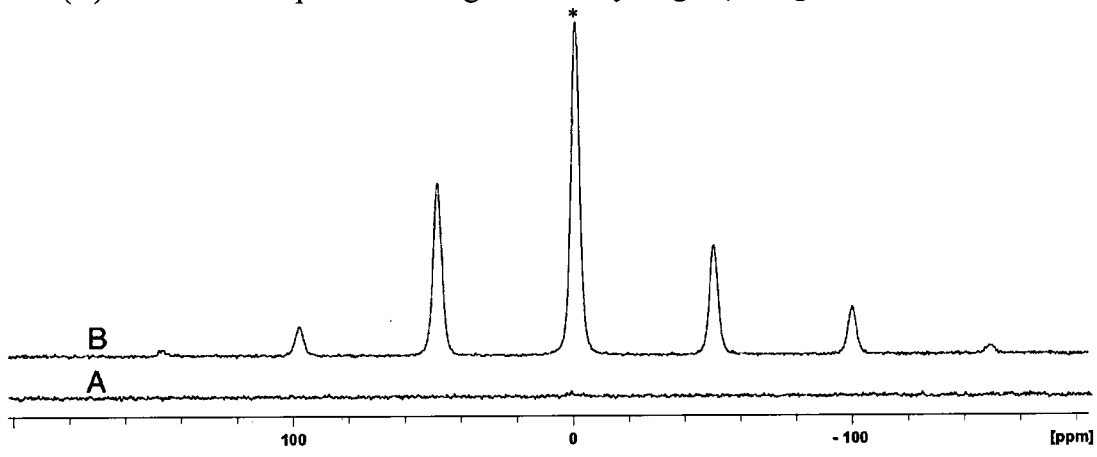

Fig. 2. The solid state ^{31}PNMR spectra of freeze-dried (A) pure porcine collagen hydrogel and (B) APS-initiated porcine collagen-MPC hydrogel (collagen:MPC=1:1,w/w). The peak at -1.05ppm marked with a star "*" is from the phosphorus in MPC. Other peaks are spinning sidebands. The reference compound used for these spectra was ammonium dihydrogen phosphate which has a chemical shift of 0.81 ppm with respect to 85% phosphoric acid at 0 ppm.

3.2. Physical and mechanical properties

The key physical and mechanical properties of collagen-MPC hydrogels are summarized in Table 1.

All hydrogels contained 89 to 92% of water, and showed refractive indices of approximately 1.35. Optical clarity (% light transmission and backscatter) were either comparable to those of human corneas or superior. We noted that APS-initiated crosslinked RHCIII-MPC hydrogel in particular, had excellent light transmission properties (98.3%), but it was the UV crosslinked RHCIII-MPC samples that showed no backscatter (0%).

Table 1 shows at the outset that hydrogels fabricated from recombinant collagen are significantly stronger than those of extracted porcine collagen. For example, the average tensile strength of porcine collagen hydrogels was 0.13 MPa compared to 1.7 MPa for RHCIII hydrogel. Correspondingly, the tensile strength of porcine collagen-MPC hydrogels was significantly lower than that of RHCIII-MPC hydrogels.

Table 1. Comparison of key properties of optimized porcine and recombinant human collagen-MPC hydrogels with their respective collagen only benchmarks[a]

Materials	Human cornea	Porcine collagen hydrogel	RHCIII hydrogel [6]	Porcine collagen–MPC hydrogel[b]	RHCIII–MPC hydrogel[c]	RHCIII–MPC hydrogel[d]
Water content (%)	78 [16]	91.9 ± 0.48	89.6 ± 1.8	89.0 ± 0.5	90.1 ± 2.4	90.0 ± 0.2
Optical properties						
Refractive index	1.373–1.380 [17]	1.3493 ± 0.0011	1.3507 ± 0.0011	1.3519 ±0.0004	1.3501 ± 0.0016	1.3521 ± 0.0003
Transmission (%)	>87 [18]	92.0 ± 2.9	89.8 ± 0.9	87.9 ± 2.2	98.3 ± 1.5	87.4 ± 2.2
Backscatter (%)	<3 [19]	1.9 ± 0.1	0.8 ± 0.4	1.6 ± 0.2	1.8 ± 0.0	0
Mechanical properties						
Tensile strength (MPa)	3.81 ± 0.40 [20]	0.13 ± 0.42	1.70 ± 0.21	0.69 ± 0.17*	1.29 ± 0.31	1.86 ± 0.44
Elongation at break (%)	–	48.58 ± 15.14	13.88 ± 0.69	49.08 ± 6.73	37.89 ± 10.31**	33.08 ± 4.55**
Elastic modulus (MPa)	3–13 [21,22]	0.60 ± 0.26	20.26 ± 2.04	2.09 ± 1.12*	5.26 ± 1.50**	11.42 ± 3.57**
Thermodynamic properties						
T_d (°C)	65.1 [13]	59.6	58.6	57.0	54.1	55.2
Permeability						
Glucose (cm^2/s)	2.4×10^{-6} [23]	$1.60 \pm 0.00 \times 10^{-6}$	$1.19 \pm 0.07 \times 10^{-6}$	$2.39^* \pm 0.13 \times 10^{-6}$	$1.45^{**} \pm 0.06 \times 10^{-6}$	ND
Albumin (cm^2/s)	1.1×10^{-7} [24]	$1.60 \pm 0.60 \times 10^{-7}$	$0.85 \pm 0.18 \times 10^{-7}$	$1.90 \pm 0.38 \times 10^{-7}$	$1.09 \pm 0.07 \times 10^{-7}$	ND

*Denotes significant difference compared to porcine collagen only hydrogels.
**Denotes significant difference compared to RHCIII only hydrogels.
[a] $n = 3$ samples, for each formulation. Statistical analyses were performed using a one-way ANOVA followed by Tukey test, with statistical significance set at $P < 0.05$.
[b] Collagen:MPC (4:1 w/w) prepared with chemical initiator, APS/TMEDA.
[c] Collagen:MPC (2:1 w/w) prepared with chemical initiator, APS/TMEDA.
[d] Collagen:MPC (2:1 w/w) prepared with photoinitiator, Irgacure 2959.

Interestingly, the addition of MPC to porcine collagen resulted in an IPN with a fivefold increase in tensile strength compared to crosslinked porcine collagen alone (Table 1). However, with the already stronger RHCIII hydrogels, addition of the MPC network did not have a similar enhancing effect.

On the other hand, porcine collagen hydrogels are more elastic than RHCIII hydrogels. While addition of MPC significantly increased the elongation at break of RHCIII hydrogels, there was no significant change to the porcine collagen hydrogels.

The elastic moduli of collagen-MPC gels were all significantly different from the collagen-only bench marks. In the case of porcine hydrogels, the incorporation of the MPC-PEGDA network into crosslinked collagen increased the elastic modulus. With RHC, however, the incorporation of the MPC network decreased hydrogel stiffness, but this was still within the range of moduli documented for human corneas.

Denaturation temperatures of all hydrogels are lower than that of the human cornea. Glucose and albumin diffusion coefficients, however, are comparable to those of the human cornea.

3.3. In vitro biodegradation

In general, porcine collagen-based hydrogels were more rapidly degraded by the high concentrations of collagenase used in the degradation assay (Fig. 3). RHCIII collagen hydrogels were more robust but still fully degraded after approximately 20 hours. RHCIII-MPC hydrogels, however, showed greatly enhanced stability, remaining intact for 50h. After 50h, however, they began to lose mass. At 26 days, 73% of the initial mass of the chemically initiated collagen-MPC hydrogel remained. Human cornea controls, in contrast to hydrogels, showed a biphasic response to enzymatic incubation. A slight increase in mass was observed within 19h, after which rapid loss of mass occurred so that by 26 days, only 3% mass remained.

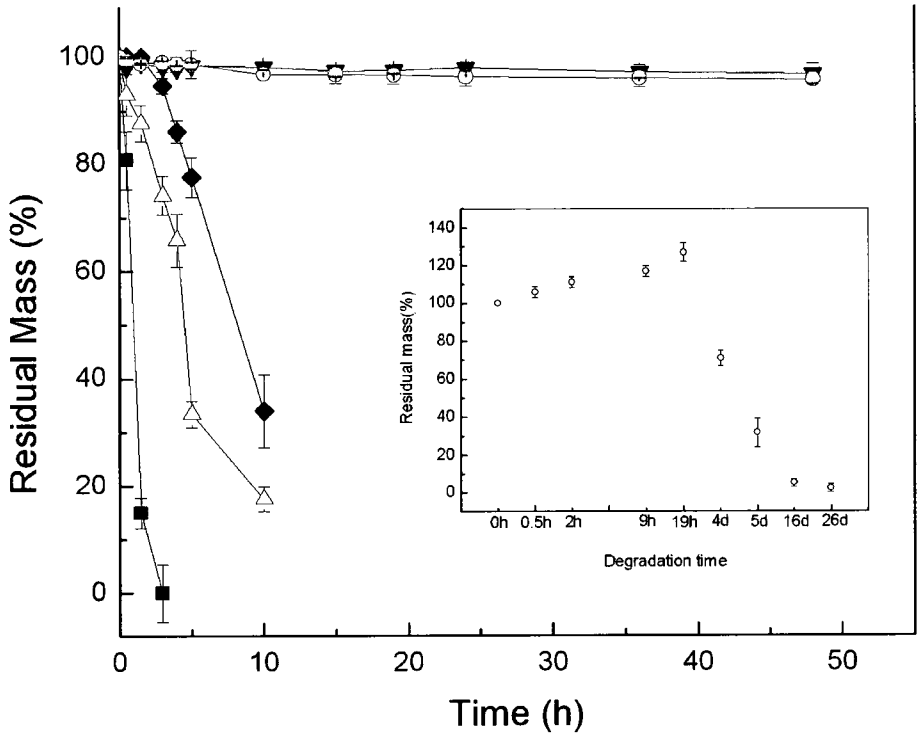

Fig. 3. *In vitro* biodegradation collagen and collagen-MPC hydrogels in collagenase. (■): porcine collagen; (▲): porcine collagen-MPC (Collagen:MPC=4:1w/w); (♦): recombinant human collagen type III (RHCIII); (▼): RHCIII-MPC (collagen:MPC=2:1w/w, chemically polymerized); (●) RHCIII-MPC (collagen:MPC=1:1w/w, photopolymerized). The inset shows biodegradation of human corneas. Error bar: standard deviation (n=3 different samples for each formulation).

3.4. UV and sunlight irradiation effects

The absorption spectrum of collagen-MPC hydrogels (Fig. 4a) and pHEMA contact lenses (Fig. 4d) showed minimal change in the UV region (300-400 nm) and no change within the visible light region (400-700 nm) after 20 hours of irradiation under simulated sunlight. Changes in the absorption spectrum were more apparent in the UV range for collagen only hydrogels (Fig. 4b), tapering off in the 400 through 560 nm range. With human corneas, a marked change in absorption occurred within the visible light range (Fig.4c).

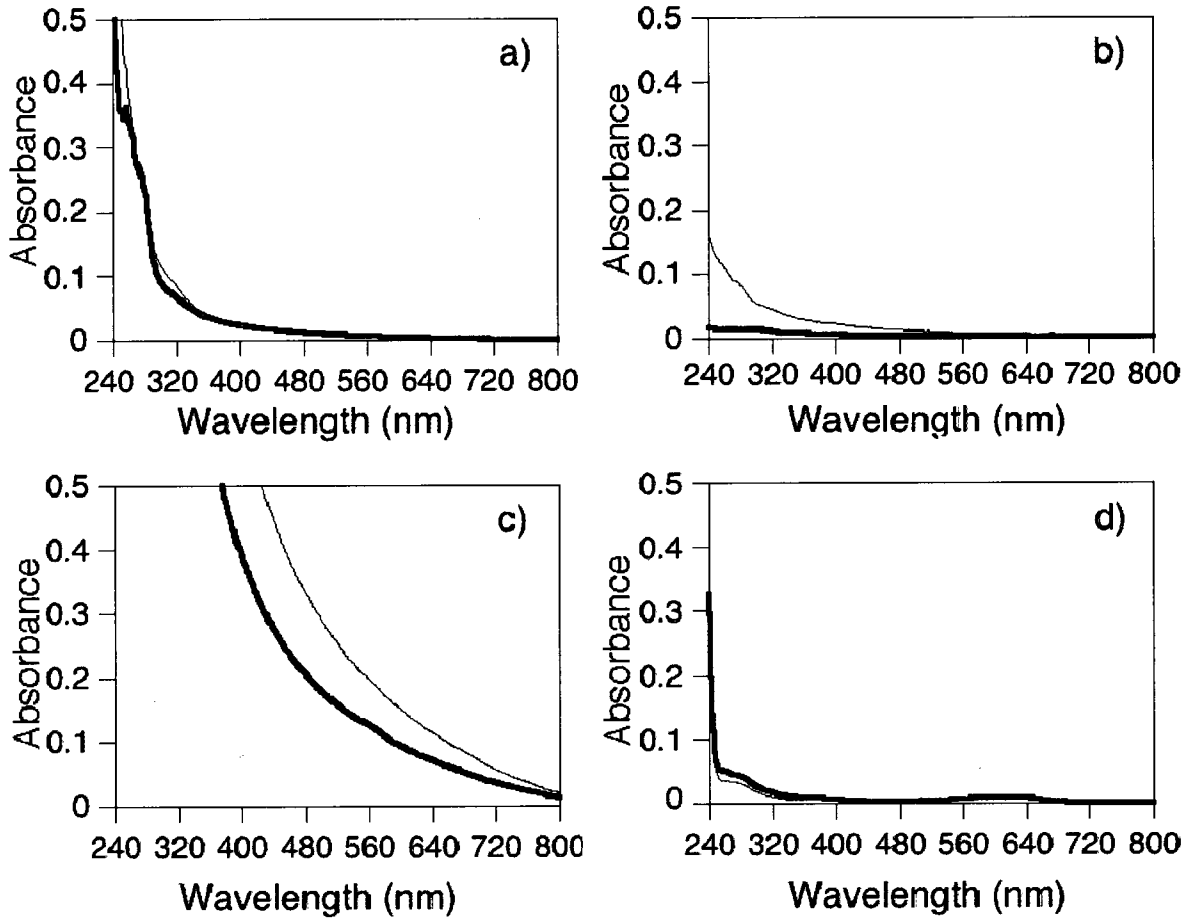

Fig. 4. Absorption spectrum before (thick) and after (thin) solar exposure for 20 hours. A) collagen-MPC hydrogel, B) collagen only hydrogel, C) human cornea, D) pHEMA contact lenses with no UV blocker.

3.5. In vitro biocompatibility

Collagen-MPC hydrogels supported attachment and proliferation of immortalized human corneal epithelial cells and the cells reached confluence at day 5, at comparable rates to those on crosslinked collagen only hydrogels and tissue culture treated polystyrene dishes. Nerve growth rates over the surface of porcine collagen-MPC hydrogels were also comparable to those of tissue culture polystyrene controls, with extended neurites reaching approximately 250 μm over five days. Neurite length on collagen only hydrogels was about 175 μm.

3.6. Implantation and clinical evaluation

No adverse inflammatory reactions were observed in either pigs or rabbits. Full epithelial coverage over the implant was completed within the first week post-surgery . Neovascularization occurred in both pigs with implants and allografts, but this was resolved by administration of steroids drops. One pig that had received a collagen-MPC hydrogel died of causes unrelated to the surgery.

Mild to moderate haze (+1 to +2) was observed in all pigs implanted with collagen-MPC hydrogel or allografts. Haze was observed up to six months post-operative in rabbits.

At nine and 12 months post-operative, all corneal implants, both porcine collagen-MPC and RHCIII-MPC hydrogels were fully repopulated with corneal epithelial and stromal cells. Corneal nerves had also re-grown into the implants, as visualized by *in vitro* confocal microscopy (Fig. 5).

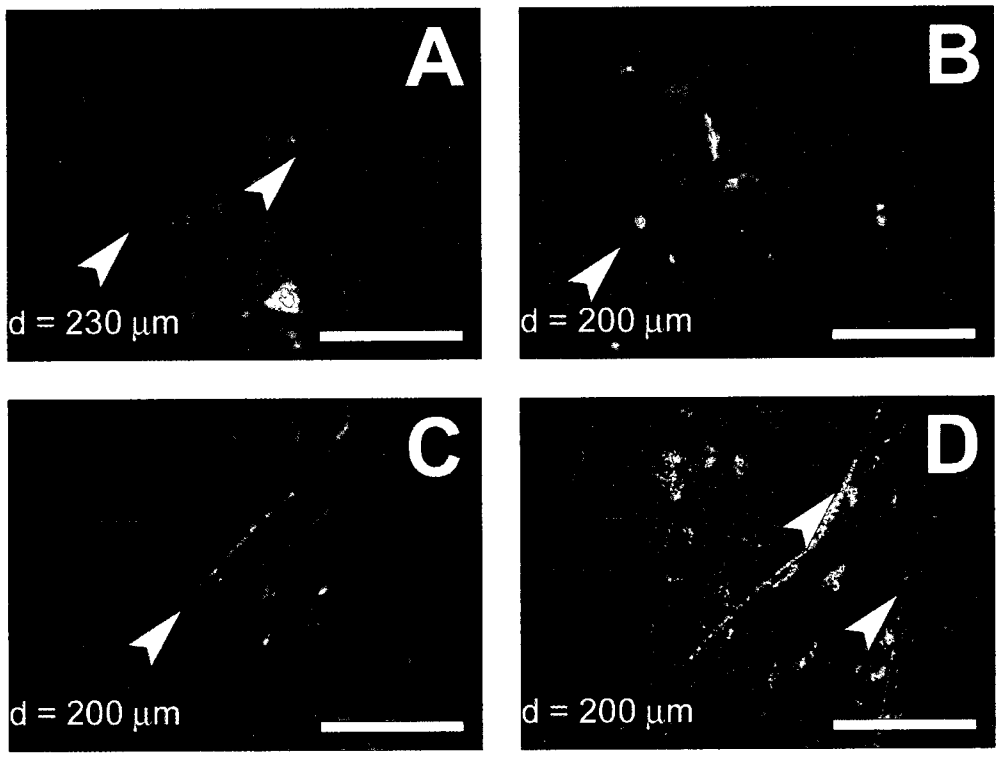

Fig. 5. Typical *in vitro* confocal images of the cornea of mini-pigs at 12 months post-operative (A-C), showing nerves in corneas that were either (A) untreated, or implanted with (B) porcine collagen-MPC hydrogels or (C) allografts. A nine month confocal image of a RHCIII-MPC implant into a rabbit cornea is shown in (D). Scale bar, 50 μm. The "d" value indicates the depth of confocal imaging.

3.7. Histopathological Evaluation

H&E sections of untreated corneas (Fig. 6A), collagen-MPC implanted corneas (Fig. 6B) and allografts in pigs after 12 months post-surgery (Fig. 6C), all show seamless host-graft integration. All corneas show the typical stratified, non-keratinizing epithelium and underlying stroma cells in a lamellar arrangement. Positive staining for AE-5 indicated the presence of terminally differentiated corneal epithelial cells in all samples (Figure. 6D-F). UEA staining showed the regeneration of tear film mucin over collagen-MPC implants (Fig. 6H). Procollagen I staining was detected in collagen-MPC implants (Fig. 6K) and allografts

(Fig. 6L), illustrating the synthesis of new matrix. However, all samples were negative for F4/80 (data not shown) indicating the absence of macrophage activity at implantation sites. The allografts contained a small number of smooth muscle actin positive cells just beneath the epithelium (data not shown), but both the collagen-MPC and the control samples were unstained.

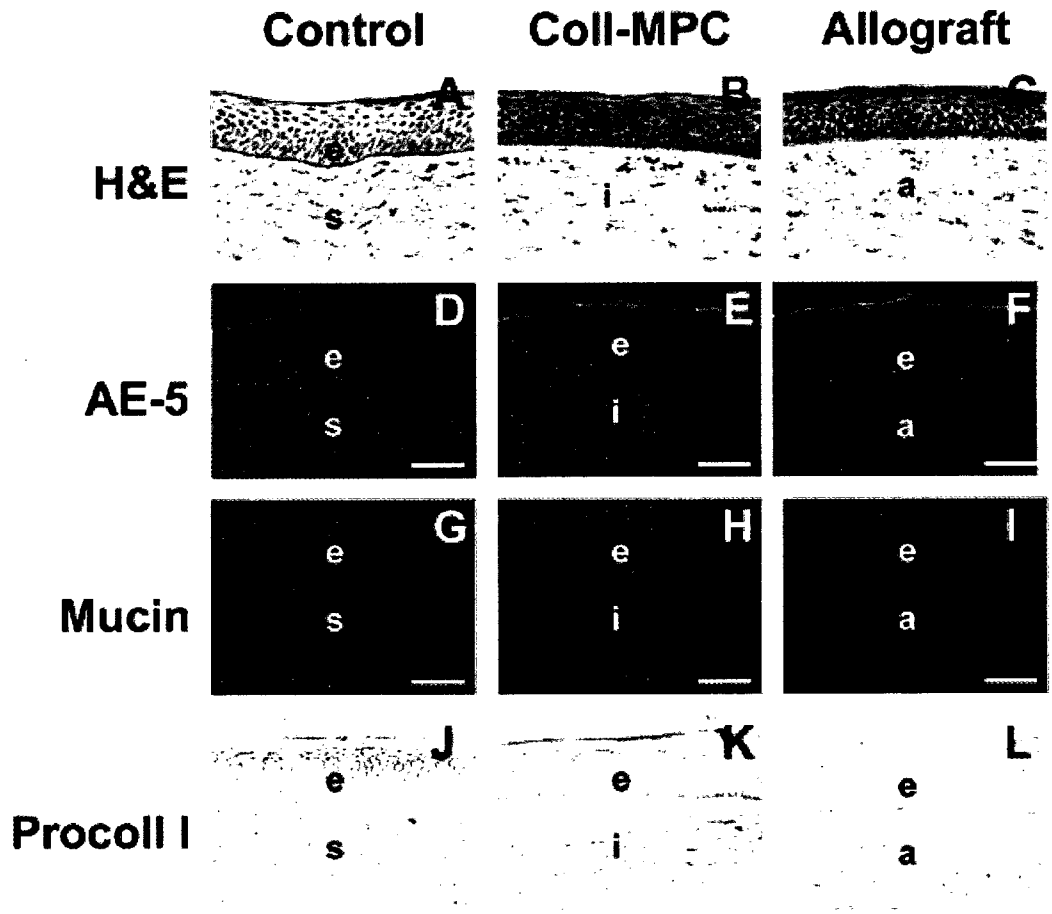

Fig. 6. Sections through representative pig corneas at 12 months post-implantation; e: epithelium; s: stroma. (A-C) Haematoxylin and eosin stained sections showing stratified epithelium and stroma cells in unoperated control (A), implanted (B), allograft control (C). (D-F) AE-5 staining in unoperated control (D), implanted (E), allograft control (F), showing cytokeratins. (G-I) Mucin binding to the epithelial surface on the implant (H) and allograft (I) indicating the restoration of tear film mucin layer in both the cases comparable to unoperated control (G). (J-L) Procollagen deposition. Positive procollagen deposition at the interface in the implant (K) and allograft control (L). Procollagen was not observed in unoperated control (J). (Bar = 50 μm for A-C and J-L Bar = 25 μm for D-I).

TEM observations of the epithelial-stromal interface (Fig. 7) show the restoration of the lamellar arrangement of stromal cells within the implant area. The regenerated epithelium rests on a regenerated basement membrane; and the presence of hemidesmosomes indicate stable cell attachment. Sub-epithelial nerves were also present in implants, allografts and unoperated corneas.

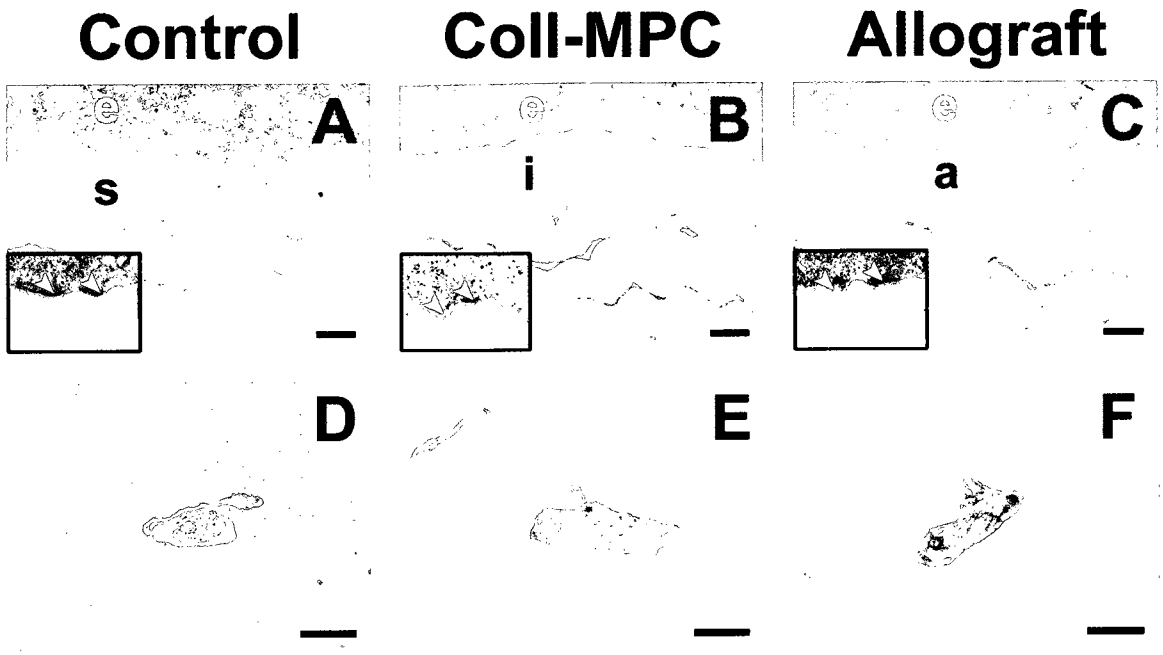

Fig. 7. TEM of the epithelial-stromal interface region of mini-pig implant. (A-C) Epithelial cells are overlying either a stroma (s), implant (i) or allograft (a), all of which contain stromal cells. Bars =5 μm. (D-F) Higher magnification of regenerated nerves, show the staining of clear and dense vesicles. Bars =2 μm.

A TEM image with high magnification (Fig.8) reveals the typical arrangement of collagen fibrils in the regenerated stroma. The diameters of the regenerated collagen fibrils are 24.3±2.4nm, 28.4±6.2nm and 22.7±5.4nm, respectively, for 3 different pigs.

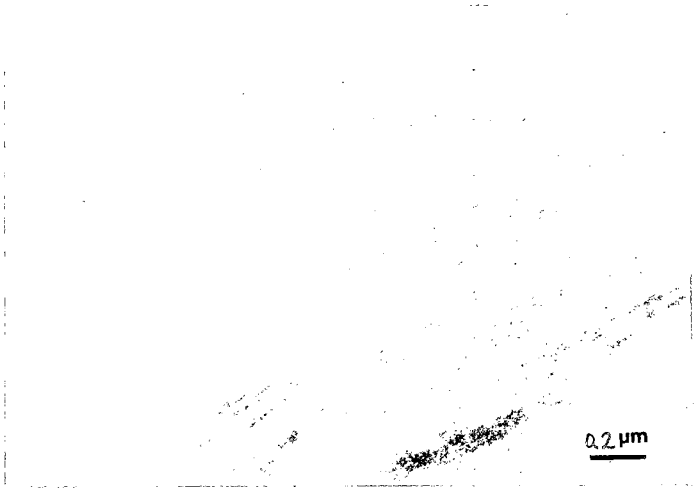

Fig. 8. TEM image showing regenerated collagen fibrils in the stroma of the mini-pig cornea received implant. Bar=0.2 μm. The average diameter of the fibrils: 22.7±5.4 nm (averaged from n=50 fibrils).

4. Discussion

In this study, both medical grade porcine collagen, commonly used in cosmetic procedures as dermal fillers or as components of face creams, and the more recently available RHC were examined as IPN scaffolds for artificial corneas. The porcine collagen comprised primarily type I collagen, the main biochemical component of the cornea, making up 71% of the dry weight of the corneal ECM [25]. The RHC used in this study was type III collagen (RHCIII). Although a more minor component of the corneal extracellular matrix [26], we recently reported that when implanted into pigs, they showed very similar performance to RHCI in terms of biocompatibility and promoting cellular and nerve regeneration [13]. Type III collagen has also been reported to have superior light transmission properties to type I collagen [27], and when fabricated into corneal implants, the resulting RHCIII hydrogels showed higher optical clarity as compared to RHCI hydrogels[13]. This is likely due to the smaller fibril diameter of type III collagen [28,29].

Poly(MPC) hydrogels are known for their high water content and ability to uptake enormous amounts of water, swelling more than 1000% [30]. This high water content renders

the hydrogels too weak for use as tissue substitutes. Kiritoshi and Ishihara [30] developed a novel MPC derivative, 2-(methacryloyloxy)ethyl-[N-(2 methacryloyloxy)ethyl]phosphorylcholine(MMPC), to crosslink MPC. The swelling degree of MMPC-crosslinked MPC hydrogels was markedly suppressed, but still as high as 200% at the highest crosslinking density they used. The mechanical properties of the crosslinked hydrogels were not reported.

In the fabrication of our IPN network, MPC was entrapped within the concentrated collagen solution. After completion of the EDC/NHS mediated amidation, as well as chemical/photo- initiated polymerization of PEGDA, these two networks intertangle with each other, preventing the polymerized MPC from swelling. As illustrated in Table 1, the water content (swelling ability) of the IPN hydrogels basically reflects that of its collagen component.

Although mechanically weak on its own, our results show that MPC incorporation in bulk enhanced the tensile strength of porcine collagen-MPC hydrogels, quintupling it from 0.13 MPa to 0.69 MPa. However, the tensile strength of RHCIII-MPC hydrogels was almost unchanged by incorporation of the MPC. In contrast to tensile strength measurements, MPC incorporation imparted an increase in elasticity (% elongation at break) to RHCIII hydrogels and a stiffness (elastic modulus) increase to porcine collagen hydrogels. The difference in mechanical strength between porcine type I collagen and RHCIII hydrogels could be due to the small fibril diameter of type III collagen, as mentioned above, which may allow for a more tightly packed hydrogel that is more robust. In this case, although RHCI-MPC hydrogels could be fabricated, their overall optical and mechanical properties were inferior to

those of RHCIII-MPC hydrogels, and therefore are not good candidates for potential clinical application (data not shown).

The resistance of MPC to collagenase digestion [10,11] was also conferred to the hybrid IPN. However, while porcine collagen-MPC hydrogels were more resistant to collagenase digestion than collagen alone, the increased resistance of RHCIII-MPC hydrogels to collagenase digestion was phenomenal by comparison. Optimized, fully synthetic RHCIII-MPC hydrogels showed almost no loss of mass for up to 50 h in concentrated collagenase, with retention of 73% of the initial mass after 26 days in collagenase. The human corneal controls showed an initial increase in mass, due to swelling (stromal edema), consistent with previous reports of excised human corneas that have been harvested for transplantation and placed in a hypotonic solution [31]. However, after this initially swelling, the human corneas showed a loss in mass, with only 3% of the initial mass remaining at day 26.

Given the exposed location of a corneal substitute with the eye, determination of implant stability following sunlight exposure/irradiation is critical. Also a patient may need appropriate eye protection if most UV irradiation from sunlight passes through the implanted hydrogel. The minimal change in the absorption spectrum of collagen-MPC hydrogels after 20 hours of irradiation suggests that the hydrogels are stable and that the patient's vision will not be affected by sunlight irradiation. On the contrary, the absorption spectrum of the human cornea is drastically altered, with significant light absorption. This finding is in keeping with previous reports that the human cornea acts as a UV filter, absorbing light in particular in the UV region [32, 33] and resulting in loss of clarity. The loss of clarity is likely due to a conformational change of collagen molecules and swelling of collagen fibrils, resulting in

light scattering [34]. The intertangled collagen-MPC networks therefore most likely act to prevent such conformational changes. Because collagen-MPC hydrogels show very limited UV absorption, UV light may pass through the implants readily to the retina. However, it is also important to note that the corneal epithelium also has an important role in UV absorption and protective effects [32], so fully epithelialized implants may be UV-protective. In any case, patients receiving collagen-MPC implants could wear UV-protective sunglasses to protect their retinas from sun-damage. Alternatively, a UV blocking agent could also be incorporated into collagen-MPC implants.

The IPN hydrogels support epithelial cells and nerve overgrowth *in vitro* at rates that are comparable to benchmark collagen hydrogel and tissue culture polystyrene, indicating that they are good candidate materials for corneal substitutes.

In vivo pig implantation results demonstrated a re-epithelialization rate that is comparable to the rate of wound healing in normal healthy human cornea and our previous implants with collagen-only hydrogels [4, 13]. The morphology of the regenerated epithelium, expression of differentiation markers, along with TEM observations showing regenerated basement membrane and hemidesmosomes demonstrate that this epithelium is stable, and comparable to that of the untreated, contralateral control corneas. Although previously reported synthetic IPN hydrogels that were surface grafted with collagen supported the epithelial cell migration, e.g. in rabbit models, the rate of migration and morphology of the epithelium were not normal [35]. In addition, nerves were not regenerated in these synthetic IPNs, whereas the collagen-MPC IPNs, including the fully synthetic recombinant human collagen-MPC hydrogels, clearly supported nerve regeneration. Along with the stromal cell ingrowth observed, the histological results therefore show successful

regeneration of corneal tissue and associated nerves, and full integration of the implant into the host tissue and the restoration of a functional cornea.

The positive albeit low levels of procollagen staining observed in the implants as well as TEM images show the presence of collagen fibrils elaborated by corneal cells, suggesting gradual remodeling of the implant matrix. The diameters of the regenerated collagen fibrils in the implant region at 12 months post-operative were 24.3±2.4nm, 28.4±6.2nm and 22.7±5.4nm, respectively, for the three different pigs. These values are close to our previously reported collagen diameters for allograft and untreated pig controls [6] and accounting for the optical clarity of the hydrogels. The absence of macrophages and lack of anti-smooth muscle staining (indicating the absence of myofibroblasts) further demonstrate that the implants are well-tolerated by the host.

The recombinant human collagen-MPC in rabbits showed similar host-graft integration, and regeneration of epithelium, stroma and corneal nerves by slit lamp biomicroscopy and *in vivo* confocal microscopy. Although these implants are part of a more extensive comparative study of implant performance in healthy corneas versus an injury model, the results presented here show that a fully synthetic IPN comprising recombinant collagen made in yeast and a synthetic phosphorylcholine, is able to support regeneration of corneal epithelium, stroma as well as nerves, unlike previously reported fully synthetic, primarily core-and-skirt corneal implants designed as prostheses [2, 3, 35], where there may/may not be epithelial overgrowth over the central optical core, and stromal cell growth into the surrounding skirt to anchor the devices.

The in bulk incorporation of MPC, as opposed to surface immobilization [10], resulted in IPNs with the desired characteristics of both original components, along with

novel features. For example, MPC and polymeric MPC-derivatives are well-established anti-fouling agents [36, 37]. However, with polymeric MPC as part of the collagen-MPC IPN, the resulting hydrogels were fully bio-interactive, capable of promoting corneal cellular regeneration from surrounding host stem or progenitor cells. In addition, the hydrogels are capable of allowing nerve regeneration following injury or surgery.

5. Conclusions

Here we demonstrate that by incorporating MPC as a network, using PEGDA as a crosslinker into a collagen network to form an IPN, a hydrogel with significant mechanical strength, high stability against degradation by collagenase enzyme or UV exposure and capable of sustaining an ECM-like environment was produced. Furthermore, this hydrogel is able to interact with host tissues to promote tissue regeneration by mobilizing endogenous host stem or progenitor cells. These properties make collagen-MPC hydrogels potential candidates for use as future corneal matrix substitutes.

Acknowledgements

We thank Mr. Minoru Fukuda at Kyorin University for excellent TEM assistance and Subhadra Dravida for technical assistance with immunohistochemistry. Funding support from NSERC and CIHR Canada CHRP grant no. 337436 to M. Griffith and J.C. Scaiano; NSERC studentship to C.R. McLaughlin.

Chapter 5

5.1 Manuscript 4

Regeneration of Functional Nerves within Full Thickness Collagen-phosphorylcholine Corneal Substitute Implants in Guinea Pigs.

Accepted for publication in Biomaterials December 11th, 2009 manuscript number jbmt12423

While the previous manuscript investigated the use of carbodiimide crosslinked type 1 porcine collagen MPC corneal substitutes in partial thickness lamellar keratoplasty, it did not examine full thickness penetrating keratoplasty. Also, it has not been shown whether the nerves are functioning normally compared to the unoperated controls. In the present manuscript, it was found that after six months, the regeneration of the corneal tissue was observed (epithelium, stromal cells). Electrophysiology showed evidence of mechano-nociceptors, cold sensing, and polymodal units. The incidence of units exhibiting ongoing activity and the frequency value of their spontaneous firing was higher in fibers recorded from implanted corneas than in control eyes, which has been reported for regenerating fibres. Following eight months, the spontaneous firing of the nerve terminal impulses was similar to contralateral unoperated corneas.

Regeneration of Functional Nerves within Full Thickness Collagen-Phosphorylcholine Corneal Substitute Implants in Guinea Pigs.

Christopher R. McLaughlin,[1,2,*] M. Carmen Acosta,[3,*] Carolina Luna,[3] Wenguang Liu,[1,2] Carlos Belmonte,[3] May Griffith,[1,2,§] and Juana Gallar.[3,§]

[1]*University of Ottawa Eye Institute, The Ottawa Hospital, General Campus, 501 Smyth Road, Ottawa ON K1H 8L6, Canada*

[2]*Dept. of Cellular and Molecular Medicine, University of Ottawa, Ottawa, ON, Canada*

[3]*Instituto de Neurociencias de Alicante, Universidad Miguel Hernandez-CSIC, Avda. Santiago Ramón y Cajal s/n, San Juan de Alicante 03550, Spain*

[*,§]*Equal Contribution*

Short title: Functional nerves in corneal substitutes

Corresponding Author:

email: mgriffith@ohri.ca; phone: (613) 737-8899, ext. 74011; fax: (613) 739-6070

Key words:

Cornea, nerve regeneration, collagen structure, scaffold, ophthalmology

Co-author Contributions to Manucript

Acosta, M. Carmen

Dr. Acosta is a post doctoral fellow at the Universidad Miguel Hernandez in Alicante. She was responsible for performing electrophysiological recordings of the implanted artificial corneas.

Luna, Carolina

Dr. Luna is a post doctoral fellow at the Universidad Miguel Hernandez in Alicante. She was responsible for assisting with the electrophysiological recordings of the implanted artificial corneas.

Liu, Wenguang

Dr. Liu was a post doctoral fellow who developed the chemically crosslinked collagen MPC formulation, and prepared the hydrogels.

Belmonte, Carlos

Dr. Belmonte is an electrophysiologist at the Universidad Miguel Hernandez in Alicante, who developed the experimental design for the recordings of corneal nerves.

Griffith, May

Dr. Griffith was my supervisor, and was responsible for the overall design and management of all the project, and manuscript revision.

Gallar, Juana

Dr. Gallar is a corneal electrophysiologist at the Universidad Miguel Hernandez in Alicante, and contributed to the project design, and analysis of the electrophysiology data.

Abstract

Our objective was to evaluate promotion of tissue and nerve regeneration by extracellular matrix (ECM) mimics, using corneal implantation as a model system. Porcine type I collagen and 2-methacryloyloxyethyl phosphorylcholine (MPC) were crosslinked using 1-ethyl-3-(3-dimethyl aminopropyl) carbodiimide (EDC) and *N*-hydroxysuccinimide (NHS) and moulded into appropriate corneal dimensions to serve as substitutes for natural corneal ECM. These were implanted as full-thickness grafts by penetrating keratoplasty into the corneas of guinea pigs after removal of the host tissue, and tracked over eight months, by clinical examination, slit-lamp biomicroscopy, and esthesiometry. Histopathology and *ex vivo* nerve terminal impulse recordings were performed at three months and at eight months. The implants promoted regeneration of corneal cells, nerves and the tear film, while retaining optical clarity. After three months, electrophysiological recordings showed evidence of mechano-nociceptors, and polymodal units inside the implants, while cold sensitive units were present only on the peripheral host cornea. Following eight months, the incidence of nerve activity and the frequency of spontaneous firing were higher than in control eyes as reported for regenerating fibers. Active cold nerve terminals also innervated the implant area. We show that ECM mimetic materials can promote regeneration of corneal cells and functional nerves. The simplicity in fabrication and demonstrated functionality shows potential for ECM substitutes in future clinical applications.

1. **Introduction**

The cornea is the transparent outer covering of the eye and major refractive element. Corneal function depends on its transparency and any trauma or disease that leads to irreversible opacification will result in vision loss and blindness. It is estimated that there are 50 million people worldwide who possess bilateral blindness, as well as at least 150 million people who have impaired vision in both eyes [1, 2]. Treatment consists of transplantation of human donor corneas, and unfortunately, there is a shortage in most countries.

Artificial corneas are being developed [3-5]. Most artificial substitutes developed are prostheses (keratoprostheses) designed to restore minimal function of light transmission and protection of the delicate internal structures of the eye. Most importantly, they do not address the loss of corneal innervation, even though it is now recognized that the cornea, being an avascular organ, is unique in its dependence upon its sensory nerves and the interaction of these nerves with corneal cells for maintenance of tissue integrity and wound healing [6]. In general, the prostheses have been in limited use.

Very recently, we completed a Phase I human clinical trial with a biomimetic corneal substitute designed to promote endogenous regeneration, as a possible alternative to allografting as a treatment, and to alleviate donor tissue shortage. We showed for the first time in humans that implants mimicking the bioactive extracellular matrix scaffolding of the cornea are able to promote regeneration of corneal tissue and nerves [7]. Despite the success of this clinical trial, these implants, made from carbodiimide-crosslinked recombinant human collagen, were designed to turnover and only address clinical indications that affect the epithelium and superficial stromal layers. To extend the functionality of our biomaterials for use in full-thickness grafts or to address disease conditions where excessive enzyme

production occurs, tougher and more enzyme resistant interpenetrating networks (IPNs) of collagen and phosphorylcholine (2-methacryloxy-ethylphosphorylcholine) (MPC) were developed and tested in pig models as lamellar grafts [8]. The collagen-MPC implants remained stably integrated over the 12 month study period, with regeneration of corneal tissues and nerves.

However, there are many different types of nerves innervating the cornea (see Belmonte et al., 2004 for a review) [9]. Corneal neurons can be classified morphologically as either thin myelinated A-delta, or unmyelinated C axons. Immunohistochemical analysis reveals that approximately 60% of corneal sensory neurons are immunoreactive to calcitonin gene related peptide (CGRP), and 20% contain the neuropeptide substance P [10, 11]. Approximately 20% of corneal fibers respond to mechanical forces and are thus characterized as mechanonociceptors, similar to those found in the skin but with activation thresholds orders of magnitude lower. They fire impulses transiently in response to contact of the corneal surface. The majority of corneal fibers (70%) are polymodal nociceptors which are activated by near noxious mechanical insult and present thermoresponsiveness to corneal temperatures above 39°C and noxious cooling below 29°C. Also, they respond to exogenous chemical irritants, as well as to endogenous chemical mediators produced from damaged corneal tissue, by inflammatory cells [12, 13]. Additionally, about 10% of corneal sensory fibers are thermosensitive cold units recruited only by low to moderate temperature drops [13, 14].

To date, there is no information on whether collagen-phosporylcholine hydrogel scaffolds or other ECM mimetic corneal substitutes are able to promote regeneration of all the different sub-types of sensory nerves, or whether there are sub-types that regenerate while

others do not. Information on the activity of various sub-types of regenerated nerves would provide information on the function of the regenerated cornea. We also have no information on whether nerves would regenerate in a full-thickness graft as well as in partial thickness grafts as we had previously observed [8]. Thus, the aim of the present study was to examine in detail the functional regeneration of corneal nerves by studying the spontaneous and stimulus-evoked activity of corneal sensory afferents regenerating in collagen-MPC hydrogels. In order to ensure that this was a viable model of nerve regeneration, we also had to demonstrate in parallel, the safety and efficacy of these hydrogels as full-thickness corneal substitutes that promoted regeneration of both nerves and the corneal tissue they interact with.

2. Materials and Methods

2.1. Materials

Type I porcine atelocollagen was purchased from Nippon Meat Packers Inc. (Tokyo, Japan). 2-methacryloxy-ethylphosphorylcholine (MPC) was from Biocompatibles, UK. Poly(ethylene glycol) diacrylate (Mn=575), 1-ethyl-3-(3-dimethylaminopropyl) carbodiimide (EDC), ammonium persulphate (APS), and N,N,N',N'- tetramethyl ethylene diamine (TEMED) were supplied by Sigma-Aldrich, USA. N-hydroxyl-succinimide (NHS) was purchased from Fluka (Buchs, Switzerland). Morpholinoethanesulfonic acid (MES) was provided by EMD chemicals Inc, USA. All other reagents were of analytical grade and used as received.

2.2 Preparation of Collagen-MPC hydrogels with chemical initiator–APS/TEMED

400 mg of 20 % (w/w) porcine type I acidic atelocollagen solution was buffered with 150 µl of 0.625 M MES buffer and thoroughly mixed with calculated volumes of 2-methacryloxy-ethylphosphorylcholine (MPC) solution and a poly(ethylene glycol) diacrylate (PEGDA) solution, at 4 °C. A syringe pump, that we previously described, was used. The collagen:MPC ratio was 4:1 (w/w). The MPC:PEGDA ratio was 3:1 (w/w). Both solutions were prepared in 0.625 M MES with 25ul of 4% (w/w) ammonium persulphate (APS) / N,N,N',N'- tetramethyl ethylene diamine (TEMED). MES solution was added to the collagen-MPC-PEGDA solution and thoroughly mixed at 0°C. Calculated volumes of 1-ethyl-3-(3-dimethylaminopropyl) carbodiimide (EDC), and N-hydroxysuccinimide (NHS) solution (both at 20% wt/vol, EDC:NHS:collagen-NH_2=1.5:1.5:1) were then added to crosslink the collagen and again thoroughly mixed at 4°C. The final mixed solution was immediately dispensed onto a glass plate. The hydrogels were cured at 100% humidity under nitrogen at room temperature for 16 h and then at 37 °C for 5 h. After demoulding, they were washed thoroughly with 0.1M phosphate buffered saline (PBS) and then stored in PBS containing 1 % chloroform to maintain sterility. Hydrogels with different collagen to MPC ratios, 2:1 or 1:1 were similarly prepared.

2.3. Physical and mechanical characterization

Optical properties (white light transmission, backscatter and refractive index), equilibrium water content, thermal properties and glucose and albumin permeability of the implants were determined as we had previously described [15]. Mechanical properties

(tensile strength, % breaking strain and elastic modulus were also measured as we previously described using an Instron electromechanical universal tester [15]. Physical and mechanical properties are reported in Liu et al 2009 [8]. In addition, the ability of the implants to tolerate the placement of interrupted and continuous sutures was also examined.

2.4. In vitro biocompatibility and performance

Epithelial coverage and nerve surface growth on collagen-MPC gels and crosslinked collagen controls were evaluated as previously described in detail, using an immortalized human epithelial cell line and dorsal root ganglia isolated from embryonic day 8 chick embryos [15, 16].

2.5. Implantation and clinical evaluation

With ethics approval from both the University of Ottawa (Protocol EI-14) and University Miguel Hernández and in accordance with animal care guidelines through ARVO, collagen-MPC hydrogels (150 μm thick and 3.5 mm diameter) were implanted into the corneas of Duncan Hartley guinea pigs. Experiments were carried out on male Dunkin Hartley guinea-pigs (Harlan, Barcelona, Spain) weighing about 400 g at the beginning of the procedure. Animals were housed on a 12 h/12 h light/dark cycle with food and water available *ad libitum* for at least 1 week prior to initiating the experiments. Guinea-pigs were anaesthetized by isofluorane. A circular incision was performed with a 3.0 mm diameter trephine in the central cornea of the right eye, and the host tissue was removed manually. Then, a tissue-engineered corneal substitute (3.5 mm diameter, 150 μm thick) was implanted, as in penetrating keratoplasty, and held in place with 10-0 continuous suture. Immediately after

implantation, topical antibiotic (two drops of 3 mg/ml tobramycin; Tobrex, Alcon, Spain) was administered to the surgical eye. Upon full recovery from the anesthesia the animals were returned to their home cages. Postoperative medication included 0.02 mg/kg buprenorphine hydrochloride (Buprex, Schering-Plough, Madrid, Spain) and topical tobramycin during 2 and 7 days after surgery, respectively. Within 48 hours after surgery, two out of 20 implants were extruded and animals were euthanized according with the endpoint criteria. The remaining animals remained healthy, as assessed by their normal weight gain, activity, and grooming.

At different times after surgery (1-2 days, and 2, 3, 6 and 8 months), corneas were subjected to slit-lamp examination and fluorescein staining to ascertain the success of the surgical procedure. Corneal sensitivity was evaluated measuring the corneal touch threshold (CTT) with a Cochet-Bonnet esthesiometer. As nerves start to invade the type of implant used in this study at two months post-surgery [17], nerve activity was recorded at 3 and 8 months.

2.6. Histopathological Evaluation

Eight guinea pigs were sacrificed after 6 months post-implantation. Operated right eyes from guinea pigs were enucleated and fixed in 4% paraformaldehyde for 45 minutes. Corneas were excised under a surgical scope, cut into quarters and washed with 0.1M Tris Buffered Saline (TBS). One quarter was taken for wholemount staining, while the remainder was processed for histopathological analysis. Permeabilization and blocking was performed for 1 hour in 0.2% Triton X-100, 4% foetal bovine serum, 1% bovine serum albumin in TBS. Corneas were incubated in a 1:200 dilution of neural specific β III tubulin antibody (Tuj1)

overnight at 4°C. After three washes in blocking solution, the corneas were incubated with 1:300 anti-mouse CY3 conjugated secondary antibody for 5 hours at 4°C. The corneas were then coverslipped in mounting medium and imaged on a Nikon microscope. Multiple images were taken and overlayed using Nikon software.

Corneas with implants and control unoperated corneas were processed for histopathological examination by light microscopy. Sections were stained with H&E for routine histopathological examination. Frozen sections were stained with Collagen VII, a marker for anchoring fibrils in hemidesmosomes, AE-5, a differentiated epithelial cell marker, vimentin, a stromal cell marker, and Na^+/K^+ ATPase, an endothelial marker, by standard immunofluorescence. Sections were blocked with 4% FCS + 1% BSA in 0.1 M PBS, pH 7.4, 0.2% Triton X-100 and incubated in primary antibody (1: 200) overnight at 4°C. They were then incubated with 1:400 FITC conjugated secondary antibody (Sigma) and visualized on a Zeiss Axioskop 2.

2.7. Electrophysiology

2.7.1. Nerve recording

Two types of preparations were used for electrophysiological recording of single unit electrical activity from the superfused eye of the guinea pig *in vitro*. The first (Fig. 1A) was preferably suitable for recording the units that were characterized as mechanonociceptive or as polymodal nociceptors, while in the second one (Fig. 1B), cold sensitive units could be easily identified. At 24-48 hours and three and eight months after corneal surgery, animals were euthanized with an overdose of sodium pentobarbitone and both eyes (contralateral and implanted) were immediately excised.

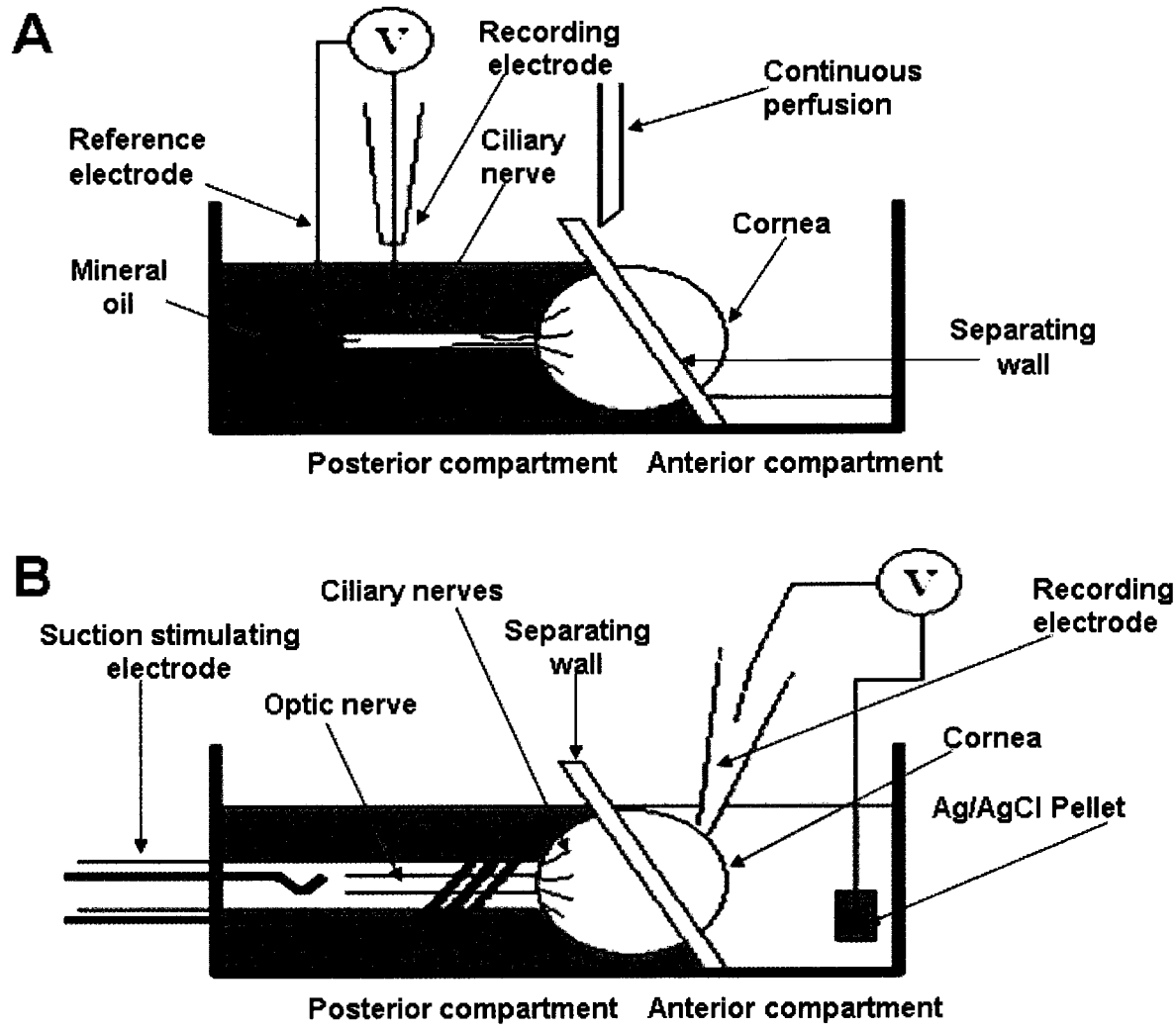

Fig. 1. Schematic diagram of the recording set-ups used in the experiments.

2.7.2. Recording of corneal nerve fiber impulse activity (Fig. 1A)

The eyes were enucleated including the bulbar and tarsal conjunctiva, with the optic and ciliary nerves. The connective tissue and extraocular muscles were carefully removed from the back of the eye and the ciliary nerves around the optic nerve were exposed. The

excised eye was then placed in a double chamber specially designed to keep the anterior segment of the eye with the conjunctiva separated from the back pole and the ciliary nerves. In the front part of the chamber the conjunctiva was pinned to the separating wall in order to segregate both compartments, which were perfused separately. Thus, only the nerve terminals on the cornea were affected by stimuli applied to the front part of the chamber, but not the axons located in the back part. The anterior compartment was perfused with warmed (32-34°C) physiological saline solution of the following composition (in mM): NaCl, 133.4; KCl, 4.7; $CaCl_2$, 2; $MgCl_2$, 1.2; $NaHCO_3$, 16.3; NaH_2PO_4, 1.3; glucose, 7.8. This solution was gassed with carbogen (95%O_2, 5%CO_2) to pH 7.4. In the rear division of the chamber, filled with warmed mineral oil, nerve filaments were teased apart from the ciliary nerves and placed on an Ag-AgCl electrode for monopolar recording of single unit impulse activity, using conventional electrophysiological equipment (gain x10000, high pass 300Hz, low pass 3 KHz, DAM50 amplifier, WPI, Sarasota, FL, USA). Electrical signal was collected to a PC with an acquisition system (CED Micro1401, Cambridge Electronic Design, Cambridge, UK), and analyzed with Spike 2 software (v 6.0, also from CED). Spontaneous activity was measured for 1 min before any stimulation. Mechanical threshold was determined with calibrated von Frey hairs (range 0.25-32.00mN). Receptive fields (RF) of corneal afferent fibers were located using mechanical stimulation with a fine paintbrush and mapped using a suprathreshold von Frey hair. For chemical stimulation a gas jet of 98.5% CO_2 was applied on the corneal RF during 30s [18]. Thermal stimulation was performed heating (up to 45°C) or cooling (down to 20°C) the perfusion solution using a custom-made Peltier device. Electrical pulses (0.1-1.5mA, 0.5ms, 1Hz; S48 stimulator, Grass, Warwick, RI, USA) applied

on the receptive field were used to measure conduction latency and then calculate conduction velocity of the recorded fibers (see below).

2.7.3. Recording of corneal nerve terminal impulses (Fig. 1B)

Single unit extracellular recordings from cold-sensitive corneal nerve terminals were made using a method adapted after Brock et al [19]. Briefly, the eyes were enucleated and mounted in a recording chamber also divided in two compartments to separate the cornea from the back of the eye and the optic and ciliary nerves. The eyes were continuously superperfused with the physiological solution at 32-34°C. In the back part of the chamber the optic nerve and associated ciliary nerves were drawn into a suction electrode for electrical stimulation to measure the latency of electrically-evoked spikes. Conduction velocity then was calculated from the values of conduction latency and the distance between the stimulating and recording electrodes, measured with an 8.0 gauge thread placed along the trajectory of the nerve [18].

Nerve terminal impulse activity was recorded using glass micropipette electrodes applied to the surface of the cornea and secured with slight suction. The pipettes had a tip diameter of around 60μm and were filled with physiological solution. Signals were recorded with respect to an Ag/AgCl pellet in the bath. Electrical activity was amplified (1000x, AC preamplifier NL 103, Digitimer, Welwyn, UK), filtered (high pass 150Hz, low pass 5KHz; NL 125, Digitimer), collected to a PC with a CED micro1401 acquisition system, and analyzed with the indicated software.

Spontaneous and stimulus evoked impulse activity were registered from recording sites where the electrical activity originated from a single nerve terminal. Mechanical stimulation was made applying light suction to the recording pipette with a syringe, or by pushing the recording electrode gently against the corneal surface with a slight displacement of the micromanipulator. Thermal stimulation was done modifying the temperature (from control temperature down to 20°C or up to 50°C) of the physiological solution bathing the cornea with a Peltier cell. Nerve impulses originating from single cold-sensitive nerve endings were identified by their rhythmic ongoing discharge which increased upon cooling and decreased upon warming the perfusion solution. Spontaneous activity at basal temperature was recorded for at least 1 minute prior to the application of a cooling pulse (20°C over approximately 10 s), followed by re-warming to the baseline temperature. After re-establishing stable baseline activity, the solution bathing the cornea was heated to about 50°C and re-cooled again to baseline temperature.

2.7.4. Data analysis

Data were collected and processed for statistical analysis (SigmaStat, v 3.5; Systat Software, Erkrath, Germany). Data are expressed as mean ± SEM, with n being the number of explored nerve terminal or fiber impulses. Changes of firing in response to CO_2 pulses or temperature changes (cooling or heating) in implanted and contralateral corneas were compared using the Mann-Whitney rank sum test and t-test, as indicated. Z-test or Fisher's exact test were using to compare proportions, as indicated. $P<0.05$ or below was considered significant.

3. Results and Discussion

3.1. Clinical and histopathological evaluation of corneal regeneration

No adverse inflammatory reactions were observed in guinea pigs, with full epithelial coverage complete within the first week post-surgery, as demonstrated by fluorescein staining. Neovascularization occurred in all guinea pigs with implants, but this was resolved by administration of steroids drops two weeks post implantation.

Mild to moderate haze (+2 to +3) was observed in all guinea pigs implanted with collagen-MPC hydrogels at three weeks post implantation (Fig. 2B), when the sutures were removed. It was present for the next four to five weeks but was typically resolved at around eight weeks post implantation. We have previously observed similar haze in mice transplanted with full thickness porcine collagen implants, which resulted in a low grade immunological response, and caused the formation of a retro corneal membrane [20]. In these guinea pigs, by six months post-operative, all implanted grafts recovered transparency (Fig. 2C).

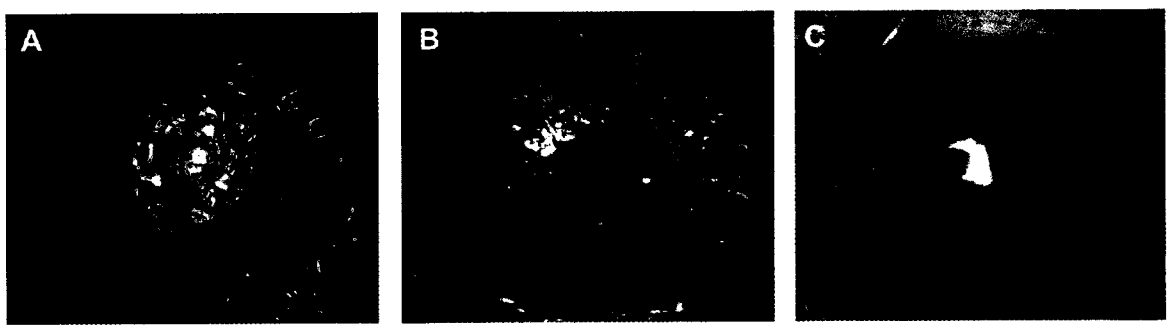

Fig. 2. Corneal implantation by penetrating keratoplasty showing the implant at (A) 1 hour post-operative. Neovascularization and a mild to moderate haze (arrow) was observed at 3 weeks post-operative (B) and remained for another 4-5 weeks. The haze then resolved so that the cornea was optically clear at 6 months post-operative (C).

H&E sections of untreated corneas (Fig. 3A) and collagen-MPC implanted corneas (Fig. 3B) at six months post surgery all showed seamless host-graft integration, suggesting a correlation of recovery of transparency with the recovery of corneal microarchitecture and/or function. A non-keratinized, stratified epithelium was observed in all corneas, along with stromal cells in a lamellar arrangement. Both the implants (Fig. 3D) and controls (Fig 3C) were positive for AE – 5, an antibody directed towards keratin 3 and keratin 12, and an indicator for terminally differentiated epithelial cells. Staining for collagen VII was also positive, indicating the presence of anchoring fibrils and stable attachment of the epithelium to the underlying corneal substitute (Fig. 3F). Vimentin staining positive cells were present in both the control and implanted eyes (Fig. 3H), showing that infiltration of host stromal keratocytes had occurred in grafts. At six months post-operative, they show a lamellar arrangement that we have previously observed in partial thickness grafts in pigs [8]. These observations along with recent human clinical trial *in vivo* confocal microscopical observations (unpublished) suggests that the early transient haze observed likely coincides with the in-growth of stromal cells. Endothelial cells were also present, as visualized by the positive staining for sodium/potassium ATP-ase (Na^+/K^+ ATPase) observed in implanted eyes (Fig. 3J). Unlike the case in mice [20], there was no retrocorneal membrane formation.

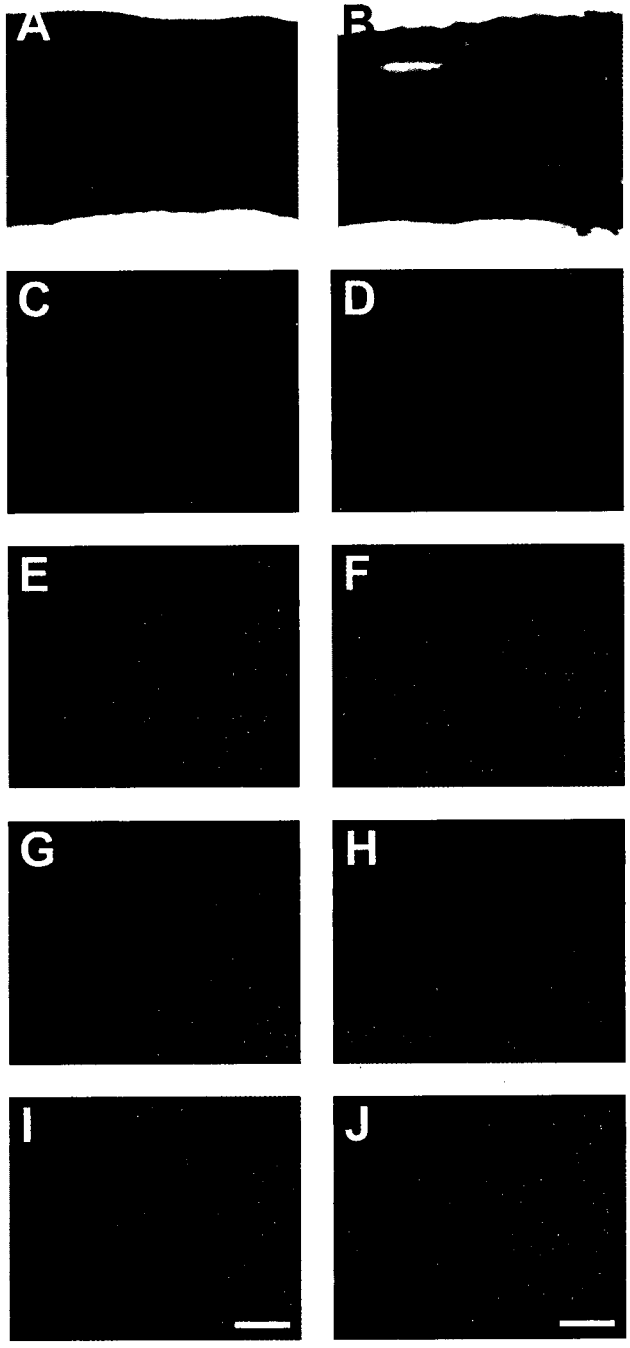

Fig. 3. Histology of control (left panels) and collagen MPC corneal substitute (right panels) at 6 months post implantation. (A-B): H&E staining of unoperated (A) and operated cornea (B), both showing a stratified epithelium over a stroma. (C-D) Cytokeratin staining showing the presence of a normal, differentiated, stratified, non-keratinizing epithelium in the unoperated (C) and operated cornea (D). (E-F) Collagen VII staining at the epithelial/stromal junction in the operated cornea indicate the presence of anchoring fibrils in both operated (F) and control (E) corneas. (G-H) Vimentin staining of the stromal keratocytes indicating infiltration of the corneal substitute (H) by host corneal cells. (I-J) Na^+/K^+ ATPase staining shows an intact endothelium covering the implant (J) compared to the unoperated eye (I). Scale bars, 50 μm.

Na^+/K^+ ATPase is an ion transporter found on the lateral membrane of corneal endothelial cells and serves to actively transport Na^+ ions from the corneal stroma to the aqueous humor. Its combined pump/leak action maintains corneal hydration, stromal

thickness, and overall corneal clarity [21, 22]. In humans, the corneal endothelium does not undergo proliferation at a rate sufficient to replace damaged or dead cells [23, 24]. Loss of central corneal endothelial cells occurs at a rate of 0.5% to 0.6 % per year [25], and to compensate for this, neighbouring endothelial cells will migrate and spread from the periphery and enlarge to cover the defect. As in humans, cellular division plays a minor role in the coverage of small to medium-sized defects in the corneal endothelium of guinea pigs. No mitotic activity is observed in normal endothelium or during re-growth after small or medium size lesions [26]. However, unlike humans, after full cellular denudation, cell division will occur to repopulate the endothelium [27]. The occurrence of endothelial cell division, therefore, depends both upon the species, and on the size and type of injury [26]. The implantations performed in the present study cover approximately 20-25% of the corneal surface, representing a medium size lesion, and most likely, coverage of the implant involved migration and spreading, like the human cornea, rather than cell proliferation.

Even though the human corneal endothelium does not undergo cell division *in situ*, endothelial cells can be expanded *in vitro*. We have shown that our collagen-based scaffolds promote the growth of human endothelial cells *in vitro* [28]. An ideal scenario would be to use the patients own endothelial cells to replace those that are lost. This could either be accomplished by inducing the patient's endothelial cells to grow *in vivo*, or by explanting precursor cells onto the scaffold prior to implantation. Due to the low *in vivo* proliferation, there have been attempts to stimulate the endothelial cells through gene therapy, to develop an *in situ* treatment method [29], but this has only been tested *ex vivo*. Another method that is being employed, involves the identification of corneal endothelial precursor cells. In 2005, it was observed that some peripheral corneal endothelial cells would incorporate BrdU,

which increased upon wounding [30]. Adult stem cell colonies have been isolated from various human tissues using the sphere forming assay [31, 32], and corneal endothelial precursors have been isolated. They expressed neuronal (glial fibrillary acidic protein, beta III tubulin) and mesenchymal markers (alpha smooth muscle actin), however they had a limited self renewing capacity, and were subsequently deemed as progenitors, or precursors. Upon differentiation, the cells show normal endothelial cell morphology and pump functions [33]. Precursors isolated from rabbits and humans shows that the sphere forming capacity (number of spheres/cells isolated) is highest in the periphery of the endothelium compared to the centre [34]. Therapy has been investigated for treatment of small endothelial defects through direct injection of spheres into the anterior chamber in a rabbit model [35]. There are early indications that sphere-forming precursors could be seeded on denuded amniotic membranes, and be induced to differentiate into endothelial cells with normal hexagonal morphology [36].

3.2 Corneal Nerve Regeneration: Wholemount Observations

In the intact cornea, sensory nerves from the ophthalmic branch of the trigeminal ganglion [37-39] enter the periphery of the cornea in a radial manner, losing their myelin sheath and subdividing into thinner nerve trunks that bifurcate and anastomose forming a dense stromal plexus, which then enters the basal epithelium and forms the subbasal nerve plexus (SBP). There, nerve bundles run parallel to the surface forming the so called "epithelial leashes", from where single nerve fibers split off and bend, ascending between the epithelial cells, eventually terminating in the most superficial epithelium as free nerve

endings [11], the structures where transduction of natural stimuli into nerve impulses take place [40].

In the collagen-MPC implants, nerve fibers entered the periphery of the cornea in a similar manner, as nerve trunks that branched in the stroma into thinner nerve bundles. (Fig 4B), and even originating a subbasal nerve plexus with identifiable epithelial leashes (Fig 4C). We have previously shown that nerves will regenerate into collagen based artificial corneas implanted through lamellar keratoplasties [8], but this is the first time it has been observed in full thickness implants. Corneal innervation is important for maintaining proper function of the cell types of the cornea [6]. Current keratoprosthesis design does not permit the regrowth of nerves, which might explain the increased complications and extrusion rates following implantation [26]. The collagen – MPC implants, however, allowed for the regeneration of corneal nerves into the implanted area, which is beneficial for proper corneal homeostasis and function.

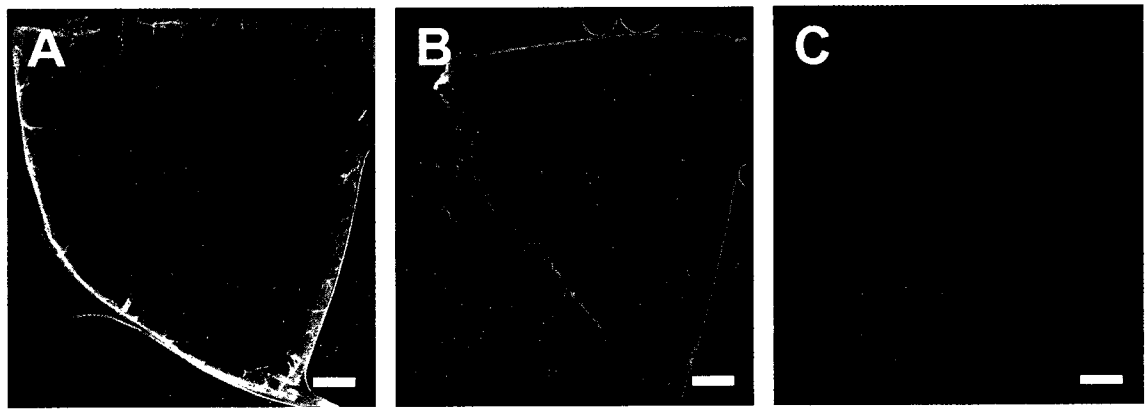

Fig. 4. Penetration of corneal nerves into collagen MPC corneal substitutes. Stromal nerves bundles were localized in wholemounts from unoperated (A) and operated corneas (B) using immunostaining for anti β–III tubulin. Both large and small diameter nerve bundles were observed to enter the implant, and were present at varying depths through the cornea, reaching finally the subbasal nerve plexus level (C). Scale bar for A-B = 500 μm, for C = 50μm.

3.3. Electrophysiology

3.3.1 Post surgical recording of nerve activity

Electrical activity was recorded from operated and from contralateral (control) corneas. At 1-2 days after surgery, no electrical activity could be recorded inside the implant in three separate eyes, while nerve activity was present outside the corneal substitute (n=20 units, data not shown). Nine units recorded from implanted corneas at three months post-surgery and nineteen recorded after eight months were analyzed. Nineteen units recorded from contralateral eyes were recorded as control. When the cornea is subjected to surgical manipulation, and the corneal nerves are severed as during penetrating keratoplasty, the axons undergo Wallerian degeneration within hours following the injury [39]. Gradually, the axonal stumps regenerated and form microneuromas, which lead to sprouts that enter the denervated tissue [38] or in this case, the artificial cornea.

3.3. Electrophysiology

3.3.1 Post surgical recording of nerve activity

Electrical activity was recorded from operated (n=10) and from their contralateral (control) corneas. At 1-2 days after surgery, no electrical activity could be recorded inside the implant in three separate eyes, while nerve activity was present outside the corneal substitute (n=20 units, data not shown). Nine units recorded from three implanted corneas at three months post-surgery, and 19 units recorded from four corneas after eight months were analyzed. Nineteen units recorded from contralateral eyes were recorded as control. When the cornea is subjected to surgical manipulation, and the corneal nerves are severed as during

penetrating keratoplasty, the axons undergo Wallerian degeneration within hours following the injury [41]. Gradually, the axonal stumps regenerate and form microneuromas, which lead to sprouts that enter the denervated tissue [40] or in this case, the artificial cornea. These results support the suitability of these full thickness artificial scaffolds as an adequate milieu to allow reinnervation of functionally active corneal nerves.

3.3.2 Electrophysiological recordings at three and eight months post surgery

3.3.2.1 Conduction velocity

Determination of conduction latency was intended to be measured in all studied sensory receptors recorded from implanted and contralateral corneas. However the electrically-evoked nerve impulse was not always detectable because of the large electrical artifact, resulting only in two occasions in implanted corneas at three months. This is probably due to the small size of guinea-pig eyes and, thus, the short distance between stimulating and recording electrodes, resulting that the electrically-evoked spike is overlapped with the much larger artifact originated by electrical stimulus. Conduction velocities measured in these two units were 2.3 m/s and 7.0 m/s, in the A-delta range. Conduction velocity was also measured in six out of 19 fibers recorded from contralateral eyes, being also in the A-delta range (mean value of 4.8±0.3 m/s) (Table 1).

Table 1. Functional properties of corneal sensory units, recorded from contralateral and implanted eyes at 3 months post-surgery.

	Implanted	Contralateral
Conduction velocity (m/s)	4.7±1.7 (2.3-7) 2/28	4.8±0.3 (2-7) 6/19
Receptive field diameter (mm)	3.0±0.0 (3)	3.0±0.1 (2-4)

Data are expressed as the mean ± SEM; the range is shown in brackets. No. of responding units/No. of explored units is also shown.

3.3.2.2 Incidence of response to mechanical, chemical and thermal stimulation

Based on their response to mechanical, chemical and thermal stimulation, fibers functionally identified as mechano-nociceptors (MN, those responding only to mechanical forces applied to their receptive field), polymodal nociceptors (PN, with response to mechanical, chemical and heat stimulation) and cold thermoreceptors (CT, showing sensitivity to temperature reductions) were recorded from implanted and contralateral eyes. In addition to these three types of functionally classified sensory receptors, three fibers firing spontaneously and not responding to any intended stimulation except to electrical stimuli were found in implanted corneas. This may be due to an abnormal activity of regenerating nerve fibers due to changes in the expression of membrane channels involved in the stimulus transduction, altering their response to natural stimuli, or in nerve impulse propagation thus increasing nerve impulse transmission [42].

3.3.2.3 Nociceptive units

3.3.2.3.1 Location of receptive fields

Using suprathreshold mechanical stimulation with von Frey hairs, the receptive fields of 11 corneal nociceptive units recorded from four eyes with implanted corneas, and of 14

nociceptors recorded from four contralateral eyes were mapped and their size measured. No differences were found between receptive field diameters of nociceptive units measured in implanted and contralateral corneas (Table 1). In contralateral eyes, RF of nociceptors usually covered a quadrant of the corneal surface, sometimes including also part of the adjacent sclera. At three months after surgery, some nociceptors presented RF that reached the limits of the implants and even penetrated into them.. At eight months post-implant, both nociceptors with RF covering areas within and outside the transplanted area (Fig. 5), and nociceptors with RF restricted to the host cornea with their borders reaching the limits of the implant were identified. This indicated that nerve sprouts had regenerated within the implant by eight months, which is similar to what we have found in our lamellar keratoplasties in other species [16, 43].

The presence of active nociceptors, particularly polymodals, in implanted corneas may contribute to maintain corneal trophic status after surgery. Neuropeptides contained in nociceptive terminals are released by nociceptors upon activation, and contribute to trophic maintenance of corneal tissue [9, 40].

3.3.2.3.2 Ongoing activity

Nociceptors recorded from implanted eyes at three and eight months after surgery showed at rest an irregular spontaneous activity of low frequency. The spontaneous mean discharge rate measured before any intended stimulation in nociceptive fibers innervating areas inside or near the wounded area was significantly higher than in contralateral eyes (1.83 ± 0.28 imp/s vs. 0.02 ± 0.02, $n=9$; $p<0.003$, Mann-Whitney Rank Sum Test), being the incidence of spontaneous activity also significantly higher in nociceptive units recorded from

implanted corneas than in those recorded from non-operated corneas (89% vs. 11%, n=9; p=0.009, z-test). This increased ongoing activity may be due to a state of hyperactivity of regenerating nociceptive endings or to alterations of the corneal environment, mainly chemical mediators, providing an ongoing stimulus to nociceptors, although no clinical or histopathological evidences of corneal inflammation have been found. Following surgical damage, there are profound morphological and functional changes in regenerated nerves that cause a change in the overall excitability, which results in increased spontaneous activity compared to unoperated nerves [40].

3.3.2.3.3 Mechanical threshold

Mechanical threshold was determined in nine nociceptive fibers recorded from implanted corneas at three (n=6) or eight months (n=3), through stimulation with the 0.25mN von Frey hairs. In contralateral unoperated corneas, mechanical threshold measured in eight nociceptive units was similar (0.30±0.4 mN) to that from implanted corneas.

3.3.2.3.4 Response to chemical stimulation

The response of nociceptive units to chemical stimulation with air puffs of 98.5% CO_2 was also analyzed. At three months after the implant, a positive response to chemical stimulation was obtained in six units out of nine explored nociceptors with receptive fields covering an area located inside and outside the implant (Fig. 5) that were classified as polymodal nociceptors (Table 2). Increase of firing discharge induced by CO_2 in these polymodal units recorded from implanted corneas was slightly lower than in contralateral eyes but the difference was not significant (p=0.078, t-test) (Table 2). Most units sensitive to

chemical stimulation presented also a high frequency postdischarge after the end of the CO_2 pulse [9, 13], firing with high frequency during 30s after the end of the CO_2 pulse, before recovering the basal ongoing discharge (Fig. 5). Postdischarge after CO_2 pulses was similar in implanted and contralateral eyes ($p=0.422$, t.-test) (Table 2). Overall, the response of polymodal nociceptors to chemical stimulation presented a delayed temporal course in operated eyes, as reflected by the increased post-discharge observed (Table 2). In two of the polymodal units recorded in implanted corneas, the impulse frequency during application of the CO_2 pulse inside the implant was lower than that obtained when the CO_2 stimulus was applied in the intact area of the RF (data not shown). This finding, together with the slightly reduced response to CO_2 may indicate that although they are functional, polymodal nerve endings regenerating inside the corneal substitute have an altered response to chemical acidic stimulation [44].

Table 2. Response to chemical stimulation (a 30s-pulse of 98.5% CO_2) of corneal polymodal nociceptors recorded from implanted and contralateral eyes.

	Implanted	Contralateral
Spontaneous activity (30s before the pulse, imp/s)	1.09±0.40	0.62±0.58
Mean discharge rate in response to CO_2 (during the 30s-pulse, imp/s)	1.76±0.68	3.86±1.14
Postdischarge (30 s after the pulse, imp/s)	2.08±0.42	1.14±0.92

The gas jet was applied to the center of the receptive field. In implanted corneas, the stimulated area was a zone of the receptive field covering part of the implant. Data are mean ± SEM, n = 6 and 8 polymodal nociceptors. The response to CO_2 was slightly reduced in implanted eyes, but the differences were not significant (t-test).

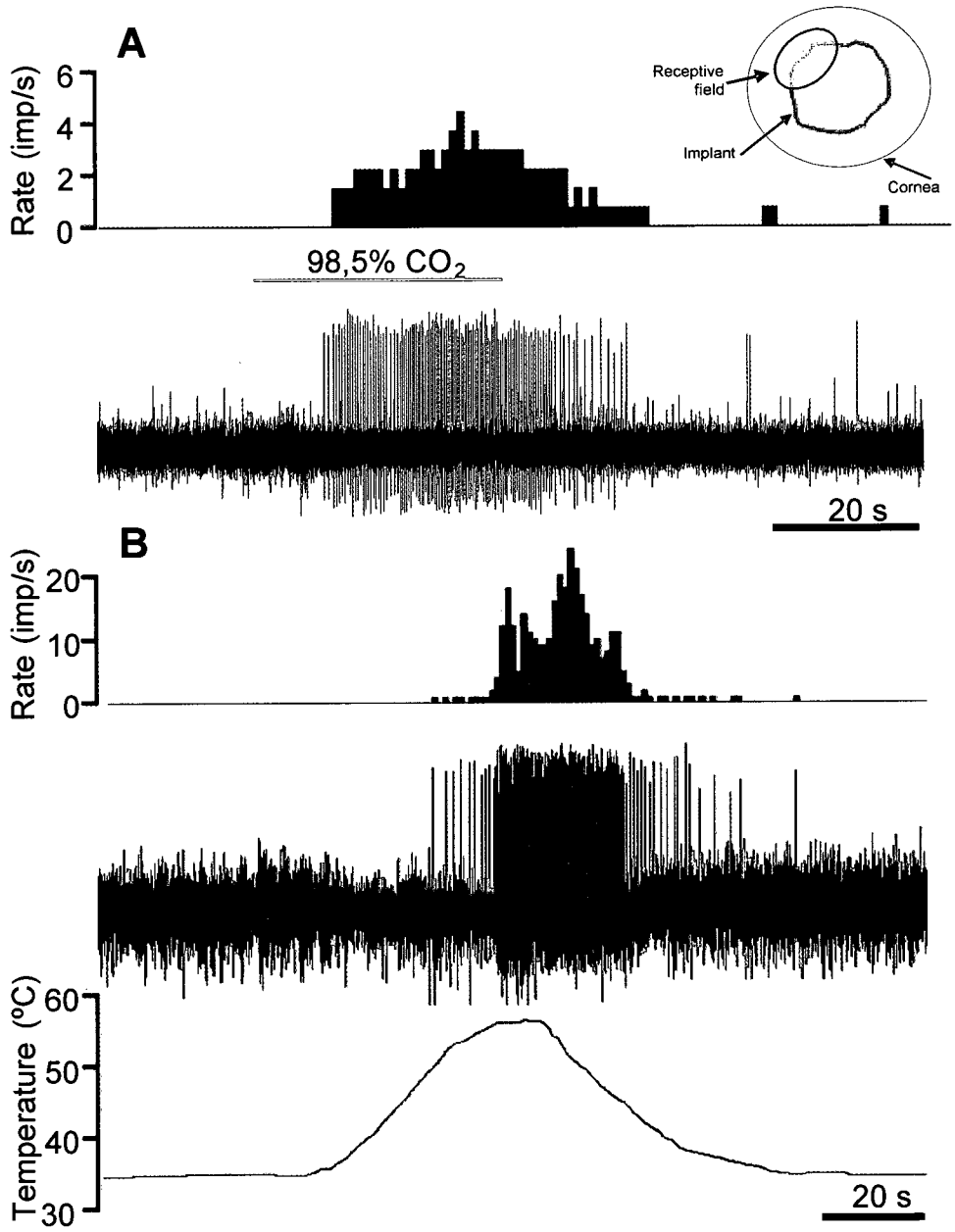

Fig. 5. Response of regenerating corneal polymodal nociceptive units to noxious stimuli. Sample recording showing the response to injurious stimuli of a polymodal unit recorded in an implanted cornea at 3 months after surgery. A. Chemical stimulation. The upper trace represents the frequency histogram of the impulse discharge (lower trace) evoked when a 30 s-duration gas puff containing 98.5% CO_2 is applied to the corneal receptive field near the implant border. B. Thermal stimulation. Response to heating of the same corneal polymodal unit. Frequency histogram, nerve impulse recording and thermal stimulus waveform (34° to 52°C) are shown. The inset shows a schematic representation of the cornea, depicting the area covered by the implant and the location of the polymodal nociceptor receptive field.

3.3.2.3.5 Cold thermosensitive units

3.3.2.3.5.1 Location of receptive fields

Receptive fields of cold-sensitive units present small diameter (1 mm approximately) and in native corneas are scattered throughout the corneal surface [13]. No electrical activity evoked by cold stimuli was recorded inside the implant at 1-2 days and three months post-surgery, while active cold-sensitive units were already present in the vicinity of the implant (data not shown). At eight months after implant, cold sensory nerve terminals were recorded either from areas inside (n=5) (Fig. 6) or outside (n=4) the implant. Five cold sensitive units located throughout the entire corneal surface of control corneas were recorded for comparison.

3.3.2.3.5.2 Ongoing activity

Cold terminals recorded from implanted eyes showed at rest a regular spontaneous activity of high frequency (6.14±0.45 imp/s) (Fig. 6) only slightly higher (p=0.615, t-test) than that recorded from non-operated corneas (5.73±0.66 imp/s), and being in cold terminals located inside the implant (4.87±0.13 imp/s, n=5) significantly lower than in those located outside (7.42±0.86 imp/s, n=4) (p=0.013, t-test). An increased ongoing activity has also been described in corneal nociceptors and cold nerve terminals regenerating after photorefractive keratectomy (PRK) or corneal microkeratome lesions [13, 44], and it is probably due to an abnormal expression of TTX-resistant Na+ channels after lesion [42].

3.3.2.3.5.3 Response to thermal stimulation

Cold nerve terminals were characterized by the increase of firing in response to temperature reductions (Fig. 6). The characteristics of the response to cooling of cold nerve terminals studied in contralateral and operated eyes were similar (cooling threshold range: -0.25°C to -2.50°C; peak frequency from 11 to 34 imp/s, reached around 25°C). The characteristics of the response to cold of thermosensitive units regenerating in corneal implants are similar to that recorded from intact corneas [13, 14].

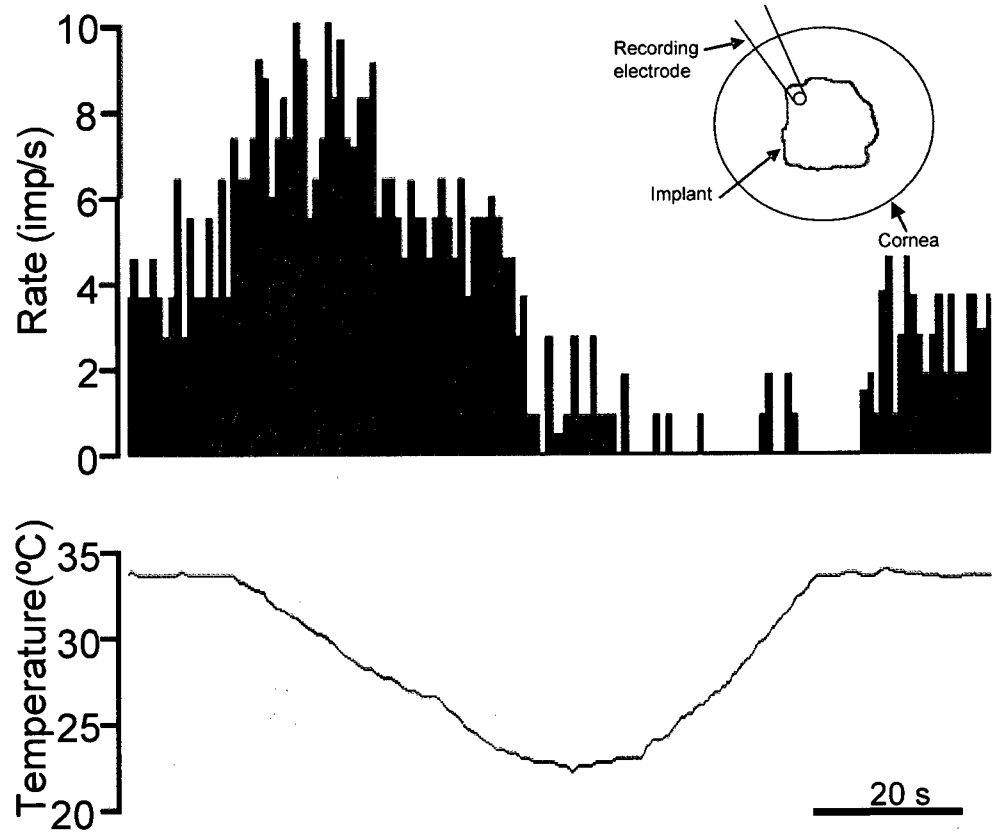

Fig. 6. Sample recording of the response to temperature reduction of a cold corneal nerve terminal located inside a corneal implant at eight months after surgery. A pulse to 25°C was applied from a basal temperature of 33°C. The upper trace represents the frequency histogram of the impulse discharge and the lower trace shows the temperature change registered in the recording chamber. Inset: schematic representation of the cornea, illustrating the area covered by the implant and the location of the cold nerve terminal.

4. Conclusion

The collagen-MPC hydrogels were well-tolerated as full-thickness implants in the guinea pigs, where they seamlessly integrated into the host corneas and promoted regeneration of corneal tissue and nerves. Electrical activity recorded from regenerating corneal nerves within the implants constitute the first demonstration of the functional state of sensory nerves regenerating *in vivo* inside an implant. Corneal nerves started to re-innervate the implant at three months post-surgery and were functionally active within the implant by eight months. The ability of this simple ECM mimetic to allow functional nerve regeneration after implantation will in turn ensure stability of the regenerated corneal tissue due to the important trophic role these nerves have in maintaining corneal integrity. Hence, such corneal substitutes may in the future be good candidates for clinical applications.

Acknowledgements

Supported by grants SAF2008-00529, BFU2008-04425 and CSD2007-00023 (Ministerio de Ciencia e Innovación), and Fundación Marcelino Botín, Spain (MCA, CB, JG) and NSERC Canada Discovery grant (MG). CRM was supported by an NSERC Canada doctoral scholarship. Technical assistance of Alfonso Pérez-Vegara and Manuel Bayonas is acknowledged.

Chapter 6

6.1 Manuscript 5

Tissue Engineered Recombinant Human Collagen-based Corneal Substitutes for Implantation: Performance of Type I versus Type III Collagen

Invest Ophthalmol Vis Sci. 2008 Sep;49(9):3887-94. Epub 2008 May 30.

Although the previous manuscripts showed successful implantation of type 1 porcine collagen implanted through both DLKP and full thickness penetrating keratoplasty, the ultimate goal is implantation into humans. With concerns for the use of animal collagen including risk of disease transmission, and immunological response, we utilized type I and type III recombinant human collagen crosslinked with carbodiimide chemistry, and implanted through deep lamellar keratoplasty into mini pigs. Although the majority of the cornea is type I collagen, a small portion of it is comprised of type III collagen. We found that the constructed corneal substitutes had similar mechanical properties to each other, with RHC-III implants showing increased optical clarity. Implants supported regeneration of corneal cells, and sensory nerve re-innervation.

Tissue Engineered Recombinant Human Collagen-based Corneal Substitutes for Implantation: Performance of Type I versus Type III Collagen

Kimberley Merrett[1], Per Fagerholm[2], Christopher R. McLaughlin[1,3], Subhadra Dravida[1], Neil Lagali[1], Naoshi Shinozaki[4], Mitchell A. Watsky[5], Rejean Munger[1], Yasuhiro Kato[4], Fengfu Li[1], Christopher J. Marmo[6] and May Griffith[1,3]

[1]University of Ottawa Eye Inst, 501 Smyth Road, Ottawa, ON K1H 8L6, Canada

[2]Linköping University Hospital, Dept. of Ophthalmology, Se-58185 Linköping, Sweden.

[3]Dept. of Cellular and Molecular Medicine, Univ. of Ottawa, 451 Smyth Road, Ottawa, ON K1H 8M5, Canada

[4]Cornea Centre and Eye Bank and Oral Health Science Center, Tokyo Dental College, Chiba, Japan

[5]Dept. of Physiology, Univ. of Tennessee Health Science Center, Memphis, TN, USA 38163

[6]CooperVision Inc., Pleasanton, CA 94588-4520

Grant Information:

NSERC Canada Grant STPGP 246418-01 to MG and MAW; Canadian Stem Cell Network grant to MG; CIHR Canada post-doctoral fellowship to NL.

Commercial interests: N (PF, CRM, SD, NL, NS, MAW, YK); F (RM); F, P(MG, CJM)

Corresponding Author:

May Griffith, PhD

University of Ottawa Eye Institute

The Ottawa Hospital – General Campus

501 Smyth Road

Ottawa, ON K1H 8L6, Canada

Phone: (613) 737-8899, ext. 74011

Fax: (613) 739-6070

E-mail: mgriffith@ohri.ca

Co-author Contributions to Manuscript

Merrett, Kimberley

Ms. Merrett is a chemical engineer and research associate at the University of Ottawa who developed the recombinant human collagen formulation, fabricated the implants, and tested their mechanical and physical properties

Fagerholm, Per

Dr. Fagerholm, an ophthalmologist at Linköping University Hospital in Sweden, was responsible for the implantation of the artificial corneas into the pigs.

Dravida, Subhadra

Mrs. Dravida was a research associate who assisted in processing the samples for immunohistochemistry

Lagali, Neil

Dr. Lagali, was a post doctoral fellow in the Munger Lab who was mainly responsible for the *in vivo* confocal microscopy images.

Shinozaki, Naoshi

Dr. Shinozaki, Director of the Ichikawa General Hospital Cornea Center in Japan, provided guidance in obtaining the electron microscopy images of the implanted corneas.

Watsky, Mitchell

Dr. Watsky is a corneal physiologist at the University of Tennessee. He performed all the glucose and albumin permeability assays, as well as the statistical analyses.

Munger, Rejean

Dr. Munger, an optical physicist at the University of Ottawa Eye Institute, aided in analysis of the in vivo confocal microscopy images of the artificial cornea.

Kato, Yasuhiro

Dr. Yasuhiro is a post doctoral fellow at the Ichikawa General Hospital Cornea Center in Japan, and provided the electron microscopy images of the implanted corneas.

Li, Fengfu

Dr. Li is research fellow at the University of Ottawa who helped to direct the mechanical characterizations of the artificial corneas and prepare the manuscript.

Marmo, Christopher

Dr. Marmo is a research scientist at CooperVision who provided insight on material development.

Griffith, May

Dr. Griffith was my supervisor. She helped guide the study and helped me with editing the manuscript.

My role in this manuscript was to design the study, perform the *in vitro* testing of the gels to determine which formulations were suitable for implantation, as well as the histopathological analysis of the implants. I also assembled the figures for the documents, and wrote up the manuscript.

Abstract

Purpose: To compare the efficacies of recombinant human collagens types I and III as corneal substitutes for implantation.

Methods: 13.7% recombinant human collagen, either type I or type III, was thoroughly mixed with 1-ethyl-3-(3-dimethylaminopropyl)carbodiimide and N-hydroxysuccinimide. The final homogenous solution was either moulded into sheets for *in vitro* studies or into implants with the appropriate corneal dimensions for transplantation into mini-pigs. Animals with implants were followed for up to 12 months post-operative. Clinical examinations of the cornea included detailed slit lamp biomicroscopy, *in vivo* confocal microscopy and fundus examination. Histopathological examinations were also performed on corneas harvested after 12 months.

Results: Both crosslinked recombinant collagens had refractive indices of 1.35, with similar optical clarity to human corneas. Their chemical and mechanical properties were similar, although RHC-III implants showed superior optical clarity. Implants into pig corneas over 12 months show comparably stable integration, with regeneration of corneal cells, tear film and nerves. Optical clarity was also maintained in both implants, as evidenced by fundus examination.

Conclusions: Both RHC-I and RHC-III implants can be safely and stable integrated into host corneas. The simple crosslinking methodology and recombinant source of materials make them potentially safe and effective future corneal matrix substitutes.

Introduction

The current and projected shortage of high quality donor human corneas for transplantation in many countries have prompted the development of viable, long term alternatives to human donor tissue. As the cornea is the main refractive element of the eye and serves as a protective barrier, it has several key properties that need to be replicated in any artificial replacement. These include high optical clarity, appropriate refractive index and toughness, ability to seamlessly integrate into host tissues and remain avascular. To date, corneal substitutes that have been tested clinically are prostheses that address replacement of the cornea's function with synthetic polymers that are either compatible with or non-harmful to host tissue. More recent approaches, however, have been to develop bio-interactive materials that would allow some host tissue regeneration, such as reconstitution of a healthy epithelium[1-3] or epithelium, stroma and nerves.[4, 5]

We previously developed optically clear cornea stromal matrix substitutes based upon crosslinked porcine or bovine collagen, that when implanted into mini-pigs, promoted regeneration of corneal cells, nerves and tear film mucin. [4, 5] However, these animal collagen-based corneal substitutes gave low level but observable immunogenic reactions when implanted into mice as xenogeneic grafts.[6] Furthermore, heading towards human clinical implantation, identification of an implant material that is safe as well as efficacious is essential to overcome safety concerns around the use of animal source collagen, including the potential for transmission of disease[7] and immune response within the host.[8] Recombinant human collagen or artificial collagens based on repeats of Gly-X-Y would circumvent these issues. However, most artificial collagen chains reported to date are short (<10 nm), or utilize

chemical synthesis methods[9] that are not readily adapted to sequence modification and glycosylation as they would if made recombinantly.

In this study, we compared the efficacy of two recombinantly produced human collagens, types I and III for use in tissue engineering corneal substitutes. These highly purified, recombinant collagens have been fully characterized and resemble natural fibrils in their ultrastructure, ability to form triple helices and by Western blotting. While collagen I is the species most commonly found within the human cornea, collagen III has several properties including smaller fibril diameter[10] which may allow for a more tightly packed hydrogel that is more robust. We show that despite differences between type I and III fibrils, hydrogels fabricated from both collagens shared many similar properties and implants of both collagens gave similar results *in vivo*.

Materials and Methods

Fabrication of Corneal Implants

Recombinant human collagens I and III (RHC-I and RHC-III, respectively) produced in yeast cells (*Pichia pastoris*), were purchased from FibroGen Inc. (South San Francisco, CA), freeze-dried and then reconstituted.

To fabricate collagen hydrogels, 250 µl aliquots of either 13.7% (wt/wt) of RHC-I or RHC-III in aqueous solution were each loaded into a syringe mixing system free of air bubbles.[5] Calculated volumes of 1-ethyl-3-(3-dimethylaminopropyl)carbodiimide (EDC) and N-hydroxysuccinimide (NHS) solutions were added and solutions were thoroughly mixed at 4°C (ice water). The final solution was immediately dispensed as flat sheets or into curved polypropylene contact lens moulds (500 µm thick, 12 mm diameter) and cured at 100%

humidity, at 21 °C for up to 24 h and then at 37 °C for up to 24 h. The implants were washed three times with fresh 1X PBS and then stored in PBS containing 1% chloroform to maintain sterility.[5] Optimal RHC-I and RHC-III hydrogels were prepared using EDC:collagen-NH_2 ratios of 0.5:1 and 0.4:1, respectively.

Physical, Chemical and Mechanical Characterization

Optical Properties

Refractive indices of fully hydrated RHC-I and RHC-III hydrogels were recorded using an Abbe refractometer (Model C10, VEE GEE Scientific Inc., Kirkland, WA) at 21°C with bromonaphthalene as the calibration agent. Light transmission and back-scattering were measured using a custom-built instrument as described previously.[11] Briefly, transmission and back scattering measurements were made for both white light (quartz-halogen lamp source) and for the narrow spectral regions centered at 450, 500, 550, 600 and 650 nm. Differences in the optical properties between the hydrogels were analysed statistically using a one-way analysis of variance (ANOVA), followed by the Tukey-Kramer Multiple Comparisons Test. Statistical significance was set at $p<0.05$.

Mechanical Properties

The tensile strength, elongation at break, and elastic moduli of the hydrogels were determined on an Instron electromechanical universal tester (Model 3342, Instron Corporation, Norwood, MA) with Series IX/S software. Statistical analyses as described above were performed.

Diffusion Permeability

Glucose permeability of hydrogels was determined as described previously[5] at the cornea's normal physiological temperature (35 °C) using a modified Ussing chamber (Warner Instruments, Hamden, CT) with air-lift mixing. Measurements were made colorimetrically at 540 nm using a glucose assay kit (GAG020, Sigma-Aldrich) with a Shimadzu UV-1601 spectrophotometer. FITC-labelled bovine serum albumin (BSA; 66 kDa; Sigma) was used for measuring albumin diffusion. A side-by-side diffusion chamber, with magnetic stirring in each chamber (to avoid foaming problems (PermeGear, Bethlehem, PA), set at 35°C was used. Both the receptor and permeation chambers were 3 ml volume, with 0.5 mM albumin used in the permeation chamber. Sampling was performed as in the glucose measurements. Receptor chamber albumin concentrations were determined by fluorophotometry (Gilford Fluoro IV) and fitting the values to a regression line of standards of known concentration. Diffusion coefficients were calculated using these values.

Toxicology

Toxicological tests were performed as we had previously described[5] by North American Science Associates (NAMSA, Northwood, Ohio) in accordance to International Organization for Standardization (ISO) protocols. These tests included agarose overlay for cytotoxicity and the cytotoxicity test specific for extractables that may leach out of the materials (ISO 10993-5) [12], genotoxicity tests using a bacterial reverse mutation study (ISO 10993-3)[13] and systemic toxicity tests (ISO 10993-11). [14]

In Vitro Biocompatibility

Immortalized human corneal epithelial cells (HCEC) were used to evaluate epithelial coverage as we previously described. [5, 15] Briefly, HCECs were seeded on top of 1.5 cm^2 flat hydrogels of either RHC-I or RHC-III and supplemented with a serum-free medium containing epidermal growth factor, Keratinocyte Serum-Free Medium (KSFM; Invitrogen, Burlington, Canada) and grown until confluent. They were then switched to a serum-containing modified SHEM medium for the next 2 days, followed by maintenance at an air/liquid interface. Time taken by the cells to attain confluence was compared to plasma-treated, tissue culture plastic controls, and the ability of hydrogels to support epithelial stratification was evaluated.

To determine the ability of the hydrogels to support nerve growth, dorsal root ganglia from chick embryos (E 8.0) were positioned onto gels with a collagen-based adhesive. Neurite outgrowth was observed for up to 7 days, after which the gels were fixed in 4% paraformaldehyde in 0.1M PBS, pH 7.2-7.4, and stained for neurofilaments using mouse anti-NF200 antibody (Sigma), diluted 1:40 in Tris-buffered saline (TBS) containing 4% foetal bovine serum (FBS), overnight at 4^0C. They were visualized the following day by immunofluorescence after conjugating with a donkey antimouse-Cy2 neurofilament secondary antibody (Amersham, Baie D'Urfe, Canada; 1:200 dilution in TBS/FBS).

In Vivo Biodegradation

RHC-I and RHC-III gels, 5 mm X 5 mm x 500 μm, were implanted subcutaneously into the backs of male SD rats of at least 300g (*Rattus norvegicus,* Hla® (SD)CVF®, Hilltop

Lab Animals, Inc.) for 30, 60, 90 and 180 days at NAMSA, to evaluate the sub-chronic and chronic effects of implantation following ISO 10993-6.[16] This test also provides a measure of the biodegradation rate of implanted materials. For surgery, animals were anaesthetized by interperitoneal injection of ketamine hydrochloride and xylazine (66 mg/kg + 9 mg/kg), dosed at 2.25 ml/kg and subcutaneous injection of 0.05 mg/kg buprenorphine. Small incisions (7 mm in length) were made paravertebrally in the thoracic and lumbar region (2 cm away from the vertebral column) for up to four samples per rat. After sample insertion, incisions were closed with wound clips that were removed 11 days later. At each time point, animals were euthanized and the skin over each implant site was incised and reflected to expose the implant sites. One sample each was randomly selected for macroscopic evaluation while the other four samples were processed for histopathological examination.

Corneal Implantation and Clinical Evaluation

Procedures were performed in accordance to the ARVO Statement for the Use of Animals in Ophthalmic and Vision Research, and with ethics approval from the University of Ottawa (Protocol EI-5), as we previously described.[5] Briefly, in a blinded study, pigs anaesthetized with a mixture of 4.4 mg/ kg Telazol® (Wyeth, Carolina, Puerto Rico) and 2.2 mg/ kg xylazine (Rompun®; Bayer Inc., Ontario, Canada) were implanted with one of either RHC-I or RHC-III hydrogels (6.26 mm diameter, 500 μm thick), after removal of the equivalent host corneal tissue. The implants were held in place by overlying sutures that were removed four weeks later. All animals received steroids (Prednisolone®, Sandoz, Quebec, Canada) and antibiotics (Zymar®, Allergan, Irvine, CA) q.i.d.. The non-operated,

contralateral corneas served as controls. Additional controls consisted of four animals that received allograft transplants.

Follow-ups were performed daily on each pig up to 7 days post-operative, then weekly for a month, followed by detailed examinations at 2, 6 and 12 months. Examinations included slit-lamp and fundus biomicroscopy (to image the retina) to assess implant optical clarity, Schrimer's to assess tear film regeneration, sodium fluorescein staining to assess integrity and barrier function. Intraocular pressure measurements were taken to ensure that implants were not blocking aqueous humour flow.

In vivo confocal microscopy (ConfoScan3, Nidek, Japan) was used to assess cell and nerve in-growth, as well as to measure corneal thickness in live animals. Corneal touch sensitivity was measured using a Cochet-Bonnet aesthesiometer (Handaya Co., Tokyo, Japan). The density of nerve fibers within the central 5mm of all corneas was quantified by analysis of *in vivo* confocal images. Full details of the nerve density quantification methodology are given in the paper by Lagali et al.[17] Nerve density was reported as the total length of all nerve fibers detected within a corneal depth zone divided by the zone volume (confocal microscope image cross-sectional area multiplied by the corneal zone depth of field), expressed in μm/mm3. Central corneal nerve density 12 months postoperatively was compared within the various graft types by corneal depth zone[17], using the Kruskal-Wallis analysis-of-variance (ANOVA) on ranks method. Additionally for each graft type, nerve density was compared to levels in control corneas for the same depth zone using either a t-test (where data was normally distributed) or a Mann-Whitney rank sum test (for non-normally distributed data). For all nerve density comparisons, normality was determined using the Kolmogornov-Smirnov test, and for all statistical tests $P<0.05$ was considered

statistically significant. All statistics were calculated using SigmaPlot v9.0 with SigmaStat integration (Systat Software Inc., Point Richmond, CA).

Histopathological Evaluation

Corneas with implants, and controls were cut into four pieces for light and electron microscopy. Two were fixed in 4% paraformaldehyde in 0.1M PBS, processed, paraffin embedded and sectioned at 10 μm. One quarter of each cornea was also prepared for cryosectioning. Sections were stained with H&E for histopathological examination. Immunofluorescence was performed as described above on deparaffinized sections, for type VII collagen, a hemidesmosome marker[18], procollagen I, smooth muscle actin (SMA) and type III collagen. On frozen sections, samples were stained with *Ulex europaeus* agglutinin (UEA), AE-5, CD45 and F4/80. Antibody details are in Table 1.

Table 1. Primary antibody specifications.

Primary Antibody	Dilution	Company	Specificity
AE-5	1:100	Chemicon, Temecula, CA	Corneal epithelial cell-specific marker
Ulex europaeus agglutinin	1:200	Sigma-Aldrich, Oakville, ON, Canada	Mucin of tear film
Collagen VII	1:100	Sigma-Aldrich	Hemidesmosome complex marker
SP8-D1 (procollagen I)	1:60	Developmental Studies Hybridoma Bank, Iowa City, IA	De novo collagen synthesis
Smooth muscle actin (SMA)	1:100	Cell Marque Corp, Rocklin, CA	Myofibroblasts
F4/80	1:400	Serotec USA, Raleigh, NC	Pan macrophage marker
CD45	1:40	BD Biosciences, San Diego, CA	Bone marrow-derived cells
Type III collagen-biotin	1:100	Southern Biotech Co., U.S.A.	Type III collagen

Slides used for procollagen I, SMA and type III collagen staining were deparaffinized and treated with 3% H_2O_2. Samples were then blocked for non-specific staining with 4% FBS + 1% BSA in PBS followed by antigen retrieval performed by reacting with proteinase K (2 mg/ml) for 20 min at 37 °C, followed by primary antibody incubation overnight at 4°C. The sections were incubated with a 1:400 dilution of the biotinylated anti-mouse IgG antibody (Amersham) after washing, followed by a 1:400 dilution of avidin-horseradish peroxidase

(Amersham) and visualized with diaminobenzidine (Roche, Mannheim, Germany). Sections stained for type VII collagen, UEA, CD45, AE-5 and F4/80 were blocked with 4% FCS + 1% BSA in PBS, and incubated in primary antibody overnight at 4°C. They were then incubated with 1:400 FITC conjugated secondary antibody (Sigma) and visualized on a Zeiss Axioskop 2.

For ultrastructural examination, ¼ of each sample was fixed in Karnovsky's fixative, post-fixed in osmium tetroxide and processed for routine transmission electron microscopy.

Results

RHC-I hydrogels crosslinked with an EDC-collagen ratio of 0.5, and RHC-III hydrogels with EDC-collagen ratios of 0.4 had optimal physical and mechanical properties. These were therefore the hydrogels used for further comparison in this study.

Physical and Mechanical Characterization

The physical and mechanical properties of the RHC hydrogels are summarized in Table 2. Both had water content of over 90%, which most likely correlates with a refractive index of 1.35, that of water. Light transmission through RHC-III gels was significantly higher than that of RHC-I gels at 89.8±.9 % versus 80.7±2.6 % ($P<0.01$), but backscatter for both gels was very low, < 1%.

There were no statistically significant differences in tensile strength, elongation at break and moduli between RHC-I and RHC-III gels. No significant differences were recorded in the thermodynamic properties either. However, neither hydrogel was as thermally stable as the human cornea.

The glucose diffusion coefficients for type I and type III were $1.39\times^{-6}cm^2/s$ and $1.19\times^{-6}cm^2/s$, respectively, in agreement with that of human corneal stroma at $2.4\times^{-6}cm^2/s$ [19]. The bovine serum albumin diffusion coefficient for type I and type III implants were 1.456 x 10^{-7} and 8.512 x 10^{-8} respectively. RHC-I gels were within the same range as the diffusion coefficient of albumin in human corneal posterior stroma at $1.10\times^{-7}$ cm^2/s [19] but RHC-III had a diffusion coefficient that was slightly lower.

Table 2. Comparison of key properties of optimized EDC/NHS cross-linked recombinant human collagen type I (RHC-I) and type III (RHC-III) corneal substitutes to excised human eye bank corneas. $n \geq 3$ samples for each test.

	Human Cornea	RHC-I (EDC Ratio = 0.5)	RHC-III (EDC Ratio = 0.4)
Water content	80%[18]	91%	90%
Optical properties			
Refractive index	1.3375[19]	1.35	1.35
Transmission (%)	>85[14]	80.7 ± 2.6	89.8 ± 0.9
Backscatter (%)	6–8	0.54	0.81
Mechanical properties			
Tensile strength (MPa)	3.8[20]	1.126 ± 0.154	1.700 ± 0.205
Elongation at break (%)	—	15.33 ± 1.45	13.89 ± 0.69
Elastic modulus(MPa)	3–13[21,22]	16.7 ± 1.49	20.26 ± 2.04
Thermodynamic properties T_d (°C)	65.1	59.2	58.6
Permeability			
Glucose (cm^2/s)	2.5×10^{-6} [23]	$1.4 \pm 0.083 \times 10^{-6}$	$1.2 \pm 0.069 \times 10^{-6}$
Albumin (cm^2/s)	10^{-7} [23]	1.5×10^{-7}	8.5×10^{-8}

$n \geq 3$ samples for each test. T_d, dissolution temperature.

Toxicology

Both RHC-I and RHC-III were non-reactive or negative for all the *in vitro* toxicology tests performed. They were non-toxic in *in vivo* tests, as none of the mice treated with hydrogel extracts showed any mortality or evidence of systemic toxicity.

Biodegradation

Subcutaneous implants in rats up to 12 weeks (90 days) are considered short term, while those beyond 12 weeks are considered long-term. Results show no evidence of any significant inflammation or fibrosis of host tissues at the implantation sites, indicating

good biocompatibility over both the short and long-term. The polymers were intact at all time points tested at macroscopic levels. Microscopic examination, however, showed sections of implants with continuous, smooth edges at 90 days (Fig. 1A, B) but macrophage attachment to the cut surfaces at 180 days (Fig. 1C, D). The latter are possible indications of early degradation.

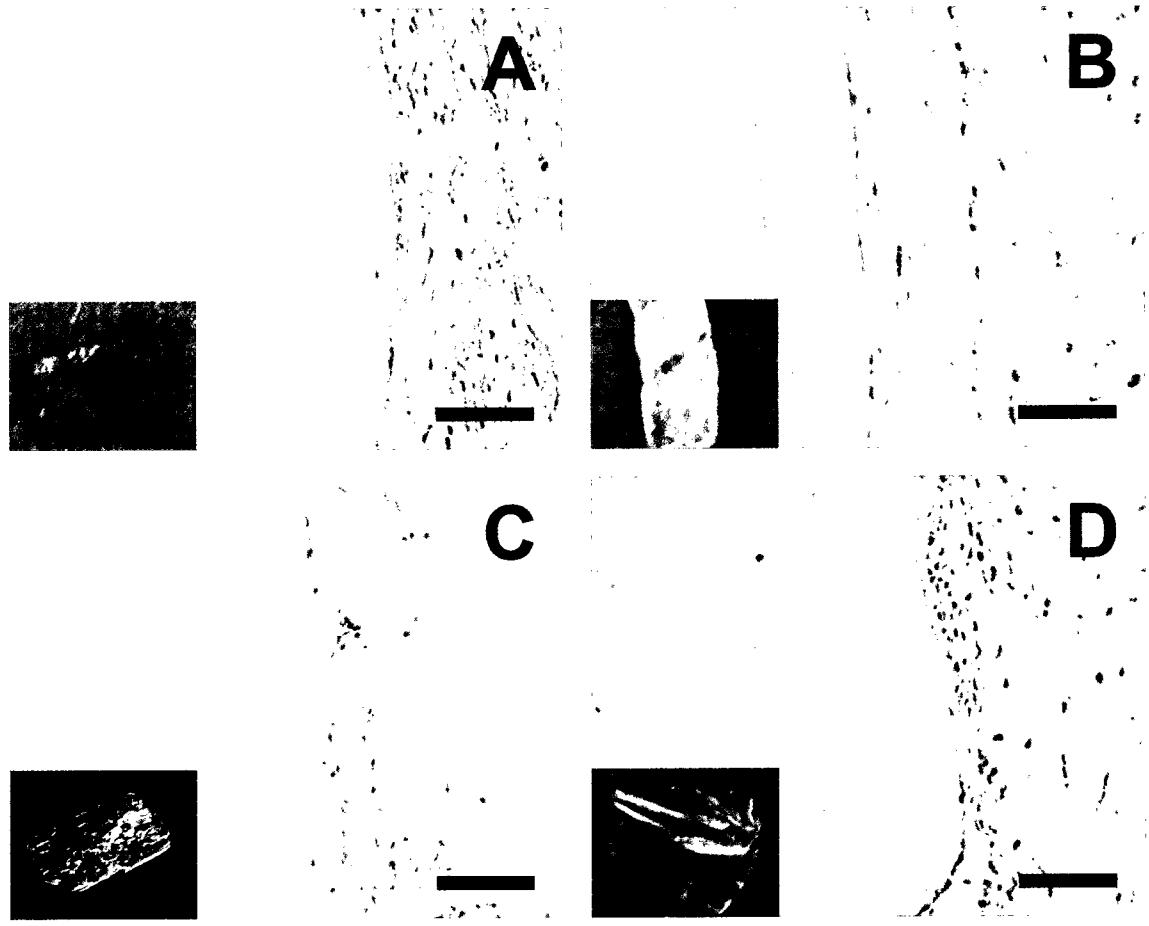

Fig. 1. H&E stained sections through RHC-I and RHC-III hydrogels implanted subcutaneously into rats. After 90 days, both RHC-I (**A**) and RHC-III (**B**) gels have smooth, continuous edges, i.e. no signs of biodegradation. Insets show intact samples retrieved after implantation. After 180 days, there is evidence of loss of smooth continuous edge, showing the beginning of possible biodegradation of the RHC-I (**C**) and RHC-III (**D**) implants. Bars: 100 μm.

In Vitro biocompatibility

Both RHC-I and RHC-III gels supported attachment and proliferation of corneal epithelial cells, reaching confluence over 4 days, and stratifying after air-lifting. Nerve overgrowth and ingrowth was also observed but there were no differences observed between RHC-I and RHC-III gels (data not shown).

Implantation and Clinical Evaluation

No adverse inflammatory or immune reaction was observed after implantation of either RHC matrices or allografts. Epithelial coverage of implants was complete by 4 days post-operative. Slit lamp examinations showed mild haze up to six months for both RHC-I and RHC-III. Very mild haze (+ 0.5) was observed in one of four pigs implanted with RHC-I gels at 12 months post-operative. A diffuse +1 haze was observed in one of four pigs in the corresponding RHC-III group. Animals that had received allografts were at +1 for two animals and +2 for a third animal, out of four operated animals. All control, untreated corneas were haze free (0). The regenerated epithelium showed exclusion of sodium fluorescein dye, indicating that the epithelium was intact and had re-established barrier properties. Schirmer's tests indicated comparable tear production in all operated and unoperated corneas. Intraocular pressures were unchanged, showing that the implants did not block flow of aqueous humour within the eye. Fundus camera images of the retinal vessels (Fig. 2 B, C) were comparable to those of unoperated corneas (Fig. 2).

Clinical *in vivo* confocal microscopy of the implanted stromal matrices at 6 weeks post-surgery showed presence of fine sub-epithelial nerves (Fig. 2E, F) and corresponding stromal cells and nerves (Fig. 2H, I) with morphology mimicking that of unoperated controls

(Fig. 2D, G). All operated corneas showed comparable touch sensitivity to unoperated controls by aesthesiometry. Touch sensitivity was extinguished by application of lidocaine.

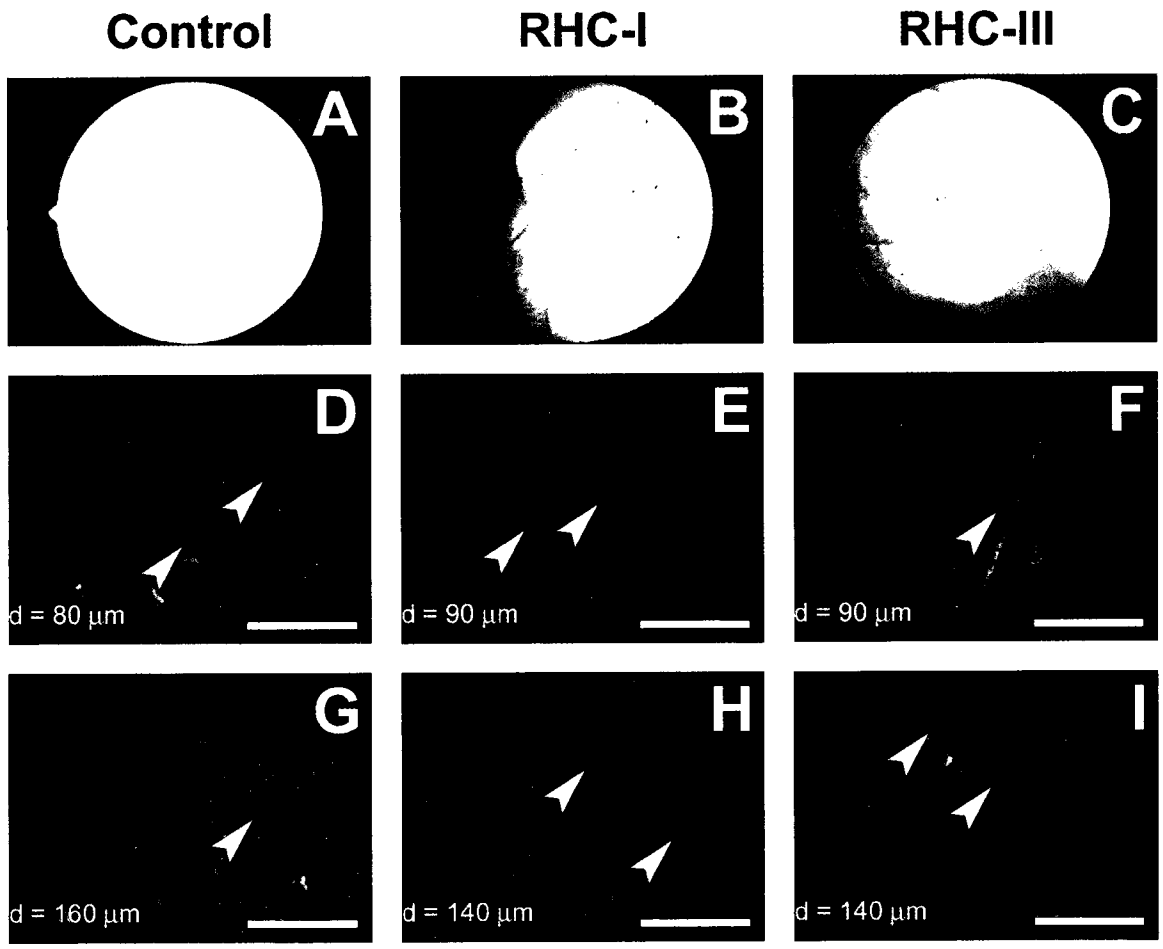

Fig. 2. Fundus and IVCM images at 12 months from pigs. Fundus images of the retina. Proper morphology of the retinal vessels are seen in operated eyes of RHC-I (**B**), RHC-III (**C**) implants compared to unoperated corneas (**A**). IVCM images show fine, regenerated sub-epithelial nerves in both RHC-I (**E**), RHC-III (**F**) implanted corneas. Larger, stromal nerves were also observed in both RHC-I (**H**) and RHC-III (**I**) implants. Corresponding unoperated controls are shows in (**D**) and (**G**). Bars: 50 µm.

Histopathological Evaluation

H&E sections through controls (Fig. 3A), RHC implants (Fig. 3 B,C) or allografts (Fig. 3D showed typical corneal morphology: the epithelium was stratified and overlies a

matrix containing stromal cells. All epithelia were fully differentiated as indicated by positive AE5 staining (Fig. 3 E-H). The allografts contained a small number of smooth muscle actin positive cells (Fig. 3 L) but both RHC samples were unstained (Fig. 3 J, K). All samples were positive for Type VII collagen, a marker for hemidesmosomes[18] at the basement membrane-epithelium interface (Fig. 3 M-P) and UEA staining showed the presence of a tear film in all samples (Fig. 3 Q-T) . All samples were negative for F4/80 and CD45, respectively (data not shown) indicating that implants had minimal/no macrophage activity, and very few/ no marrow-derived cells. Samples of corneas implanted with RHC-III hydrogels for 12 months were negative for type III collagen while control, non-implanted RHC-III hydrogels were intensely stained (data not shown). Observable procollagen I staining, however, was present in RHC-III implants (Fig. 3 W).

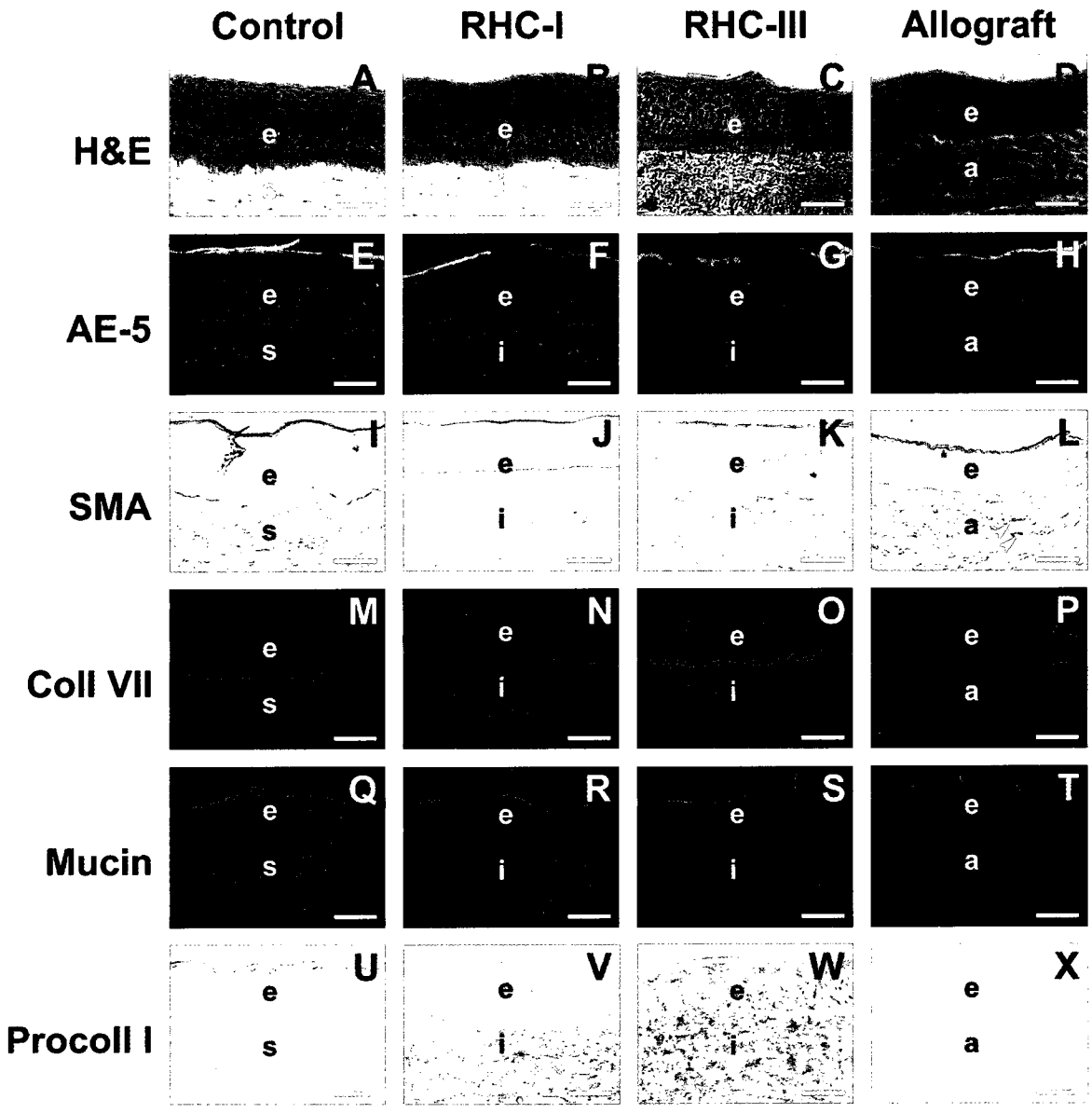

Fig. 3. Postsurgical corneal regeneration at 12 months. (**A-D**) H&E sections show stratified epithelia (e) over the stroma (s), implants (i) and allograft (a). Both RHC-I and RHC-III implants were populated by stromal cells. (**E-H**) Regenerated epithelia over RHC implants were AE5 positive as were the controls. (**I-L**) Smooth muscle actin staining, indicative of activated stromal cells or myofibroblasts, was only found in a few cells (arrowheads) in the allograft.(**L**). (**M-P**) Type VII collagen staining seen at the epithelium–implant interface of corneas with RHC-I (**N**) and RHC-III (**O**) implants is comparable to that observed in unoperated controls (**M**) and allograft (**P**). (**Q-T**) UEA staining indicating presence of tear film mucin was seen in all samples. (**U-X**) Procollagen I staining was more pronounced in RHC-III (**W**) implants compared to others. Bars: 50 μm.

TEM observations of the epithelial-stromal interphase region (Fig. 4) confirmed the presence of stromal cells in RHC-I and RHC-III implants. Sub-epithelial nerves were also observed in implants, allograft and control corneas (Fig. 4E-H). Epithelial-implant interface showed the presence of hemidesmosomes in all samples (Fig. 4 I-L).

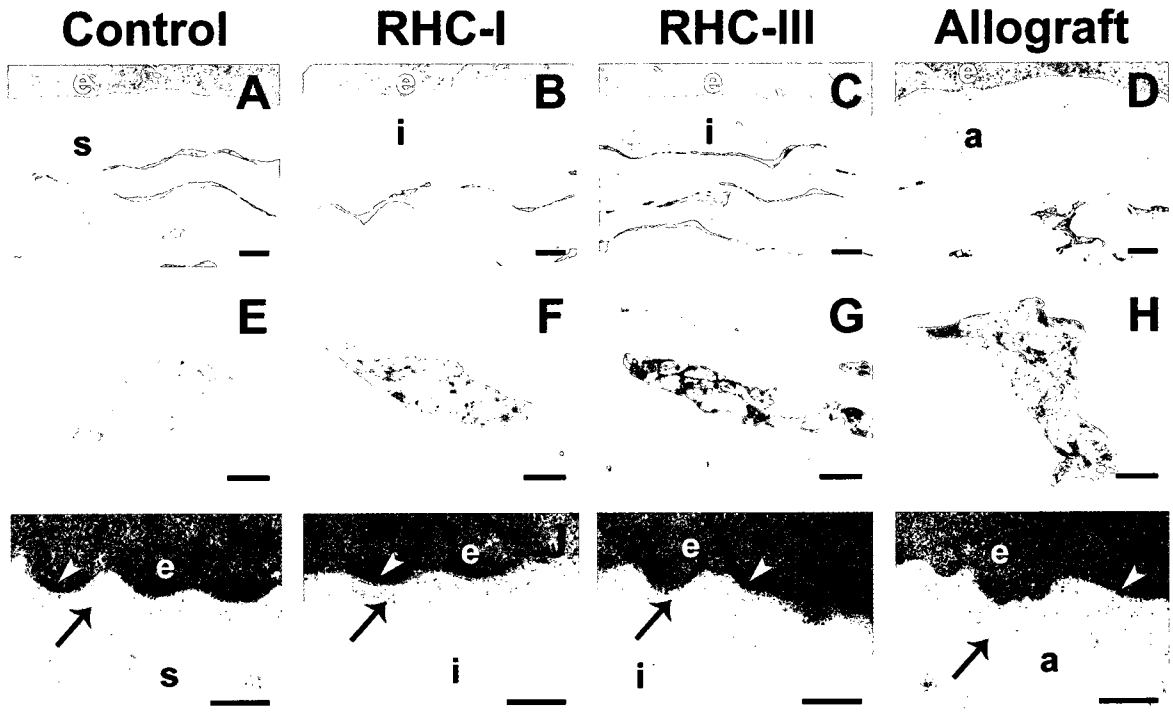

Fig. 4. (**A-D**) TEM of epithelial-stromal compartment interface. Epithelial cells are overlying either a stroma (s), implant (i) or allograft (a), all containing stromal cells. Bars: 5 μm. (**E-H**) Higher magnification of regenerated nerve, show the staining of clear and dense vesicles. Bars: 1 μm. (**I-L**) Hemidesmosome plaques (arrowheads) and basement membrane (arrows) have formed within the ECM between the epithelial cells and underlying RHC implants, emulating the structures normally found at the epithelial–stromal interface of unoperated corneas. Bars: 0.1 μm.

Analysis of central corneal nerve density are given in Figure 5. No significant nerve density differences were found among allografts, RHC-I or RHC-III grafts in any corneal depth zone ($P = 0.80, 0.74, 0.06$ for zones 1, 2, 3, respectively). All graft types, however, had a significantly reduced nerve density in corneal depth zone 1 relative to unoperated

control corneas ($P < 0.01$ for all graft types). Additionally in RHC-III grafts and allografts, nerve density in depth zone 3 were significantly increased over that in untreated corneas ($P = 0.04, 0.03$ for RHC-III and allograft, respectively).

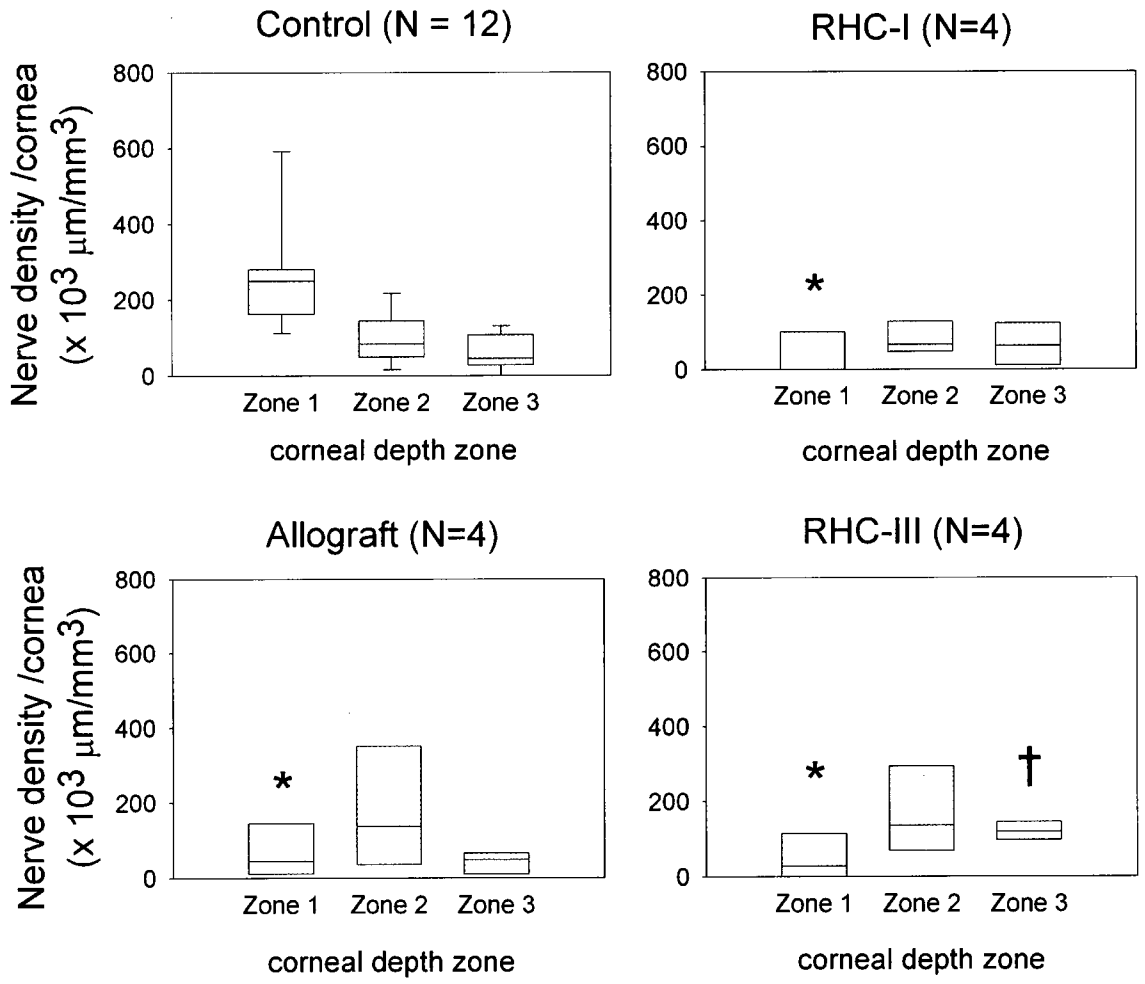

Fig. 5. Nerve density per central cornea 12 months after surgery in unoperated control corneas and in various corneal graft types. For control corneas, box plots indicate medians, 1st and 3rd quartiles, and 5th and 95th percentiles (whiskers). In grafts only medians and 1st and 3rd quartiles are shown. Asterisks (*) indicate a significant reduction in nerve density from control levels, while † denotes a significant increase relative to controls.

Discussion

The human corneal stromal matrix comprises 71% collagen by dry weight.[20] The predominant collagen is type I but smaller amounts of types III and V are present.[21] All are fibrillar collagens with structural supporting roles. Type I collagen is a heterotrimer comprising two alpha 2(I) and one alpha 1(I) chain, while type III is a homotrimer of alpha 1(III). [22] *In vivo*, collagen crosslinking allows for the tensile strength of tissues, since it increases the resistance of the fibres against proteolysis.[23] It is believed that both type I and type III collagens undergo similar crosslinking, though the lysine aldehyde pathway in the cornea, and heterotrimers of both collagens exist. However, type III collagen chains are characterized by the disulphide bonds [21] that form between the 3 chains in the triple helical domain and are more resistant to digestion by collagenases secreted by granulocytes.[24] This suggests that type III collagen is likely to be more resistant to degradation when used as implants. Furthermore, Beuerman and co-workers [25] reported that the inclusion of type III collagen in hydrated matrices significantly increased the optical transmittance and reduced contraction of the hydrogels by stromal cells. This suggests that type III collagen gels may be more robust and optically clear than type I gels.

As reported by Beuerman using extracted collagens, RHC-III gels had significantly superior light transmission. While there were no significant differences in tensile strength, elongation at break and moduli between optimized RHC-I and RHC-III gels, we noted that "optimized" gels were crosslinked using an EDC/coll-amine ratio of 0.5 and 0.4, respectively. This shows that type III collagen can therefore be crosslinked at lower EDC ratios than type I collagen, with no significant loss in terms of mechanical properties.

Albumin diffusion was decreased suggesting that the thinner type III collagen fibrils may allow for tighter packing of the hydrogel.

Both RHC-I and RHC-III hydrogels supported corneal epithelial cell proliferation and stratification at similar rates *in vitro*. Neurite extensions on these two hydrogels were also similar. These *in vitro* results were predictive of the *in vivo* results as implants.
Both implanted RHC-I and RHC-III gels were optically clear at 12 months, as evidenced by clear fundus images of retinal vessels and minimal/no haze compared to allograft controls. Both hydrogels were equally effective in allowing re-epithelialization, stromal cell and nerve in-growth. Hemidesmosomes and positive type VII collagen immunohistochemistry (as well as manipulations during fundus and *in vivo* confocal imaging) demonstrated stably anchored epithelia.

There were no significant differences in the patterns of re-innervation between RHC-I and RHC-III gels. Nerve density in corneal depth zone 1 (representing subepithelial and subbasal nerves), however, was significantly reduced after 12 months in both RHC gels and in allografts relative to the untreated controls. While the recovery of zone 1 nerve density to control levels is expected to take longer than 12 months, the rate of nerve recovery in RHC-based gels did not significantly differ from that of allograft tissue. At 12 months post-operative, both RHC-I and RHC-III implanted corneas were quiet, i.e. there were no noticeable numbers of macrophages. Our sections were also negative for CD45 marrow-derived cells in either implants or stromas of controls, in contrast to previous reports by Yamagami et al.[26] This may be due to either a difference in sample preparation or a species difference. Procollagen I staining was found, in particular, in RHC-III implanted corneas, suggesting that there is synthesis of type I collagen, suggesting that corneal stromal cells are

probably laying down type I collagen, but in a very gradual manner since optical clarity was unaffected. While we were unable to definitively determine that both RHC-I and RHC-III implants had been completely remodelled, the lack of type III collagen staining in RHC-III implanted corneas at 12 months post-operative compared to positive controls of unimplanted hydrogels together with the increased procollagen I staining very strongly suggest remodelling and turnover of the collagen scaffold.

We have therefore shown that although type III collagen is a minor component in the human cornea, it is nevertheless a suitable alternative to type I collagen in the development of stromal matrix substitutes that allow for both corneal cell and nerve regeneration after implantation. The use of recombinant materials allows for control over batch homogeneity and since it is fully synthetic, circumvents the safety issues associated with animal source proteins. In addition, as corneal nerves are regenerated, such synthetic, biomimetic corneal implants could circumvent potential problems such as dry eye that results from lack of corneal nerve regeneration after transplantation.[27]

Acknowledgements

Research support from NSERC STGP #246418 to MG and MAW; the Canadian Stem Cell Network. Partial support for animal studies and samples were provided by CooperVision, Inc. The authors thank Minoru Fukuda, Kyorin University for the excellent TEM assistance, Lea Muzakare and the ACVS staff at the University of Ottawa for excellent technical assistance; and Dr. Yuwen Liu, CooperVision for preparation of implant samples.

Chapter 7

General Discussion

The role of sensory nerve innervation for proper tissue function in the cornea has long been recognized. The cornea is highly innervated, about 100x more than tooth pulp (Lambiase et al. 1999). Being avascular, it is unique in its dependence upon sensory nerves and their interactions with corneal cells for maintenance of tissue integrity and wound healing.

Typically, in tissue engineering, there has been great interest in creating materials that allow for the regeneration of functional nerves in the host tissue following damage or disease. With respect to the field of artificial corneas, however, the role of nerves has been seriously undervalued. The majority of materials that have been employed, have served as simple prosthetic devices which address minimum replacement of the cornea's function, to permit the passage of light onto the retina for vision and providing protection for the delicate inner structures of the eyeball. These keratoprostheses, fabricated from plastics, often suffer from post implantation complications as they are minimally biocompatible but not necessarily cell friendly, and can result in graft extrusion, and ultimately, rejection.

Therefore, several issues with synthetically fabricated corneal substitutes have yet to be fully addressed. These include: 1) Creation of tissue engineered artificial corneas that permit integration with the host tissue, and repopulation with the corneal cell types including epithelial and stromal cells, as well as nerve regeneration; 2) a biomimetic artificial cornea that is strong enough to implant through full thickness penetrating keratoplasty; 3) demonstration of functional regenerated nerves within the artificial cornea to show proper impulse conduction comparable to the unoperated eye; and 4) the use of non animal sourced

biomimetic material for the development of materials for human implantation. Our previous experience in developing an *in vitro* human corneal quivalent provided the rationale behind our artificial cornea for animal implantation (Griffith et al. 1999; Suuronen et al. 2004).

7.1 Significant Scientific Contributions

Corneal transplantation with allograft tissue is currently the gold standard treatment for treating corneal damage following trauma or disease, however the supply of donor tissue cannot meet the demand, especially in developing countries. Currently, the only alternative treatment option has been keratoprostheses which do not permit integration with the host tissue. Our results in artificial cornea research have shown significant advances with respect to several issues that have yet to be fully addressed:

1. The creation of a tissue engineered innervated corneal model comprised of type I collagen, allowed for the study of corneal wound healing, in a controlled environment. It showed a proof of concept, that the ECM microenvironment found inside the native cornea would permit and sustain the growth of corneal cell types within and overlying the scaffold, as well as having the appropriate microstructure to allow nerve fibres to extend. We were also able to generate methodologies to create *in vitro* tests for determining the suitability of formulations for *in vivo* implantation.
2. Previous iterations of artificial corneas created from biological molecules have resulted in scaffolds with mechanical properties that were significantly lower than that of the native cornea, and therefore were only amenable to implantation through lamellar keratoplasties. By utilizing biomimetic and biocompatible synthetic molecules, we have been able to create stronger artificial corneas which could be

implanted for the first time in a full thickness penetrating keratoplasty animal model successfully, and allow subsequent corneal regeneration.

3. Prior prosthetic or tissue engineered corneas to date have not addressed the importance of reinnervation for proper function. We have shown that our iterations of artifical corneas have allowed for the regrowth of corneal nerves to densities that are either comparable to the unoperated eye, or at least to allograft controls, and are functionally responsive when tested via aesthesiometry. Furthermore, in our full thickness model, we have observed through electrophysiology that the nerves express the normal array of various functional nociceptors that respond to the appropriate stimuli, post surgery.
4. Artificial corneas that have been approved for clinical human implantation have been comprised of completely synthetic biocompatible materials, with no aim for regeneration. We have been able to adapt our methods for creating artificial corneas by using recombinant human collagen, produced in yeast. Not only does it provide a safe, chemically defined material for tissue engineering which alleviates the concern for the risk of disease transmission or immune reaction that could follow the implantation of animal sourced collagen, but the recombinant collagen provided stronger artificial corneas with better light transmission properties then our previous porcine collagen based corneas.

7.2 Novel Technologies, Methods, or Results

1. The development of an innervated three dimensional *in vitro* corneal model for studying the interactions of nerves with their target cells.

2. Innervation of the tissue engineered cornea affects the properties of the corneal cells, resulting in a more physiologically accurate model which better represents the human cornea and its response to chemicals
3. The creation of *in vitro* testing methods for characterizing and selecting appropriate artificial cornea formulations for *in vivo* implantation.
4. The development of a non toxic labelling method using biotin to track the artificial corneas within the host tissue.
5. EDC/NHS can be used to crosslink collagen, resulting in a non toxic final product, due to the fact that the crosslinkers are not incorporated into the artificial cornea post crosslinking, which circumvents the possibility of toxic release products resulting from breakdown.
6. The discovery that the collagen artificial corneas are remodelled by the host cells in a stable and seamless fashion, and restoration of mechanical properties occurs as a result of this.
7. Collagen based artificial corneas could be strengthened through the addition of a biomimetic molecule, MPC, which increased the mechanical strength of the scaffolds, without changing the biointeractive properties, allowing for cell overgrowth and ingrowth as well as nerve regeneration.
8. Collagen MPC artificial corneas were robust mechanically to hold sutures and be implanted through full thickness penetrating keratoplasty in an *in vivo* animal model, and permit regeneration of functional nerves.
9. The fabrication of artificial corneas from human collagen, which resulted in mechanically strong gels that could be implanted *in vivo*, and allow for stable

integration, with the regeneration of corneal cells, tear film, and nerves. Specifically, artificial corneas constructed from type III collagen, a minor component of the native cornea, were shown to have superior optical properties to those constructed from type I collagen.

7.3 Current Progress

Following the success of the implantation of biomimetic artificial corneas in animal models, we have begun clinical trials of our type III recombinant human collagen artificial corneas in 10 patients in a small Phase I clinical study in Sweden. All the patients presented with significant visual loss as a result of keratoconus or corneal scarring, and received implants through anterior lamellar keratoplasty. Following 12 month implantations, it was observed that all implants were stably integrated, and showed a morphologically-normal epithelium, with a normal tear film, although a delay in re-epithelialization was observed due to the use of overlying sutures. All grafts were well integrated, with remodelling observed, and the in growth of stromal cells and corneal nerves, as evidenced by *in vivo* confocal microscopy. Touch sensitivity was returned to the eyes, which is indicative of functional nerves, and visual acuity improved in nine of the ten patients (Fagerholm *et al*, submitted). The results of this study are promising, showing for the first time, the implantation of a corneal substitute that allowed regeneration of the corneal epithelium, nerves, and stroma in humans.

Indications for corneal transplantation do not always present as simple trauma, or keratoconus, rather, they can be long grade inflammation, or infection. Herpes simplex virus type 1 (HSV-1) is implicated as a cause of corneal graft failure in transplantation of donor

cornea and corneal prostheses (De Kesel et al. 2001; Hicks et al. 2002). The pathogenesis of this virus is complex. Initial exposure generally results in a primary infection during which the clinical signs most commonly include blepharitis, conjunctivitis, and keratitis, usually consisting of punctuate or dentritic ulceration, resulting in a characteristic superficial branching corneal ulcer (Darougar et al. 1985). After the primary infection resolves, the virus enters into a latency period, by residing in the cell body of the trigeminal ganglion, which provides sensory innervation to the ocular surface (Cleator and Klapper 2000). While the virus is dormant, there are no clinical signs that are present, nor are any viral antigens present that would stimulate the immune system to mount a defense and try to eliminate the virus. As well, the cornea may also be a site of viral latency (O'Brien and Taylor 1989). Latent virus may reactivate at various times and return to the ocular surface where it again produces ocular disease (Cleator and Klapper 2000). Reactivation of the virus can be caused by various reasons which are nonspecific including stress, immunosuppression, sunlight, and ingestion of certain foods (Cleator and Klapper 2000). Corneal graft failure in patients with herpes simplex virus (HSV) keratitis may be due to reactivation of latent HSV-1 following surgical corneal trauma and postoperative corticosteroid therapy.

We have had prior experience with conjugating our artificial corneal matrices with the laminin derived pentapeptide YIGSR, to promote nerve regeneration (Li et al. 2003). The artificial corneas would be modified to contain photocaged acyclovir, which is an antiviral used in the treatment of HSV infection. They will be tested in both primary, and latent infection cases, and could potentially improve corneal graft acceptance in higher risk cases.

In many cases, damage only occurs to one corneal layer. In general, the outermost epithelial layer that is exposed to the environment may be prone to injury such as chemical burns or dry eye syndrome. However, the stem and progenitor cells found in the corneal sclera limbus that are normally responsible for affecting the repair may also be decimated. As such, there have been various attempts to repopulate the cornea.

During reconstruction of the epithelium, corneal stem cells from the surrounding limbus are isolated either from the undamaged contralateral eye (autograft) or from allogeneic sources. These explants are most frequently seeded on prepared human amniotic membranes (Nakamura et al. 2006) or fibrin substrates (Rama et al. 2001). Outgrowing cells are allowed to form sheets that are transplanted onto the damaged eye. More recently, the authors and other collaborators have seeded corneal limbal cells onto fully synthetic, crosslinked human recombinant collagen substrates. It has been demonstrated that fully stratified corneal epithelia can be reconstituted on these. We showed that both type I and type III human recombinant collagens supported limbal epithelial proliferation and differentiation (Dravida et al. 2008).

In some patients, both corneal surfaces have been depleted of stem cells. This has been observed in patients with Steven's Johnson syndrome, chemical and thermal injury, pseudo-ocular cicatricial pemphigoid, and idiopathic ocular surface disorder. In these cases, successful autologous reconstruction of the corneal surface by transdifferentiation of oral mucosal epithelium has been performed (Inatomi et al. 2006). The oral mucosal cells were cultured on human amniotic membranes, and then transplanted onto 15 eyes in 12 patients. Kinoshita and co-workers further suggested the use of transdifferentiated autologous oral mucosa precursor cells. These cells may be safer for ocular resurfacing than with allogeneic

corneal grafts, in particular for younger patients with the most severe ocular surface disorders. However, it should be noted that all transplanted eyes had some peripheral corneal neovascularization.

Failure of the monolayered corneal endothelium is one of the more common reasons for transplantation, especially in patients with congenital or age-related conditions requiring transplantation. Various methods have been tested for corneal endothelial tissue engineering and transplants of engineered endothelial sheets have been tested in animal models, mainly rabbits (Hsiue et al. 2006). Rabbits, unlike humans, can rapidly regenerate the endothelium. That being said, human corneal endothelial cells have also been grown successfully *in vitro* on a range of supports including Descemet's membrane (Hsiue et al. 2006). In the author's lab, we show that human corneal endothelial cells grow well on amniotic membrane and also crosslinked type I recombinant human collagen. However, unlike the limbal cells, we found that corneal endothelial cells proliferate better on type I recombinant human collagen membranes. Poor growth is observed on type III collagen membranes.

In conclusion, the creation of corneal substitutes that promote the *in vivo* reconstruction of healthy and viable tissue, as well as innervation, is an important advancement in the field of corneal transplantation. The manuscripts presented showed that the use of tissue engineered biomimetic materials designed to mimic the ECM of the native cornea were suitable for both lamellar and full thickness corneal implants and allowed for the regeneration of corneal cell types, and functional nerves, to produce a seamless and stable graft.

References

Chapter 1

Albers, K. M., D. E. Wright and B. M. Davis (1994). "Overexpression of nerve growth factor in epidermis of transgenic mice causes hypertrophy of the peripheral nervous system." J. Neurosci. **14**(3 Pt 2): 1422-32.

Araki, K., Y. Ohashi, S. Kinoshita, K. Hayashi, Y. Kuwayama and Y. Tano (1994). "Epithelial wound healing in the denervated cornea." Curr. Eye Res. **13**(3): 203-11.

Aucoin, L., C. M. Griffith, G. Pleizier, Y. Deslandes and H. Sheardown (2002). "Interactions of corneal epithelial cells and surfaces modified with cell adhesion peptide combinations." J. Biomater. Sci. Polym. Ed. **13**(4): 447-62.

Badylak, S. F. (2002). Modification of natural polymers: Collagen. Methods of Tissue Engineering. A. Atala and R. P. Lanza. San Diego, Academic Press: 505-514.

Bakri, A., N. Farooqui, D. Myung, W. Koh, J. Noolandi, M. Carrasco, C. Frank and C. Ta (2006). "Biocompatibility of a Hydrogel Corneal inlay in vivo." Invest Ophthalmol Vis Sci (Arvo Annual Meeting) **47 (E-Abstract 3592)**.

Baldwin, H. S. (1996). "Early embryonic vascular development." Cardiovasc. Res. **31 Spec No**: E34-45.

Belmonte, C., A. Aracil, M. C. Acosta, C. Luna and J. Gallar (2004). "Nerves and sensations from the eye surface." Ocul. Surf. **2**(4): 248-53.

Borene, M. L., V. H. Barocas and A. Hubel (2004). "Mechanical and cellular changes during compaction of a collagen-sponge-based corneal stromal equivalent." Ann. Biomed. Eng. **32**(2): 274-83.

Boudreau, N., C. Myers and M. J. Bissell (1995). "From laminin to lamin: regulation of tissue-specific gene expression by the ECM." Trends Cell Biol. **5**(1): 1-4.

Brock, J. A., E. M. McLachlan and C. Belmonte (1998). "Tetrodotoxin-resistant impulses in single nociceptor nerve terminals in guinea-pig cornea." J Physiol **512 (Pt 1)**: 211-7.

Carrier, P., A. Deschambeault, M. Talbot, C. J. Giasson, F. A. Auger, S. L. Guerin and L. Germain (2008). "Characterization of wound reepithelialization using a new human tissue-engineered corneal wound healing model." Invest. Ophthalmol. Vis. Sci. **49**(4): 1376-85.

Chan, K. Y. and R. H. Haschke (1982). "Isolation and culture of corneal cells and their interactions with dissociated trigeminal neurons." Exp. Eye Res. **35**(2): 137-56.

Chen, X., C. Belmonte and H. P. Rang (1997). "Capsaicin and carbon dioxide act by distinct mechanisms on sensory nerve terminals in the cat cornea." Pain **70**(1): 23-9.

Chikama, T., M. Nakamura and T. Nishida (1999). "Up-regulation of integrin alpha5 by a C-terminus four-amino-acid sequence of substance P (phenylalanine-glycine-leucine-methionine- amide) synergistically with insulin-like growth factor-1 in SV-40 transformed human corneal epithelial cells." Biochem. Biophys. Res. Commun. **255**(3): 692-7.

Chirila, T. V., S. Vijayasekaran, R. Horne, Y. C. Chen, P. D. Dalton, I. J. Constable and G. J. Crawford (1994). "Interpenetrating polymer network (IPN) as a permanent joint between the elements of a new type of artificial cornea." J. Biomed. Mater. Res. **28**(6): 745-53.

Corcoran, J., B. Shroot, J. Pizzey and M. Maden (2000). "The role of retinoic acid receptors in neurite outgrowth from different populations of embryonic mouse dorsal root ganglia." J. Cell Sci. **113 (Pt 14)**: 2567-74.

Crabb, R. A., E. P. Chau, M. C. Evans, V. H. Barocas and A. Hubel (2006). "Biomechanical and microstructural characteristics of a collagen film-based corneal stroma equivalent." Tissue Eng. **12**(6): 1565-75.

Davis, E. A. and C. H. Dohlman (2001). "Neurotrophic keratitis." Int. Ophthalmol. Clin. **41**(1): 1-11.

de Castro, F., I. Silos-Santiago, M. Lopez de Armentia, M. Barbacid and C. Belmonte (1998). "Corneal innervation and sensitivity to noxious stimuli in trkA knockout mice." Eur J Neurosci **10**(1): 146-52.

De Felipe, C. and C. Belmonte (1999). "c-Jun expression after axotomy of corneal trigeminal ganglion neurons is dependent on the site of injury." Eur J Neurosci **11**(3): 899-906.

Dua, H. S. and A. Azuara-Blanco (2000). "Limbal stem cells of the corneal epithelium." Surv. Ophthalmol. **44**(5): 415-25.

Ehlers, M. D., D. R. Kaplan, D. L. Price and V. E. Koliatsos (1995). "NGF-stimulated retrograde transport of trkA in the mammalian nervous system." J Cell Biol **130**(1): 149-56.

Emoto, I. and R. W. Beuerman (1987). "Stimulation of neurite growth by epithelial implants into corneal stroma." Neurosci. Lett. **82**(2): 140-4.

Falcinelli, G., B. Falsini, M. Taloni, P. Colliardo and G. Falcinelli (2005). "Modified osteo-odonto-keratoprosthesis for treatment of corneal blindness: long-term anatomical and functional outcomes in 181 cases." Arch. Ophthalmol. **123**(10): 1319-29.

Foster, A. (2003). "Vision 2020--the Right to Sight." Trop. Doct. **33**(4): 193-4.

Freegard, T. J. (1997). "The physical basis of transparency of the normal cornea." Eye **11 (Pt 4)**: 465-71.

Gallar, J., M. A. Pozo, R. P. Tuckett and C. Belmonte (1993). "Response of sensory units with unmyelinated fibres to mechanical, thermal and chemical stimulation of the cat's cornea." J Physiol **468**: 609-22.

Gaudreault, M., P. Carrier, K. Larouche, S. Leclerc, M. Giasson, L. Germain and S. L. Guerin (2003). "Influence of sp1/sp3 expression on corneal epithelial cells proliferation and differentiation properties in reconstructed tissues." Invest. Ophthalmol. Vis. Sci. **44**(4): 1447-57.

Gelse, K., E. Poschl and T. Aigner (2003). "Collagens--structure, function, and biosynthesis." Adv Drug Deliv Rev **55**(12): 1531-46.

Gipson, I. K. and P. Argueso (2003). "Role of mucins in the function of the corneal and conjunctival epithelia." Int. Rev. Cytol. **231**: 1-49.

Girardot, J. M. and M. N. Girardot (1996). "Amide cross-linking: an alternative to glutaraldehyde fixation." J. Heart Valve Dis. **5**(5): 518-25.

Griffith, M., R. Osborne, R. Munger, X. Xiong, C. J. Doillon, N. L. Laycock, M. Hakim, Y. Song and M. A. Watsky (1999). "Functional human corneal equivalents constructed from cell lines." Science **286**(5447): 2169-72.

Guo, X., A. E. Hutcheon, S. A. Melotti, J. D. Zieske, V. Trinkaus-Randall and J. W. Ruberti (2007). "Morphologic characterization of organized extracellular matrix deposition by ascorbic acid-stimulated human corneal fibroblasts." Invest. Ophthalmol. Vis. Sci. **48**(9): 4050-60.

Handwerker, H. O. and P. W. Reeh (1991). "Pain and inflammation." Pain Research and Clinical Management. (Proceedings of the Vth World Congress on Pain) **4**: 59-70.

Hicks, C. R., G. J. Crawford, J. K. Dart, G. Grabner, E. J. Holland, R. D. Stulting, D. T. Tan and M. Bulsara (2006). "AlphaCor: Clinical outcomes." Cornea **25**(9): 1034-42.

Hollick, E. J., S. L. Watson, J. K. Dart, P. J. Luthert and B. D. Allan (2006). "Legeais BioKpro III keratoprosthesis implantation: long term results in seven patients." Br. J. Ophthalmol. **90**(9): 1146-51.

Holzer, P. (1988). "Local effector functions of capsaicin-sensitive sensory nerve endings: involvement of tachykinins, calcitonin gene-related peptide and other neuropeptides." Neuroscience **24**(3): 739-68.

Imamura, E., O. Sawatani, H. Koyanagi, Y. Noishiki and T. Miyata (1989). "Epoxy compounds as a new cross-linking agent for porcine aortic leaflets: subcutaneous implant studies in rats." J. Card. Surg. **4**(1): 50-7.

Jacob, J. T., J. R. Rochefort, J. Bi and B. M. Gebhardt (2005). "Corneal epithelial cell growth over tethered-protein/peptide surface-modified hydrogels." J. Biomed. Mater. Res. B Appl. Biomater. **72**(1): 198-205.

Jain, R. A. (2000). "The manufacturing techniques of various drug loaded biodegradable poly(lactide-co-glycolide) (PLGA) devices." Biomaterials **21**(23): 2475-90.

Jonas, J. B. and L. Holbach (2005). "Central corneal thickness and thickness of the lamina cribrosa in human eyes." Invest. Ophthalmol. Vis. Sci. **46**(4): 1275-9.

Khan, B. F., M. Harissi-Dagher, D. Pavan-Langston, J. V. Aquavella and C. H. Dohlman (2007). "The Boston keratoprosthesis in herpetic keratitis." Arch. Ophthalmol. **125**(6): 745-9.

Kim, M. K., S. M. Lee, J. L. Lee, T. Y. Chung, Y. H. Kim, W. R. Wee and J. H. Lee (2007). "Long-term outcome in ocular intractable surface disease with Seoul-type keratoprosthesis." Cornea **26**(5): 546-51.

Klausner, M., P. J. Hayden, B. A. Breyfogle, K. L. Bellavance, M. M. Osborn, D. R. Cerven, G. L. DeGeorge and J. Kubilus (2003). The EpiOcular Prediction Model: A Reproducible In Vitro Means of Assessing Ocular Irritancy. Alternative toxicological methods

H. Salem and S. A. Katz. Boca Raton, Fla., CRC Press: 591 p.

Lambiase, A., P. Rama, L. Aloe and S. Bonini (1999). "Management of neurotrophic keratopathy." Curr. Opin. Ophthalmol. **10**(4): 270-6.

LaVail, J. H., W. E. Johnson and L. C. Spencer (1993). "Immunohistochemical identification of trigeminal ganglion neurons that innervate the mouse cornea: relevance to intercellular spread of herpes simplex virus." J Comp Neurol **327**(1): 133-40.

Li, F., D. Carlsson, C. Lohmann, E. Suuronen, S. Vascotto, K. Kobuch, H. Sheardown, R. Munger, M. Nakamura and M. Griffith (2003). "Cellular and nerve regeneration within a biosynthetic extracellular matrix for corneal transplantation." Proc. Natl. Acad. Sci. U. S. A. **100**(26): 15346-51.

Li, F., M. Griffith, Z. Li, S. Tanodekaew, H. Sheardown, M. Hakim and D. J. Carlsson (2005). "Recruitment of multiple cell lines by collagen-synthetic copolymer matrices in corneal regeneration." Biomaterials **26**(16): 3093-104.

Liu, L., L. Kuffova, M. Griffith, Z. Dang, E. Muckersie, Y. Liu, C. R. McLaughlin and J. V. Forrester (2007). "Immunological responses in mice to full-thickness corneal grafts engineered from porcine collagen." Biomaterials **28**(26): 3807-14.

Liu, Y., L. Gan, D. J. Carlsson, P. Fagerholm, N. Lagali, M. A. Watsky, R. Munger, W. G. Hodge, D. Priest and M. Griffith (2006). "A simple, cross-linked collagen tissue substitute for corneal implantation." Invest. Ophthalmol. Vis. Sci. **47**(5): 1869-75.

Marfurt, C. F., R. E. Kingsley and S. E. Echtenkamp (1989). "Sensory and sympathetic innervation of the mammalian cornea. A retrograde tracing study." Invest. Ophthalmol. Vis. Sci. **30**(3): 461-72.

Meek, K. M. and D. W. Leonard (1993). "Ultrastructure of the corneal stroma: a comparative study." Biophys. J. **64**(1): 273-80.

Mehta, J. S., C. E. Futter, S. R. Sandeman, R. G. Faragher, K. A. Hing, K. E. Tanner and B. D. Allan (2005). "Hydroxyapatite promotes superior keratocyte adhesion and proliferation in comparison with current keratoprosthesis skirt materials." Br. J. Ophthalmol. **89**(10): 1356-62.

Meller, D., K. Peters and K. Meller (1997). "Human cornea and sclera studied by atomic force microscopy." Cell Tissue Res. **288**(1): 111-8.

Morgan, C. W., I. Nadelhaft and W. C. de Groat (1978). "Anatomical localization of corneal afferent cells in the trigeminal ganglion." Neurosurgery **2**(3): 252-8.

Muller, L. J., C. F. Marfurt, F. Kruse and T. M. Tervo (2003). "Corneal nerves: structure, contents and function." Exp. Eye Res. **76**(5): 521-42.

Muller, L. J., L. Pels and G. F. Vrensen (1996). "Ultrastructural organization of human corneal nerves." Invest. Ophthalmol. Vis. Sci. **37**(4): 476-88.

Muller, L. J., G. F. Vrensen, L. Pels, B. N. Cardozo and B. Willekens (1997). "Architecture of human corneal nerves." Invest. Ophthalmol. Vis. Sci. **38**(5): 985-94.

Myung, D., N. Farooqui, L. L. Zheng, W. Koh, S. Gupta, A. Bakri, J. Noolandi, J. R. Cochran, C. W. Frank and C. N. Ta (2008). "Bioactive interpenetrating polymer network hydrogels that support corneal epithelial wound healing." J. Biomed. Mater. Res. A.

Myung, D., W. Koh, J. Ko, J. Noolandi, M. Carrasco, A. Smith, C. Frank and C. Ta (2005). "Characterization of Poly(Ethylene Glycol)–Poly(Acrylic Acid) (PEG–PAA) Double Networks Designed for Corneal Implant Applications." Invest Ophthalmol Vis Sci (Arvo Annual Meeting) **46 (E-abstract 5003)**.

Niederkorn, J. Y. (1990). "Immune privilege and immune regulation in the eye." Adv. Immunol. **48**: 191-226.

Nimni, M. E. (1988). Collagen. Boca Raton, Fla., CRC Press.

Nimni, M. E., D. Cheung, B. Strates, M. Kodama and K. Sheikh (1987). "Chemically modified collagen: a natural biomaterial for tissue replacement." J. Biomed. Mater. Res. **21**(6): 741-71.

Nishida, T. (1997). Cornea: Fundamentals of cornea and external disease. Cornea. J. J. Krachmer, M. J. Mannis and E. J. Holland. St. Louis, Missouri, Mosby-Year Book Inc. **1:** 3-27.

Rama, P., S. Bonini, A. Lambiase, O. Golisano, P. Paterna, M. De Luca and G. Pellegrini (2001). "Autologous fibrin-cultured limbal stem cells permanently restore the corneal surface of patients with total limbal stem cell deficiency." Transplantation **72**(9): 1478-85.

Ren, H. and G. Wilson (1996). "Apoptosis in the corneal epithelium." Invest. Ophthalmol. Vis. Sci. **37**(6): 1017-25.

Riggott, M. J. and S. A. Moody (1987). "Distribution of laminin and fibronectin along peripheral trigeminal axon pathways in the developing chick." J. Comp. Neurol. **258**(4): 580-96.

Rozsa, A. J. and R. W. Beuerman (1982). "Density and organization of free nerve endings in the corneal epithelium of the rabbit." Pain **14**(2): 105-20.

Ryu, W., S. W. Min, K. E. Hammerick, M. Vyakarnam, R. S. Greco, F. B. Prinz and R. J. Fasching (2007). "The construction of three-dimensional micro-fluidic scaffolds of biodegradable polymers by solvent vapor based bonding of micro-molded layers." Biomaterials **28**(6): 1174-84.

Sack, R. A., I. Nunes, A. Beaton and C. Morris (2001). "Host-defense mechanism of the ocular surfaces." Biosci. Rep. **21**(4): 463-80.

Schaible, H. G. and R. F. Schmidt (1983). "Responses of fine medial articular nerve afferents to passive movements of knee joints." J Neurophysiol **49**(5): 1118-26.

Strampelli, B. (1963). "[Osteo-Odontokeratoprosthesis.]." Ann. Ottalmol. Clin. Ocul. **89**: 1039-44.

Suuronen, E. J., M. Nakamura, M. A. Watsky, P. K. Stys, L. J. Muller, R. Munger, N. Shinozaki and M. Griffith (2004). "Innervated human corneal equivalents as in vitro models for nerve-target cell interactions." FASEB J. **18**(1): 170-2.

Tanelian, D. L. and R. W. Beuerman (1984). "Responses of rabbit corneal nociceptors to mechanical and thermal stimulation." Exp Neurol **84**(1): 165-78.

Tervo, T. and J. Moilanen (2003). "In vivo confocal microscopy for evaluation of wound healing following corneal refractive surgery." Prog. Retin. Eye Res. **22**(3): 339-58.

Trinkaus-Randall, V. (2000). Cornea. Principles of Tissue Engineering. R. Lanza, R. Langer and J. P. Vacanti. New York, Academic Press: 471-492.

Waxman, S. G., S. Dib-Hajj, T. R. Cummins and J. A. Black (1999). "Sodium channels and pain." Proc Natl Acad Sci U S A **96**(14): 7635-9.

Wertz, P. W. (2006). Biochemistry of human stratum corneum lipids. Skin Barrier. P. M. Elias and K. R. Feingold. New York, NY, USA, Taylor & Francis: 33-42.

Whitcher, J. P., M. Srinivasan and M. P. Upadhyay (2001). "Corneal blindness: a global perspective." Bull. World Health Organ. **79**(3): 214-21.

You, L., F. E. Kruse and H. E. Volcker (2000). "Neurotrophic factors in the human cornea." Invest. Ophthalmol. Vis. Sci. **41**(3): 692-702.

Zieske, J. D., V. S. Mason, M. E. Wasson, S. F. Meunier, C. J. Nolte, N. Fukai, B. R. Olsen and N. L. Parenteau (1994). "Basement membrane assembly and differentiation of cultured corneal cells: importance of culture environment and endothelial cell interaction." Exp. Cell Res. **214**(2): 621-33.

Chapter 2

Anand, P., Terenghi, G., Warner, G., Kopelman, P., Williams-Chestnut, R. E., and Sinicropi, D. V. (1996). The role of endogenous nerve growth factor in human diabetic neuropathy. *Nat Med* **2**, 703-707.

Araki, K., Kinoshita, S., Sun, N., Kuwayama, Y., Ohashi, Y., and Manabe, R. (1992). Effect of trigeminal denervation on rabbit corneal epithelium. *Acta Soc Ophthalmol Jpn* **96**, 710-714.

Araki, K., Ohashi, Y., Kinoshita, S., Hayashi, K., Kuwayama, Y., and Tano, Y. (1994). Epithelial wound healing in the denervated cornea. *Curr Eye Res* **13**, 203-11.

Araki-Sasaki, K., Aizawa, S., Hiramoto, M., Nakamura, M., Iwase, O., Nakata, K., Sasaki, Y., Mano, T., Handa, H., and Tano, Y. (2000). Substance P-induced cadherin expression and its signal transduction in a cloned human corneal epithelial cell line. *J Cell Physiol* **182**, 189-195.

Argueso, P., and Gipson, I. K. (2001). Epithelial mucins of the ocular surface: structure, biosynthesis and function. *Exp Eye Res* **73**, 281-9.

Argueso, P., Spurr-Michaud, S., Russo, C. L., Tisdale, A., and Gipson, I. K. (2003). MUC16 mucin is expressed by the human ocular surface epithelia and carries the H185 carbohydrate epitope. *Invest Ophthalmol Vis Sci* **44**, 2487-95.

Atala, A., and Lanza, R. P., eds. (2002). *Methods of tissue engineering*. Academic Press, San Diego.

Beuerman, R. W., and Schimmelpfennig, B. (1980). Sensory denervation of the rabbit cornea affects epithelial properties. *Exp Neurol* **69**, 196-201.

Black, J. A., Renganathan, M., and Waxman, S. G. (2002). Sodium channel Na(v)1.6 is expressed along nonmyelinated axons and it contributes to conduction. *Brain Res Mol Brain Res* **105**, 19-28.

Brock, J. A., McLachlan, E. M., and Belmonte, C. (1998). Tetrodotoxin-resistant impulses in single nociceptor nerve terminals in guinea-pig cornea. *J Physiol* **512**, 211-7.

Brugge, J. S., and Erikson, R. L. (1977). Identification of a transformation-specific antigen induced by an avian sarcoma virus. *Nature* **269**, 346-8.

Danjo, Y., Watanabe, H., Tisdale, A. S., George, M., Tsumura, T., Abelson, M. B., and Gipson, I. K. (1998). Alteration of mucin in human conjunctival epithelia in dry eye. *Invest Ophthalmol Vis Sci* **39**, 2602-9.

Daston, G. P., and Freeberg, F. E. (1991). Ocular irritation testing. In Dermal and Ocular Toxicology (D. W. Hobson, ed., pp. 509-540. CRC Press, Inc., Boca Raton, FA.

Denk, W., Piston, D. W., and Webb, W. W. (1995). Two-photon molecular excitation in laser-scanning microscopy. In Handbook of biological confocal microscopy (J. B. Pawley, ed., pp. 445-458. Plenum, New York.

Denk, W., and Svoboda, K. (1997). Photon upmanship: why multiphoton imaging is more than a gimmick. *Neuron* **18**, 351-7.

Gallar, J., Pozo, M. A., Rebollo, I., and Belmonte, C. (1990). Effects of capsaicin on corneal wound healing. *Invest Ophthalmol Vis Sci* **31**, 1968-74.

Gautheron, P., Dukic, M., Alix, D., and Sina, J. F. (1992). Bovine corneal opacity and permeability test: an *in vitro* assay of ocular irritancy. *Fundam Appl Toxicol* **18**, 442-9.

Gipson, I. K., Spurr-Michaud, S. J., Tisdale, A. S., Kublin, C., Cintron, C., and Keutmann, H. (1995). Stratified squamous epithelia produce mucin-like glycoproteins. *Tissue Cell* **27**, 397-404.

Gover, T. D., Kao, J. P., and Weinreich, D. (2003). Calcium signaling in single peripheral sensory nerve terminals. *J Neurosci* **23**, 4793-7.

Griffith, M., Osborne, R., Munger, R., Xiong, X., Doillon, C. J., Laycock, N. L., Hakim, M., Song, Y., and Watsky, M. A. (1999). Functional human corneal equivalents constructed from cell lines. *Science* **286**, 2169-72.

Holzer, P. (1988). Local effector functions of capsaicin-sensitive sensory nerve endings: involvement of tachykinins, calcitonin gene-related peptide and other neuropeptides. *Neuroscience* **24**, 739-68.

Johansson, S. (1994). Graded action potentials generated by differentiated human neuroblastoma cells. *Acta Physiol Scand* **151**, 331-41.

Jumblatt, M. M., and Neufeld, A. H. (1983). Beta-adrenergic and serotonergic responsiveness of rabbit corneal epithelial cells in culture. *Invest Ophthalmol Vis Sci* **24**, 1139-43.

Keen, P., Tullo, A. B., Blyth, W. A., and Hill, T. J. (1982). Substance P in the mouse cornea: effects of chemical and surgical denervation. *Neurosci Lett* **29**, 231-5.

Kruszewski, F. H., Walker, T. L., and DiPasquale, L. C. (1997). Evaluation of a human corneal epithelial cell line as an *in vitro* model for assessing ocular irritation. *Fundam Appl Toxicol* **36**, 130-140.

Lichstein, D., Levy, T., Deutsch, J., Steinitz, M., Zigler, J. S. Jr., and Russell, P. (1999). The effects of digitalis-like compounds on rat lenses. *Invest Ophthalmol Vis Sci* **40**, 407-13.

Maggi, C. A. (1991). Capsaicin and primary afferent neurons: from basic science to human therapy? *J Auton Nerv Syst* **33**, 1-14.

Malone, J. C., Hood, A. F., Conley, T., Nurnberger, J., Baldridge, L. A., Clendenon, J. L., Dunn, K. W., and Phillips, C. L. (2002). Three-dimensional imaging of human skin and mucosa by two-photon laser scanning microscopy. *J Cutan Pathol* **29**, 453-8.

Maurer, J. K., Parker, R. D., Petroll, W. M., Carr, G. J., Cavanagh, H. D., and Jester, J. V. (1999). Quantitative measurement of acute corneal injury in rabbits with surfactants of different type and irritancy. *Toxicol Appl Pharmacol* **158**, 61-70.

Müller, L. J., Vrensen, G. F., Pels, L., Cardozo, B. N., and Willekens, B. (1997). Architecture of human corneal nerves. *Invest Ophthalmol Vis Sci* **38**, 985-94.

Neubert, J. K., Maidment, N. T., Matsuka, Y., Adelson, D. W., Kruger, L., and Spigelman, I. (2000). Inflammation-induced changes in primary afferent-evoked release of substance P within trigeminal ganglia *in vitro*. *Brain Res* **871**, 181-91.

Nishida, T., Nakamura, M., Ofuji, K., Reid, T. W., Mannis, M. J., and Murphy, C. J. (1996). Synergistic effects of substance P with insulin-like growth factor-1 on epithelial migration of the cornea. *J Cell Physiol* **169**, 159-66.

Pchejetski, D., Taurin, S., Der Sarkissian, S., Lopina, O. D., Pshezhetsky, A. V., Tremblay, J., deBlois, D., Hamet, P., and Orlov, S. N. (2003). Inhibition of Na^+,K^+-ATPase by ouabain triggers epithelial cell death independently of inversion of the $[Na^+]_i/[K^+]_I$ ratio. *Biochem Biophys Res Commun* **301**, 735-44.

Risdale, A., Micu, I., and Stys, P. K. (2004). Conversion of the Nikon C1 confocal laser-scanning head for multiphoton excitation on an upright microscope. *Appl Opt* **43,** 1669-75.

Rose, C. R., Kovalchuk, Y., Eilers, J., and Konnerth, A. (1999). Two-photon Na+ imaging in spines and fine dendrites of central neurons. *Pflugers Arch* **439**, 201-7.

Stern, M. E., Beuerman, R. W., Fox, R. I., Gao, J., Mircheff, A. K., and Pflugfelder, S. C. (1998). A unified theory of the role of the ocular surface in dry eye. *Adv Exp Med Biol* **438**, 643-51.

Suuronen, E. J., Nakamura, M., Watsky, M. A., Stys, P. K., Muller, L. J., Munger, R., Shinozaki, N., and Griffith, M. (2004). Innervated human corneal equivalents as *in vitro* models for nerve-target cell interactions. *Faseb J* **18**, 170-2.

Symposium Proceedings, technical committee on alternatives to animal testing. (1996) Replacing the Draize eye irritation test: scientific background and research needs. *J Toxicol Cut Ocular Toxicol* **15**, 211-34.

Unger, W. G. (1990). Review: mediation of the ocular response to injury. *J Ocul Pharmacol* **6**, 337-53.

Wilson, S. E., Liu, J. J., and Mohan, R. R. (1999). Stromal-epithelial interactions in the cornea. *Prog Retin Eye Res* **18**, 293-309.

Xiao, A. Y., Wei, L., Xia, S., Rothman, S., and Yu, S. P. (2002). Ionic mechanism of ouabain-induced concurrent apo.ptosis and necrosis in individual cultured cortical neurons. *J Neurosci* **22**, 1350-62.

Xu, K. P., Li, X. F., and Yu, F. S. (2000). Corneal organ culture model for assessing epithelial responses to surfactants. *Toxicol Sci* **58**, 306-314.

Chapter 3

1. Duan D, Klenkler BJ, Sheardown H. Progress in the development of a corneal replacement: keratoprostheses and tissue-engineered corneas. *Expert Rev Med Devices* 2006;3:59-72.

2. Nishida T. Cornea. In: Krachmer JH, Manis MJ, Holland EJ (eds), *Cornea.* Philadelphia: Elsevier Mosby; 2005:3-26.

3. Whitcher JP, Srinivasan M, Upadhyay MP. Corneal blindness: a global perspective. *Bull World Health Organ* 2001;79:214-221.

4. Chirila TV. An overview of the development of artificial corneas with porous skirts and the use of PHEMA for such an application. *Biomaterials* 2001;22:3311-3317.

5. Griffith M, Fagerholm P, Liu W, et al. Corneal regenerative medicine: Corneal substitutes for transplantation In: Reinhard T, Larkin F (eds), *Essentials in Ophthalmology: Cornea and external eye diseases.* Heidelberg: Springer Verlag; 2008.

6. Minami Y, Sugihara H, Oono S. Reconstruction of cornea in three-dimensional collagen gel matrix culture. *Invest Ophthalmol Vis Sci* 1993;34:2316-2324.

7. Dunn MW, Nishihara T, Stenzel KH, et al. Collagen-derived membrane: corneal implantation. *Science* 1967;157:1329-1330.

8. Willoughby CE, Batterbury M, Kaye SB. Collagen corneal shields. *Surv Ophthalmol* 2002;47:174-182.

9. Liu Y, Gan L, Carlsson DJ, et al. A simple, cross-linked collagen tissue substitute for corneal implantation. *Invest Ophthalmol Vis Sci* 2006;47:1869-1875.

10. Gratzer PF, Lee JM. Control of pH alters the type of cross-linking produced by 1-ethyl-3-(3-dimethylaminopropyl)-carbodiimide (EDC) treatment of acellular matrix vascular grafts. *J Biomed Mater Res* 2001;58:172-179.

11. Forrester JV, Kuffova L. Corneal Transplantation. Imperial College Press, London; 2004:18-21.

12. She SC, Steahly LP, Moticka EJ. A method for performing full-thickness, orthotopic, penetrating keratoplasty in the mouse. *Ophthalmic Surg* 1990;21:781-785.

13. Millodot M. A review of research on the sensitivity of the cornea. *Ophthalmic Physiol Opt* 1984;4:305-318.

14. Tervo T, Moilanen J. *In vitro* confocal microscopy for evaluation of wound healing following corneal refractive surgery. *Prog Retin Eye Res* 2003;22:339-358.

15. Plskova J, Kuffova L, Holan V, et al. Evaluation of corneal graft rejection in a mouse model. *Br J Ophthalmol* 2002;86:108-113.

16. Meijering E, Jacob M, Sarria JC, et al. Design and validation of a tool for neurite tracing and analysis in fluorescence microscopy images. *Cytometry A* 2004;58:167-176.

17. Oliveira-Soto L, Efron N. Assessing the cornea by *in vitro* confocal microscopy. *Clin Experiment Ophthalmol* 2003;31:83-84; author reply 84-86.

18. Calvillo MP, McLaren JW, Hodge DO, et al. Corneal reinnervation after LASIK: prospective 3-year longitudinal study. *Invest Ophthalmol Vis Sci* 2004;45:3991-3996.

19. Lagali NS, Griffith M, Shinozaki N, et al. Innervation of tissue-engineered corneal implants in a porcine model: a 1-year *in vitro* confocal microscopy study. *Invest Ophthalmol Vis Sci* 2007;48:3537-3544.

20. Andreassen TT, Simonsen AH, Oxlund H. Biomechanical properties of keratoconus and normal corneas. *Exp Eye Res* 1980;31:435-441.

21. Li F, Carlsson D, Lohmann C, et al. Cellular and nerve regeneration within a biosynthetic extracellular matrix for corneal transplantation. *Proc Natl Acad Sci U S A* 2003;100:15346-15351.

22. Liu Y, Griffith M, Watsky MA, et al. Properties of porcine and recombinant human collagen matrices for optically clear tissue engineering applications. *Biomacromolecules* 2006;7:1819-1828.

23. Kuffova L, Lumsden L, Vesela V, et al. Kinetics of leukocyte and myeloid cell traffic in the murine corneal allograft response. *Transplantation* 2001;72:1292-1298.

24. Holopainen JM, Moilanen JA, Sorsa T, et al. Activation of matrix metalloproteinase-8 by membrane type 1-MMP and their expression in human tears after photorefractive keratectomy. *Invest Ophthalmol Vis Sci* 2003;44:2550-2556.

25. Liu L, Kuffova L, Griffith M, et al. Immunological responses in mice to full-thickness corneal grafts engineered from porcine collagen. *Biomaterials* 2007;28:3807-3814.

26. Li F, Griffith M, Li Z, et al. Recruitment of multiple cell lines by collagen-synthetic copolymer matrices in corneal regeneration. *Biomaterials* 2005;26:3093-3104.

27. Meller D, Peters K, Meller K. Human cornea and sclera studied by atomic force microscopy. *Cell Tissue Res* 1997;288:111-118.

28. Hoeltzel DA, Altman P, Buzard K, et al. Strip extensiometry for comparison of the mechanical response of bovine, rabbit, and human corneas. *J Biomech Eng* 1992;114:202-215.

29. Kampmeier J, Radt B, Birngruber R, et al. Thermal and biomechanical parameters of porcine cornea. *Cornea* 2000;19:355-363.

30. Simonsen AH, Andreassen TT, Bendix K. The healing strength of corneal wounds in the human eye. *Exp Eye Res* 1982;35:287-292.

31. Zeng Y, Yang J, Huang K, et al. A comparison of biomechanical properties between human and porcine cornea. *J Biomech* 2001;34:533-537.

Chapter 4

[1] Yannas IV. Synthesis of organs: *In vitro* or *in vitro*? Proc Natl Acad Sci USA. 2000;97:9354–9356.

[2] Griffith M, Fagerholm P, Liu W, McLaughlin CR, Li F. Corneal Regenerative Medicine: Substitutes for Transplantation. In: Essentials of Ophthalmology, 2008. T. Reinhard, F. Larkin, Eds, Springer, Berlin, Germany, pp. 37-53.

[3] Hicks CR, Crawford GJ, Dart JKG, Grabner G, Holland EJ, Stulting RD, et al. AlphaCor – clinical outcomes. Cornea 2006; 25:1034-42.

[4] Liu Y, Gan L; Carlsson DJ, Fagerholm P, Lagali N, Watsky MA, et al. A simple, cross-linked collagen tissue substitute for corneal implantation. Invest Ophthalmol Vis Sci 2006;47 :1869-75.

[5] Liu Y, Griffith M, Watsky MA, Forrester JV, Kuffova L, Grant D, et al. Properties of porcine and recombinant human collagen matrices for optically clear tissue engineering applications. Biomacromolecules 2006;7 (6):1819-28.

[6] Liu W, Merrett K, Griffith M, Fagerholm P, Dravida S, Heyne B, et al. Recombinant collagen for tissue engineered corneal substitutes. Biomaterials 2008; 29:1147-58.

[7] McLaughlin CR, Fagerholm P, Muzakare L, Lagali N, Forrester JV, Kuffova L, et al. Regeneration of Corneal Cells and Nerves in an Implanted Collagen Corneal Substitute. Cornea 2008; 27:580-9.

[8] Kim HK, Kim K, Byun Y. Preparation of a chemically anchored phospholipid monolayer on an acrylated polymer substrate. Biomaterials 2005;26:3435–44.

[9] Wachiralarpphaithoon C, Iwasaki Y, Akiyoshi K. Enzyme-degradable phosphorylcholine porous hydrogels cross-linked with polyphosphoesters for cell matrices. Biomaterials 2007;28:984-93.

[10] Nam K, Kimura T, Kishida A. Physical and biological properties of collagen phospholipids polymer hybrid gels. Biomaterials 2007;28:3153-62.

[11] Goda T, Watanabe J, Takai M, Ishihara K. Water structure and improved mechanical properties of phospholipid polymer hydrogel with phosphorylcholine centered intermolecular cross-linker. Polymer 2006; 47: 1390-96.

[12] Li F, Griffith M, Li Z, Tanodekaew S, Sheardown H, Hakim M, et al. Recruitment of multiple cell lines by collagen-synthetic copolymer matrices in corneal regeneration. *Biomaterials* 2005;26:3093-3104.

[13] Merrett K, Fagerholm P, McLaughlin CR, Dravida S, Lagali N, Shinozaki N, et al. Tissue engineered recombinant human collagen-based corneal substitutes for implantation: performance of type I versus type III collagen. Invest Ophthalmol Vis Sci 2008; E-pub 30 May 2008.

[14] Funhoff AM, van Nostrum CF, Koning GA, Schuurmans-Nieuwenbroek NME, Crommelin DJA, Hennink WE. Endosomal escape of polymeric gene delivery complexes is not always enhanced by polymers buffering at low pH. Biomacromolecules 2004; 5:32-9.

[15] Wang SF, Lu LC, Gruetzmacher JA, Currier BL, and Yaszemski MJ. Synthesis and characterizations of biodegradable and crosslinkable poly(ε-caprolactone fumarate), poly(ethylene glycol fumarate), and their amphiphilic copolymer.Biomaterials 2006; 27:6832-41.

[16] Maurice DM. In: "The Eye". Davson H, editor, New York: Academic Press Inc; 1962. p.296.

[17] Patel S, Marshall J, Fitzke III FW. Refractive index of human corneal epithelium and stroma. J Ref Surg 1995;11:100-5.

[18] Van Den Berg TJTP, Tan KEWP. Light Transmittance of the human cornea from 320 to 700 nm for different ages. Vision Res 1994; 34(11):1453-6.

[19] Beems EM, Best JV. Light transmission of the cornea in whole human eyes. Exp Eye Res 1990; 50:393-5.

[20] Zeng Y, Yang J, Huang K, Lee Z, Lee X. A comparison of biomechanical properties between human andporcine cornea. J Biomech 2001;34:533–7.

[21] Crabb RA, Chau EP, Evans MC, BarocasVH, Hubel A. Biomechanical and microstructural characteristics of a collagen film-based corneal stroma equivalent. Tiss Eng 2006; 12: 1565-75.

[22] Jue B, Maurice DM. The mechanical properties of rabbit and human cornea. J Biomech 1986; 19:1025-39.

[23] Pettit DK, Knight PM. Glucose permeability of potential intrastromal implants. Invest Ophthal Vis Sci 1985; 26 (Suppl):151.

[24] Maurice DM, Watson PG. The distribution and movement of serum albumin in the cornea. Exp Eye Res 1965;4:355-63.

[25] Newsome DA, Foidart JM, Hassell JR, Krachmer JH, Rodrigues MM, Katz SI. Detection of specific collagen types in normal and keratoconus corneas. Invest Ophthalmol Vis Sci 1981;20:738-50.

[26] Newsome DA, Gross J, Hassell JR. Human corneal stroma contains three distinct collagens. Invest Ophthalmol Vis Sci 1982;22:376-81.

[27] Assouline M, Chew SJ, Thompson HW, Beuerman R. Effect of growth factors on collagen lattice contraction by human keratocytes. Invest Ophthalmol Vis Sci 1992; 33:1742-55.

[28] Smith LT, Holbrook KA, Madri JA. Collagen types I, III, and V in human embryonic and fetal skin. Am J Anat 1986; 175: 507-21.

[29] Fleischmajer R, Gay S, Perlish JS, Cesarini JP. Immunoelectron microscopy of type III collagen in normal and scleroderma skin. J Invest Dermatol 1980; 75: 189-91.

[30] Kiritoshi Y, Ishihara K. Synthesis of hydrophilic cross-linker having phosphorylcholine-like linkage for improvement of hydrogel properties. Polymer 2004; 45:7499-504.

[31] Ringvold A. Corneal epithelium and UV-protection of the eye. Acta Ophthalmol Scand 1998; 76: 149-53

[32] Kolozsvari L, Nogradi A, Hopp B, Bor Z. UV absorbance of the human cornea in the 240-400 nm range. Invest Ophthalmol Vis Sci 2002; 43: 2165-8.

[33] Sionkowska A, Wisniewski M, Skopinska J, Mantovani D. Effects of solar radiation on collagen-based biomaterials. Int J Photoenergy 2006. Article ID 29196, 6 pages.

[34] Myung D, Farooqui N, Zheng LL, Koh W, Gupta S, Bakri A, et al. Bioactive interpenetrating polymer network hydrogels that support corneal epithelial wound healing. J Biomed Mater Res A. 2008 May 15. DOI: 10.1002/jbm.a.32056

[35] Ringvold A. Corneal epithelium and UV-protection of the eye. Acta Ophthalmol Scand 1998; 76:149-53.

[36] Ringvold A, Anderssen E, Kjønniksen I. Impact of the environment on the mammalian corneal epithelium. Invest Ophthalmol Vis Sci. 2003; 44:10-15.

[37] Watanabe J, Nederberg F, Atthoff B, Bowden T, Hilborn J, Ishihara K. Cytocompatible biointerface on poly(lactic acid) by enrichment with phosphorylcholine groups for cell engineering. Mater Sci Eng C 2007; 27:227–31.

[38] Hsiue GH, Lo CL, Cheng CH, Lin CP, Huang CK, Chen HH. Preparation and characterization of poly(2-methacryloyloxyethyl phosphorylcholine)-block-poly(D,L-lactide) polymer nanoparticles. Journal Polymer Science: Part A: Polymer Chemistry 2007;45: 688–98.

Chapter 5

1. Foster A. Vision 2020--the Right to Sight. Trop Doct 2003;33(4):193-194.

2. Whitcher JP, Srinivasan M, Upadhyay MP. Corneal blindness: a global perspective. Bull World Health Organ 2001;79(3):214-221.

3. Griffith M, Fagerholm P, Liu W, McLaughlin CR, Li F. Corneal regenerative medicince: Corneal substitutes for transplantation. In: Reinhard T, Larkin F, editors. Cornea and External Disease, Essentials in Ophthalmology. Heidelberg, Germany, 2008.

4. Myung D, Farooqui N, Zheng LL, Koh W, Gupta S, Bakri A, et al. Bioactive interpenetrating polymer network hydrogels that support corneal epithelial wound healing. J Biomed Mater Res A 2009;90(1):70-81.

5. Sheardown H, Griffith M. Regenerative Medicine in the Cornea. In: Atala A, Lanza R, Thompson J, Nerem R, editors. Principles of Regenerative Medicine. Boston: Elsevier, 2008. p. 1066-1071.

6. Lambiase A, Rama P, Aloe L, Bonini S. Management of neurotrophic keratopathy. Curr Opin Ophthalmol 1999;10(4):270-276.

7. Fagerholm P, Lagali NS, Carlsson DJ, Merrett K, Griffith M. Corneal regeneration following implantation of a biomimetic tissue-engineered substitute. Clinical and Translational Science 2009;2(2):162-164.

8. Liu W, Deng C, McLaughlin CR, Fagerholm P, Lagali NS, Heyne B, et al. Collagen-phosphorylcholine interpenetrating network hydrogels as corneal substitutes. Biomaterials 2009;30(8):1551-1559.

9. Belmonte C, Acosta MC, Gallar J. Neural basis of sensation in intact and injured corneas. Exp Eye Res 2004;78(3):513-525.

10. Felipe CD, Gonzalez GG, Gallar J, Belmonte C. Quantification and immunocytochemical characteristics of trigeminal ganglion neurons projecting to the cornea: effect of corneal wounding. Eur J Pain 1999;3(1):31-39.

11. Muller LJ, Marfurt CF, Kruse F, Tervo TM. Corneal nerves: structure, contents and function. Exp Eye Res 2003;76(5):521-542.

12. Belmonte C, Gallar J, Pozo MA, Rebollo I. Excitation by irritant chemical substances of sensory afferent units in the cat's cornea. J Physiol 1991;437:709-725.

13. Gallar J, Pozo MA, Tuckett RP, Belmonte C. Response of sensory units with unmyelinated fibres to mechanical, thermal and chemical stimulation of the cat's cornea. J Physiol 1993;468:609-622.

14. Gallar J, Acosta MC, Belmonte C. Activation of scleral cold thermoreceptors by temperature and blood flow changes. Invest Ophthalmol Vis Sci 2003;44(2):697-705.

15. Liu W, Merrett K, Griffith M, Fagerholm P, Dravida S, Heyne B, et al. Recombinant human collagen for tissue engineered corneal substitutes. Biomaterials 2008;29(9):1147-1158.

16. Liu Y, Gan L, Carlsson DJ, Fagerholm P, Lagali N, Watsky MA, et al. A simple, cross-linked collagen tissue substitute for corneal implantation. Invest Ophthalmol Vis Sci 2006;47(5):1869-1875.

17. Lagali NS, Griffith M, Shinozaki N, Fagerholm P, Munger R. Innervation of tissue-engineered corneal implants in a porcine model: a 1-year in vivo confocal microscopy study. Invest Ophthalmol Vis Sci 2007;48(8):3537-3544.

18. Acosta MC, Belmonte C, Gallar J. Sensory experiences in humans and single-unit activity in cats evoked by polymodal stimulation of the cornea. J Physiol 2001;534(Pt. 2):511-525.

19. Brock JA, McLachlan EM, Belmonte C. Tetrodotoxin-resistant impulses in single nociceptor nerve terminals in guinea-pig cornea. J Physiol 1998;512 (Pt 1):211-217.

20. Liu L, Kuffova L, Griffith M, Dang Z, Muckersie E, Liu Y, et al. Immunological responses in mice to full-thickness corneal grafts engineered from porcine collagen. Biomaterials 2007;28(26):3807-3814.

21. Anderson EI, Fischbarg J, Spector A. Fluid transport, ATP level and ATPase activities in isolated rabbit corneal endothelium. Biochim Biophys Acta 1973;307(3):557-562.

22. Fischbarg J. Active and passive properties of the rabbit corneal endothelium. Exp Eye Res 1973;15(5):615-638.

23. Capella JA. The pathology of corneal endothelium. Ann Ophthalmol 1971;3(4):397-400.

24. Kaufman HE, Capella JA, Robbins JE. The human corneal endothelium. Am J Ophthalmol 1966;61(5 Pt 1):835-841.

25. Bourne WM, Nelson LR, Hodge DO. Central corneal endothelial cell changes over a ten-year period. Invest Ophthalmol Vis Sci 1997;38(3):779-782.

26. Ilmonen M, Lehtosalo JI, Virtanen J, Uusitalo H, Palkama A. Initial healing of posterior corneal surface following perforating trauma in the guinea pig: A scanning electron microscope study. Acta Ophthalmol. 1984;62:787-795.

27. Faure JP, Kim YZ. Obsertvations sur les effects de l'alloxane sur la cornée du cobaye. I. Destruction et réparation de l'endothélium. Arch Ophtalmol Rev Gen Ophtalmol. 1966;26:677-686.

28. McLaughlin CR, Tsai RJ, Latorre MA, Griffith M. Bioengineered corneas for transplantation and in vitro toxicology. Front Biosci 2009;14:3326-3337.

29. Pellegrini G, De Luca M, Arsenijevic Y. Towards therapeutic application of ocular stem cells. Semin Cell Dev Biol 2007;18(6):805-818.

30. Whikehart DR, Parikh CH, Vaughn AV, Mishler K, Edelhauser HF. Evidence suggesting the existence of stem cells for the human corneal endothelium. Mol Vis 2005;11:816-824.

31. Reynolds BA, Weiss S. Generation of neurons and astrocytes from isolated cells of the adult mammalian central nervous system. Science 1992;255(5052):1707-1710.

32. Tropepe V, Coles BL, Chiasson BJ, Horsford DJ, Elia AJ, McInnes RR, et al. Retinal stem cells in the adult mammalian eye. Science 2000;287(5460):2032-2036.

33. Yokoo S, Yamagami S, Yanagi Y, Uchida S, Mimura T, Usui T, et al. Human corneal endothelial cell precursors isolated by sphere-forming assay. Invest Ophthalmol Vis Sci 2005;46(5):1626-1631.

34. Yamagami S, Yokoo S, Mimura T, Takato T, Araie M, Amano S. Distribution of precursors in human corneal stromal cells and endothelial cells. Ophthalmology 2007;114(3):433-439.

35. Mimura T, Yokoo S, Araie M, Amano S, Yamagami S. Treatment of rabbit bullous keratopathy with precursors derived from cultured human corneal endothelium. Invest Ophthalmol Vis Sci 2005;46(10):3637-3644.

36. Yamagami S, Mimura T, Yokoo S, Takato T, Amano S. Isolation of human corneal endothelial cell precursors and construction of cell sheets by precursors. Cornea 2006;25(10 Suppl 1):S90-92.

37. LaVail JH, Johnson WE, Spencer LC. Immunohistochemical identification of trigeminal ganglion neurons that innervate the mouse cornea: relevance to intercellular spread of herpes simplex virus. J Comp Neurol 1993;327(1):133-140.

38. Marfurt CF, Kingsley RE, Echtenkamp SE. Sensory and sympathetic innervation of the mammalian cornea. A retrograde tracing study. Invest Ophthalmol Vis Sci 1989;30(3):461-472.

39. Morgan CW, Nadelhaft I, de Groat WC. Anatomical localization of corneal afferent cells in the trigeminal ganglion. Neurosurgery 1978;2(3):252-258.

40. Belmonte C, Aracil A, Acosta MC, Luna C, Gallar J. Nerves and sensations from the eye surface. Ocul Surf 2004;2(4):248-253.

41. Wener RG, Pinkerton RM, Robertson DM. Cryosurgical induced changes in corneal nerves. Can J Ophthalmol 1973;8(4):548-555.

42. Dib-Hajj SD, Yang Y, Waxman SG. Genetics and molecular pathophysiology of Na(v)1.7-related pain syndromes. Adv Genet 2008;63:85-110.

43. Li F, Carlsson D, Lohmann C, Suuronen E, Vascotto S, Kobuch K, et al. Cellular and nerve regeneration within a biosynthetic extracellular matrix for corneal transplantation. Proc Natl Acad Sci U S A 2003;100(26):15346-15351.

44. Belmonte C, Donovan-Rodriguez T, Luna C, Quirce S, Parra A, Acosta MC, et al. Sodium channel blockers modulate abnormal activity of regenerating corneal sensory nerves. Invest Ophthalmol Vis Sci 2009;50:E-Abstract 908.

45. Gallar J, Acosta MC, Gutierrez AR, Belmonte C. Impulse activity in corneal sensory nerve fibers after photorefractive keratectomy. Invest Ophthalmol Vis Sci 2007;48(9):4033-4037.

Chapter 6

1. Duan X, McLaughlin C, Griffith M, Sheardown H. Biofunctionalization of collagen for improved biological response: scaffolds for corneal tissue engineering. *Biomaterials* 2007;28:78-88.

2. Jacob JT, Rochefort JR, Bi J, Gebhardt BM. Corneal epithelial cell growth over tethered-protein/peptide surface-modified hydrogels. *J Biomed Mater Res B Appl Biomater* 2005;72:198-205.

3. Trinkaus-Randall V. Cornea. In: Lanza R, Langer R, Vacanti JP (eds), *Principles of Tissue Engineering.* New York: Academic Press; 2000:471-492.

4. Li F, Carlsson D, Lohmann C, et al. Cellular and nerve regeneration within a biosynthetic extracellular matrix for corneal transplantation. *Proc Natl Acad Sci U S A* 2003;100:15346-15351.

5. Liu Y, Gan L, Carlsson DJ, et al. A simple, cross-linked collagen tissue substitute for corneal implantation. *Invest Ophthalmol Vis Sci* 2006;47:1869-1875.

6. Liu L, Kuffova L, Griffith M, et al. Immunological responses in mice to full-thickness corneal grafts engineered from porcine collagen. *Biomaterials* 2007;28:3807-3814.

7. Manuelidis EE, Angelo JN, Gorgacz EJ, Kim JH, Manuelidis L. Experimental creutzfeldt-jakob disease transmitted via the eye with infected cornea. *N Engl J Med* 1977;296:1334-1336.

8. Lynn AK, Yannas IV, Bonfield W. Antigenicity and immunogenicity of collagen. *J Biomed Mater Res B Appl Biomater* 2004;71:343-354.

9. Kotch FW, Raines RT. Self-assembly of synthetic collagen triple helices. *Proc Natl Acad Sci U S A* 2006;103:3028-3033.

10. Smith LT, Holbrook KA, Madri JA. Collagen types I, III, and V in human embryonic and fetal skin. *Am J Anat* 1986;175:507-521.

11. Priest D, Munger R. A new instrument for the monitoring of the optical properties of corneas. *Invest Ophthalmol Vis Sci* 1998;39(suppl):s352.

12. International Organization of Standardization. Tests for cytotoxicity: *in vitro* method., *Biological Evaluation of Medical Devices.* Geneva, Switzerland: ISO:10993-10995.

13. International Organization of Standardization. Tests for genotoxicity, carcinogenicity and reproductive toxicology. *Biological Evaluation of Medical Devices* Geneva, Switzerland: ISO:10993-10993

14. International Organization of Standardization Tests for Systemic Toxicity. *Biological Evaluation of Medical Devices* Geneva, Switzerland: ISO:10993-10911.

15. Liu Y, Griffith M, Watsky MA, et al. Properties of porcine and recombinant human collagen matrices for optically clear tissue engineering applications. *Biomacromolecules* 2006;7:1819-1828.

16. International Organization of Standardization. Tests for local effects after implantation. *Biological Evaluation of Medical Devices* Geneva, Switzerland: ISO:10993-10996.

17. Lagali NS, Griffith M, Shinozaki N, Fagerholm P, Munger R. Innervation of tissue-engineered corneal implants in a porcine model: a 1-year *in vitro* confocal microscopy study. *Invest Ophthalmol Vis Sci* 2007;48:3537-3544.

18. Gipson IK, Spurr-Michaud SJ, Tisdale AS. Hemidesmosomes and anchoring fibril collagen appear synchronously during development and wound healing. *Dev Biol* 1988;126:253-262.

19. McCarey BE, Schmidt FH. Modeling glucose distribution in the cornea. *Curr Eye Res* 1990;9:1025-1039.

20. Newsome DA, Foidart JM, Hassell JR, Krachmer JH, Rodrigues MM, Katz SI. Detection of specific collagen types in normal and keratoconus corneas. *Invest Ophthalmol Vis Sci* 1981;20:738-750.

21. Newsome DA, Gross J, Hassell JR. Human corneal stroma contains three distinct collagens. *Invest Ophthalmol Vis Sci* 1982;22:376-381.

22. Linsenmayer TF. What is extracellular matrix? . In: Hay ED (ed), *In Cell Biology of Extracellular Matrix.* New York: Plenum Press; 1983:5-37.

23. Vater CA, Harris ED, Jr., Siegel RC. Native cross-links in collagen fibrils induce resistance to human synovial collagenase. *Biochem J* 1979;181:639-645.

24. Horwitz AL, Hance AJ, Crystal RG. Granulocyte collagenase: selective digestion of type I relative to type III collagen. *Proc Natl Acad Sci U S A* 1977;74:897-901.

25. Assouline M, Chew SJ, Thompson HW, Beuerman R. Effect of growth factors on collagen lattice contraction by human keratocytes. *Invest Ophthalmol Vis Sci* 1992;33:1742-1755.

26. Yamagami S, Ebihara N, Usui T, Yokoo S, Amano S. Bone marrow-derived cells in normal human corneal stroma. *Arch Ophthalmol* 2006;124:62-69.

27. Dartt DA. Dysfunctional neural regulation of lacrimal gland secretion and its role in the pathogenesis of dry eye syndromes. *Ocul Surf* 2004;2:76-91.

28. Tighe B. Eye Contact. *Chem Brit* 1992;28:241-244.

29. Nishida T. Cornea. In: Krachmer JH, Manis MJ, Holland EJ (eds), *Cornea.* Philadelphia: Elsevier Mosby; 2005:3-26.

30. Zeng Y, Yang J, Huang K, Lee Z, Lee X. A comparison of biomechanical properties between human and porcine cornea. *J Biomech* 2001;34:533-537.

31. Crabb RA, Chau EP, Evans MC, Barocas VH, Hubel A. Biomechanical and microstructural characteristics of a collagen film-based corneal stroma equivalent. *Tissue Eng* 2006;12:1565-1575.

32. Jue B, Maurice DM. The mechanical properties of the rabbit and human cornea. *J Biomech* 1986;19:847-853

Chapter 7

Cleator, G. M. and P. E. Klapper (2000). The Herpesviridae. Principles and Practices of Clinical Virology. A. J. Zuckerman, H. E. Banatvala and J. R. Pattison, John Wiley & Sons, Ltd.: 23-45.

Darougar, S., M. S. Wishart and N. D. Viswalingam (1985). "Epidemiological and clinical features of primary herpes simplex virus ocular infection." Br. J. Ophthalmol. **69**(1): 2-6.

De Kesel, R. J., C. Koppen, M. Ieven and T. Zeyen (2001). "Primary graft failure caused by herpes simplex virus type 1." Cornea **20**(2): 187-90.

Dravida, S., S. Gaddipati, M. Griffith, K. Merrett, S. Lakshmi Madhira, V. S. Sangwan and G. K. Vemuganti (2008). "A biomimetic scaffold for culturing limbal stem cells: a promising alternative for clinical transplantation." J. Tissue Eng. Regen. Med. **2**(5): 263-71.

Griffith, M., R. Osborne, R. Munger, X. Xiong, C. J. Doillon, N. L. Laycock, M. Hakim, Y. Song and M. A. Watsky (1999). "Functional human corneal equivalents constructed from cell lines." Science **286**(5447): 2169-72.

Hicks, C. R., G. J. Crawford, D. T. Tan, G. R. Snibson, G. L. Sutton, T. D. Gondhowiardjo, D. S. Lam and N. Downie (2002). "Outcomes of implantation of an artificial cornea, AlphaCor: effects of prior ocular herpes simplex infection." Cornea **21**(7): 685-90.

Hsiue, G. H., J. Y. Lai, K. H. Chen and W. M. Hsu (2006). "A novel strategy for corneal endothelial reconstruction with a bioengineered cell sheet." Transplantation **81**(3): 473-6.

Inatomi, T., T. Nakamura, M. Kojyo, N. Koizumi, C. Sotozono and S. Kinoshita (2006). "Ocular surface reconstruction with combination of cultivated autologous oral mucosal epithelial transplantation and penetrating keratoplasty." Am. J. Ophthalmol. **142**(5): 757-64.

Lambiase, A., P. Rama, L. Aloe and S. Bonini (1999). "Management of neurotrophic keratopathy." Curr. Opin. Ophthalmol. **10**(4): 270-6.

Li, F., D. Carlsson, C. Lohmann, E. Suuronen, S. Vascotto, K. Kobuch, H. Sheardown, R. Munger, M. Nakamura and M. Griffith (2003). "Cellular and nerve regeneration within a biosynthetic extracellular matrix for corneal transplantation." Proc. Natl. Acad. Sci. U. S. A. **100**(26): 15346-51.

Nakamura, T., T. Inatomi, C. Sotozono, L. P. Ang, N. Koizumi, N. Yokoi and S. Kinoshita (2006). "Transplantation of autologous serum-derived cultivated corneal epithelial equivalents for the treatment of severe ocular surface disease." Ophthalmology **113**(10): 1765-72.

O'Brien, W. J. and J. L. Taylor (1989). "The isolation of herpes simplex virus from rabbit corneas during latency." Invest. Ophthalmol. Vis. Sci. **30**(3): 357-64.

Rama, P., S. Bonini, A. Lambiase, O. Golisano, P. Paterna, M. De Luca and G. Pellegrini (2001). "Autologous fibrin-cultured limbal stem cells permanently restore the corneal surface of patients with total limbal stem cell deficiency." Transplantation **72**(9): 1478-85.

Suuronen, E. J., M. Nakamura, M. A. Watsky, P. K. Stys, L. J. Muller, R. Munger, N. Shinozaki and M. Griffith (2004). "Innervated human corneal equivalents as in vitro models for nerve-target cell interactions." FASEB J. **18**(1): 170-2.